Study of parameters determining inter-particle crosslinking reactions in waterborne coatings.

Sheraz Tariq

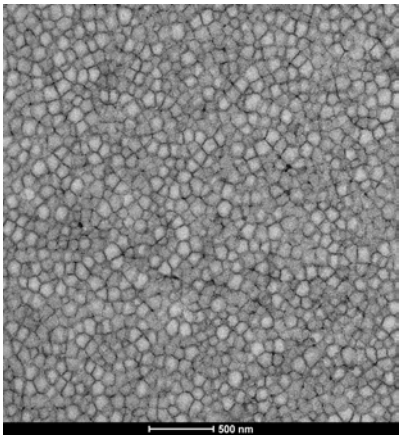

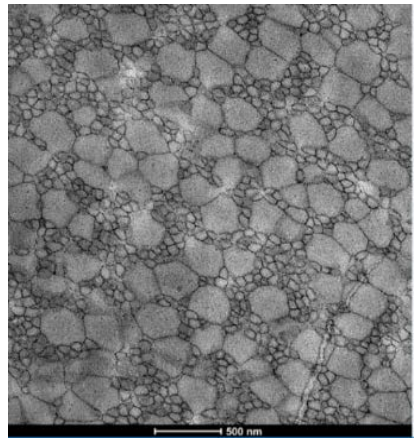

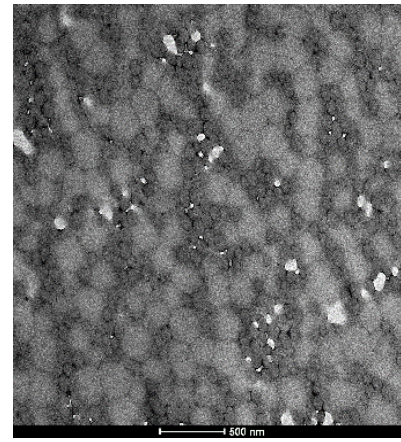

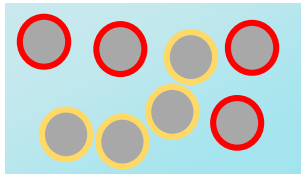

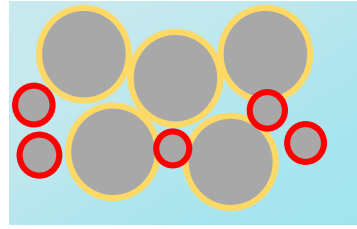

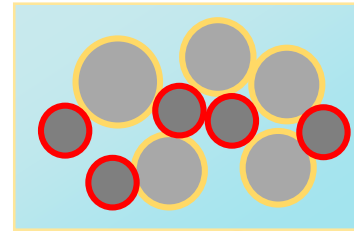

eman ta zabal zazu

Universidad del País Vasco

Euskal Herriko Unibertsitatea

2023

Study of parameters determining interparticle crosslinking reactions in waterborne coatings

Sheraz Tariq

Supervised by: Prof. María Paulis

Chemical Engineering Group

University of the Basque Country UPV/EHU

Donostia-San Sebastián

(2023)

Acknowledgements

I would like to express my sincere gratitude to my supervisor Maria Paulis for her patience and guidance throughout this journey. I believe that this work could have never been done without her continuous motivation and guidance. “Mila Esker” for the guidance and support that not only helps me to grow as a chemist but also as a person as well. You have been a role model to me.

I would like to thank all the people for their collaboration during this four-year journey. Especially, I would like to thank all the professors, post-doctorate and PhD students of the group for the discussions, suggestions and help. I would like to thank Lourdes Irusta and Mercedes Fernandez for being a part of the research work. I would like to give a special thanks to Inés Plaza for her endless help and kindness.

Thanks to the Sgiker Services, Maite Miranda and Dr. Ana Martínez for the TEM images, Dr. Loli Martin for AFM images, Dr. Mariló Gurruchaga for pendulum hardness, Dr. Beñat Olave for fluorescence experiments,Dr. Alba Gonzalez for all technical support by carrying out the DSC measurements and Dr. Dirk Mestach (Allnex) for the research discussion and suggestions.

I would like to express my gratitude to Dr. Bernd Reck, Dr. Samane Mehravar and Dr. Nico Veling for giving me the opportunity to join BASF for an internship. I would also like to thank other members of BASF company too, especially Dr. Baastian Lohmeijer and Sebastian Schmidt for their support in paint applications.

I would also like to acknowledge the financial support from the Industrial Liaison Program in Polymerization in Dispersed Media.

Contents

Chapter 3

Chapter 4

Appendix II

Appendix III

List of acronyms

AAEMA	Acetoacetoxy ethyl methacrylate
AFM	Atomic force microscope
BA	Butyl acrylate
dp	Average particle size
DLS	Dynamic light scattering
DMTA	Dynamic Mechanical Thermal analysis
FTIR	Fourier transform infrared
FRET	Fluorescence resonance energy transfer
HMDA	Hexamethylenediamine
KPS	Potassium persulfate
MAA	Methacrylic acid
MEK	Methyl ethyl ketone
MFFT	Minimum film formation temperature
MMA	Methyl methacrylate
M_w	Weight average molar mass
PEF	Pyrene excimer fluorescence
PEI	Poly ethyleneinimine
Phe-MMA	(9-phenanthryl)methyl methacrylate
PSD	Particle Size Distribution
RT	Room temperature
S	Styrene
SANS	Small-Angle Neutron Scatterings
SDS	Sodium Dodecyl Sulfate
TEM	Transmission Electron Microscopy

THF	Tetrahydrofuran
T_G	Glass transition temperature
Vc	Critical volume fraction
VOC	Volatile Organic Compounds
wbm	Weight based on main monomers
wbtm	Weight based on total monomers
wt	Total weight.

Chapter 1.

Introduction.

1.1. Waterborne coatings

The main purpose of a coating is to protect the surface and internal structure of the object it is applied on, in the same manner as skin protects the inner organs of the human body, while decoration purposes would be a secondary role. Therefore, a coating is defined as a continuous thin layer applied to the outer surface of an object for achieving the desired protective objective. During the period of early 1970s, nearly 90 % of coatings and paints were prepared from solventborne binders.[1] The binder polymer was prepared in solution and had very low solids content of around 5-20 %.[1] However, solventborne coatings have a major challenge associated with the presence of a high percentage of low boiling point volatile organic compounds (VOC) that when emitted to the atmosphere, can produce toxic responses or reactions with the ultraviolet radiation.[2] Compounds such as ether, acetone, aliphatic hydrocarbons etc. were normally used for the preparation of coatings.[3] The presence of such compounds in the atmosphere for long time may produce many diseases, from headache and to certain types of cancer.[2] Therefore, strict legislation has been enforced on the usage of VOC depending on the types of coatings (Solvent Emission Directive 1999/13/EC and Deco paint directive 2004/42/EC).[4-6]

Waterborne coatings are considered as one of the alternatives by the industry for producing low level or no VOC coatings, as water is used as the continuous phase in these coatings, instead of an organic solvent, fulfilling the VOC regulations. Some of the major advantages that make these coatings undisputable and able to revolutionize the technology are the easy availability of a wide range of resins for waterborne binders like epoxies, urethanes, polyester, acrylics etc [7] and the production of high solids content waterborne binders up to 60 wt.%.[8,9] Further increase in the solids content to 70 wt. % can also be achieved by using bimodal particle size systems.[10-12]

Waterborne coatings contain two major components apart from the waterborne polymeric binder i.e., pigments and additives. Additives are low molecular weight chemicals used in very small quantity of around 5 %. Their primary objective is to provide stability to coatings and to enhance the dispersion of pigments. Pigments are used to give decorative and aesthetic properties to the film. However, the binder is the central chemical substance used in organic coatings. This component forms a continuous film that binds all the components of the coating together and to the substrate. Most of the properties of the film depend on it, as it contains half of the formulation weight. Therefore, the study of the binders in coating applications is of utmost importance. Emulsion polymerization is mostly used in the production of the waterborne polymers for coating binders, even if adhesives, additives for paper and drug delivery systems can also be obtained by this method.[13,14] As a consequence, emulsion polymerization industry is growing in quick pace promoting clean technology.

The emulsion polymerization was greatly expanded after World War-II, when Japanese forces restricted Americans to natural rubber resources available at South East Asia. Since then

the use of emulsion polymerization has greatly increased. The product obtained from emulsion polymerization is a colloidal dispersion of polymer particles in water called “latex”.

The batch emulsion polymerization is a complex process that passes from different steps, known as intervals.[15-17] Initially, the reactor contains monomer, surfactant and water as a dispersing medium. The polymerization is initiated by the addition of initiator, which is usually water-soluble. The radicals produced from the initiator are hydrophilic and ready to react with monomer dissolved in the aqueous phase forming oligoradicals. The oligoradicals grow further by adding more monomer units present in the aqueous phase. At one point, the oligoradical will become hydrophobic enough to enter in the micelles formed by the surfactant, forming a polymer particle. This process of forming polymer particles by the entry of oligoradicals in the micelles is known as heterogeneous nucleation.[18] If oligoradicals in aqueous phase precipitate in the aqueous phase absorbing surfactant, the homogenous nucleation takes place.[19] Both homogenous and heterogeneous nucleation can be operative at the same system. This step is termed as Interval-I in which particle nucleation occurs. Generally, the number of particles per liter formed in this stage is 10^{17} to 10^{18}. In Interval-II, the monomer droplets decrease in size as the polymer particles grow. The polymer particles increase their size by mass transport and polymerization.[20] The end of interval-II, when monomer droplets disappear, depends on the swelling of polymer particles by monomer. In interval–III, a continuous decrease in the concentration of monomer in the polymer particles occurs, as polymerization proceeds. In this step, the polymerization rate decreases because the monomer concentration is decreasing. At the end, the waterborne dispersion of polymer particles is formed, also known as latex.

Nevertheless, the semibatch emulsion polymerization is the industrially preferred process to obtain latexes. This process allows better control of the polymerization process by feeding the

reactants and it is safer in terms of better control the heat generation during the exothermic reaction. The typical process followed for semibatch emulsion polymerization uses a seed (latex with a small particle size and low solids content) as an initial charge and during the polymerization, initiator, monomer and surfactant are fed in the reactor. The feeding rate plays a major role in the final properties of the polymer.

1.2. Latex film formation

Even if some latex are finally used to obtain the polymer by coagulation, many other are directly used in their dispersed form that will produce films in their final applications in coatings or adhesives. The process of transforming the colloidal dispersion of polymer particles into a continuous film is known as latex film formation. There is a general agreement to divide the film formation process into three overlapping steps i.e., water evaporation, particle deformation and coalescence and interdiffusion.[21-23] The final film properties are strongly depending on this process, depicted in Figure 1.1.

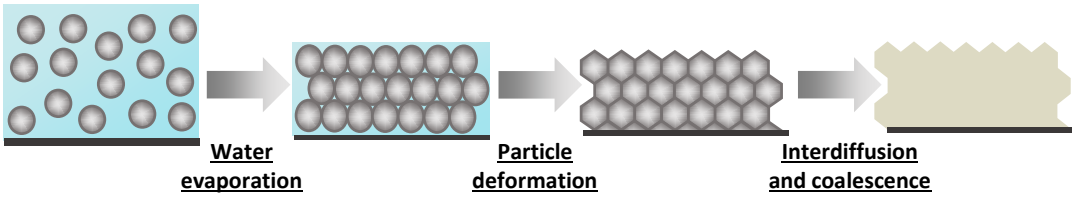

Figure 1.1 Schematic of the process of film formation: the transition from a waterborne colloidal dispersion into a continuous polymer film.

Polymer particles come closer to each other during evaporation (step-1) forming a denser and more viscous phase.[21,24,25] This step is important as it controls the packing / distribution of particles in the final film, as depending on the Péclet number, $P_{e,}$, the horizontal [26,27] or

vertical [26,28] homogeneity of the film drying will be established. P_e is defined as the ratio between characteristic time for particles diffusion and the characteristic time for water evaporation.[29] If $P_e << 1$,for low evaporation rates, low film thickness and high particle diffusion coefficient, diffusion of particles occurs much faster than water evaporation, which leads to a uniform location of the particles in the vertical direction during drying. However, if $P_e >> 1$, then evaporation rate is faster than particles diffusion, and some of them are trapped in the receding water front, forming a closed packed layer of particles on the top of the drying film, which may also increase the drying time. It has to be noted that if different particle sizes are present in a latex, each of them will have a different P_e number, and this could lead to a non-homogeneous distribution of the particles in the final film.

In step-2, particle deformation, the voids between adjacent polymer particles are eliminated due to the deformation of spherical polymer particles to a dodecahedral structure. This deformation step can take place after water evaporation, by dry sintering mechanism, before water evaporation, by wet sintering, or even during water evaporation, by capillary deformation at the water-particle-air interface.[30-32] The occurrence of one or another deformation mechanism will depend again on the rate of evaporation, the glass transition temperature of the polymer in the particles and the particle size.

However, in order to achieve full mechanical strength, particles do not need only to deform, but they also need to coalesce and the polymer chains from neighbouring particles have to interdiffuse into each other, in step-3. The rate of this step will depend again on the T_G of the polymer, the molecular weight and the branching and crosslinking density of the chains and on the nature of the stabilizing agents on the surface of the polymer particles. As it will be explained later, there are several techniques like small angle neutron scattering (SANS), fluorescence

resonance energy transfer (FRET) and pyrene excimer fluorescence (PEF) that have been used to measure the interdiffusion between polymer particles during film formation.[33-35]

Nevertheless, an easier technique to quantify the film formation ability of different latexes is the measurement of their minimum film formation temperature (MFFT). It is determined by the deposition of a thin latex film on a metallic surface in which a temperature gradient is applied. The MFFT is determined as that above which a continuous and transparent film is formed. As it has been pointed out above, the T_G of the polymer particles mainly predict their deformation and interdiffusion ability and control the MFFT of the latex. Soft particles, with T_G below room temperature, will produce good films at ambient temperature, as they will have a MFFT below that tempperature. However, it has also been reported that particle size also influences the MFFT of a latex. [36] Jensen and Morgan showed that with increasing the particles diameter from 50 to 1200 nm the MFFT suffered an increase of 5 K.[37] The reason has been attributed to the smaller voids present in the interstitial spaces between smaller polymer particles and to the predominant capillary deformation mechanism in these cases.

1.3. Film formation paradox and preparation of hard films

The film formation process in waterborne coatings is completely different from solventborne coatings. In case of solventborne coatings, the presence of solvent plasticizes the polymer during the evaporation, therefore hard polymer films can be casted from polymer solutions at room temperature. However, in case of waterborne coatings, the use of hard polymers does not allow the formation of continuous films at room temperature, because the deformation and interpenetration of particles require low T_G polymer, while hardness demands high T_G polymer.[23] This is known as the film formation dilemma. Therefore, to overcome this

challenge, different approaches have been tried to form hard films from waterborne polymeric dispersions at room temperature.

The approach most commonly followed to overcome this obstacle is the use of low molecular weight molecules, volatile organic compounds (VOC) as temporary plasticizers.[23] The main objective of these molecules is to decrease the MFFT and T_G of the polymer,[23] allowing better diffusion of the polymer chains during film formation. The effect is temporary as VOCs evaporate once the film is formed, leaving a hard film behind. The major drawback of this approach is the contamination of the environment produced by the release of these VOCs. The use of reactive plasticizers has been proposed as an alternative to solve these VOC emissions. These reactive plasticizers will react with the polymer chain and will remain in the film instead of being evaporated.[38,39] Lahtinen *et al.* reported that the use of a coalescent agent with glyceryl functionality in carboxylic acid functionalized latex, not only decreases the MFFT but also reduces VOC emissions, as the epoxy group from the coalescent agent reacts with the carboxylic group present in the latex.[40]

Another well-known and efficient compound that can be used to obtain the plasticization effect is water.[41] Its effect is known as hydroplasticization (HP) effect. The main purpose of using hydroplasticization is to decrease the MFFT without disturbing the rest of the film properties such as water resistance. To achieve the hydroplasticization effect, hydrophilic functional monomers have been included into the polymer, to favor the binding of water and its plasticization effect during film formation. A model was developed by Sundberg *et al.* to predict the functional groups that react with water and produce the plasticization effect.[42] However, the use of HP commonly relies on the use of hydrophilic protective colloids such as polyvinyl alcohol and alkali soluble resins. These ingredients work in good fashion but they may create problems in the water

and chemical resistance properties of the film. Dron *et al.* reported the use of three different functional monomers i.e., methacrylic acid, itaconic acid and polyethyleneglycol methacrylate.[43] The authors reported that use of PEGMA decreased the MFFT by 16 °C, but the water resistance properties of the final film were seriously damaged. However, with the use of itaconic acid, the MFFT decreased around 14 °C, while the water resistance was not affected. In order to improve their approach, oligomers were also produced in the polymer particles and used as a temporary oligomers plasticizer that will disturb less the chemical resistance, while reducing effectively the MFFT.[44]

The structural reinforcement is also one of the approaches followed to avoid the VOC emissions from the excess of coalescing agents. Multiphase polymer can be prepared by blending low and high T_G particles [45-48] or by combining both components in the same nanoparticles.[49,50] The soft phase helps the film formation and the hard phase assists the development of hardness in the film. The preparation of hard-core soft -shell polymer particles is one of the examples.[51,52] This morphology can be developed by encapsulating the hard domains within the polymer particles. Juhue *et al.* reported the preparation of hard-core and soft polymer particles, [53] concluding that the usage of soft layer on hard particles helps to avoid the coalescent agent by producing structured nanoparticles. Some authors have also tried the structural reinforcement by the preparation of soft-core hard-shell polymer particles.[50,54] In this system, the hard shell increases the elastic modulus of the film and the soft domain favours film formation and enhances the toughness of the film. This behavior can also been seen in the bimodal system containing polymer particles of different hardness.[55]

Physical crosslinking between polymer particles, such as ionic interaction or hydrogen bonding, is also used as an alternative to reduce the use of VOC when forming hard films at

ambient temperature from waterborne systems. Though physical interaction induces weak interactions and low bond strength, it is used in a wide variety of applications such as the synthesis of supramolecular polymers and complex polymers with self-healing properties.

The ionic interaction was first introduced in waterborne dispersions in 1967 by J.S. Johnson & Sons.[56] The authors presented the interaction between carboxylate acid latex with metal ions such as Zn^{2+}, Ni^{2+} and Cd^{2+}. The blends were stable in the solution state and crosslinking occurred on drying. As a result, hard films were produced with good mechanical strength and improved chemical resistance.[56] Kim and co-workers studied the film formation process by fluorescence resonance energy transfer (FRET) for the system having carboxylic acid containing polymer particles in the presence of different metal salts. The authors observed that interfacial crosslinking reaction occurred because of the strong ionic interaction between metal cations and carboxylic acid, and the interdiffusion of the polymer chains between polymer particles was hindered.[57] Argaiz et al. studied the effect of the blending of latexes containing a small amount of oppositely charged ionic monomers i.e., sodium styrene sulfonate and 2-(dimethylamino) ethyl methacrylate.[58] The authors found that ionic complexes were formed in the interparticle space during film formation. These complexes hindered the interdiffusion of polymer chains between polymer particles, but nevertheless, an increase in the mechanical properties was observed.[58] Furthermore, the water resistance of the films was improved if a stoichiometric neutralization between positive and negative charges was obtained.

The introduction of hydrogen bonding is another way to improve the stiffness and hardness of latex films. The electrostatic interaction between hydrogen bond donor (electron acceptor) and hydrogen bond acceptor (electron donor) is known as hydrogen bonding.[59-61] It is a relatively strong electrostatic interaction. The most widely used application area of

hydrogen bonding is the formation of supramolecular polymer [62,63] and inter-polymer complexes. [64] Basically, supramolecular polymers are formed by non-covalent interaction and contrary to the covalent crosslinking, the linkage formed are weaker and reversible. Jimenez *et al.* (2019) investigated the chemistry of tanic acid (TA), a natural occurring polyphenol and polymer latexes containing hydrogen bond acceptor groups. The high acidity of the phenolic hydroxyl group present in TA makes it a particularly good hydrogen donor. The reinforcement of the film observed in the presence of TA, which was attributed to the formation of a honeycomb microstructure, was promoted by the hydrogen bonding interactions between pyrrolidone groups in the polymer backbone and phenolic OH groups in TA.[65]

Beside the wide literature reports on physical crosslinking, the low physical bonding energy providing poor physical strength is the major drawback of this interaction. Therefore, the alternative approach is the use of chemical crosslinking, which is considered to form stronger linkages.

1.4. Overview of chemical crosslinking

The concept of crosslinking arose in 1839 when Charles Goodyear accidently added sulfur during the polymerization of rubber. Initially, the sulfur was referred to as an accelerator because its addition improved the mechanical properties and decreased the abrasion resistance of the rubber. Actually, sulfur acts as a crosslinker and makes joints between the polymer chains of rubber.[66] Though the emulsion polymerization process was invented in 1912, it took several years to realize the need of chemical crosslinking to produce hard films out of latexes.[67]

The crosslinking chemistries used for waterborne latexes were initially the same as the ones used for solventborne polymers, but trying to avoid the reactivity of the crosslinker with

water.[68] Melamine and other formaldehyde based crosslinking system were the first ones (since 1950) to be used to crosslink acrylic latexes containing hydroxyl functionalities (Figure 1.2), even if amine functional or acid functional latexes could also be crosslinked with this chemistry. In most of the cases, an additive approach was used, including water soluble or dispersable melamine derivatives to the acrylic latex. Hexamethoxymethylmelamine (HMMM) is one of the used water-soluble derivatives.[69] It acts as plasticizer at low temperatures, to favor the interdiffusion of polymer chains, and it is only activated to produce the crosslinking at 120ºC.[70] The reactive monomer approach has also been used in this crosslinking chemistry, including functional monomers having acrylamide moieties in the formulation of the acrylic latex. Melamine derivatives crosslinking were developed for high temperature applications, such as automotive and industrial coatings.

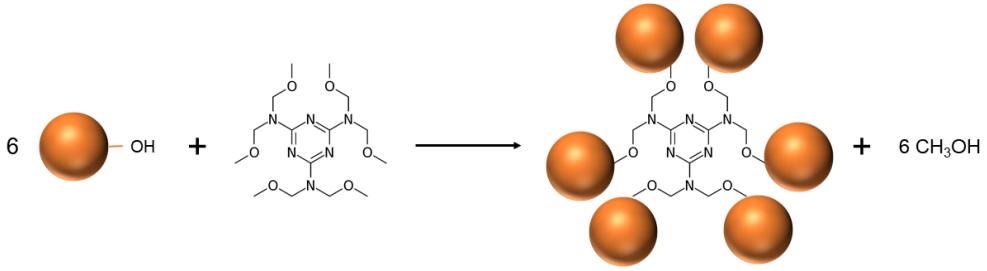

Figure 1.2. Melamine or other formaldehydes based crosslinking mechanism with hydroxylated latexes.

However, it has been seen that melamine - formaldehyde type chemistry is considered as hazardous crosslinking chemistry when operated at higher temperature. Therefore, the trend was shifted toward carboxylic acid type crosslinking chemistry as a non-toxic and ambient temperature crosslinking system. This chemistry is often used in waterborne dispersions and also gives stability to polymer particles. The mostly used functional group with carboxylate are

aziridine, carbodiimide and oxirane. The reactivity of these functionalities with carboxylate are different and it determines the shelf life, efficiency of the reaction chemistry and the toxicity.

The search for crosslinking technologies producing less formaldehyde emissions was started in the early 1970s.[71] As a result Cordova Chemical Co. developed the aziridine crosslinking technology in the late 1970s. The aziridine compound was added to the acidic latex before application.[72] In principle, the latex had to be neutralized with ammonia, so that when ammonia evaporates on drying, the crosslinking reaction would take place (Figure 1.3).[73] Nevertheless, the pot life of the mixture did not exceed 24 hours, and the aziridine compound developed severe allergic reactions.[74]

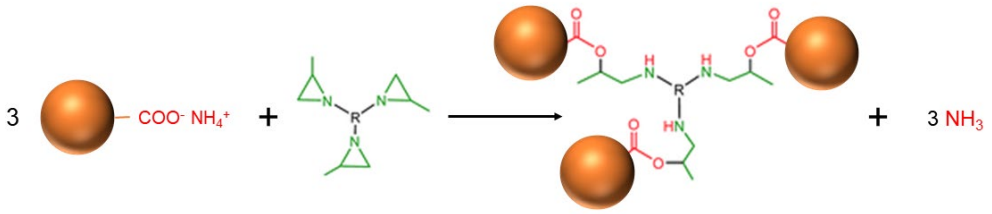

Figure 1.3. Aziridine based crosslinking of acid latexes.

Therefore, in the early 1980s Union Carbide Corp. introduced the polycarbodiimide crosslinking chemistry to get rid of the allergic problems of aziridine (Figure 1.4). The chemical structure of carbodiimide is similar of isocyanate but it is less sensitive toward the environment, which improved the shelf life of the system.[75],[76]

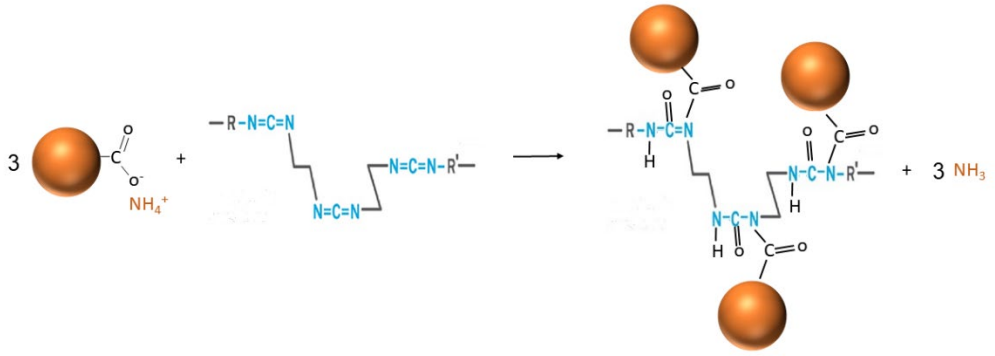

Figure 1.4. Polycabodiimide based crosslinking of acid latexes.

Oxirane and oxazoline chemistries have also been used to introduce crosslinking to latexes with functional acidic moieties (Figure 1.5 and 1.6). In the crosslinking with oxiranes and oxazolines, water soluble crosslinking oligomers can be added to the acidic latexes or those functionalities can be included in separate polymer particles. For instance, glycidyl methacrylate (GMA) has been used to include the oxirane group in polymer particles.[77,78]

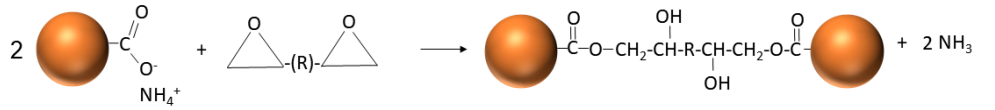

Figure 1.5. Oxirane based crosslinking of acid latexes.

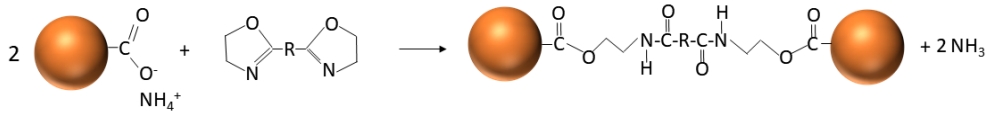

Figure 1.6. Oxazoline based crosslinking of acid latexes.

These crosslinking chemistries presented so far present the problem of the competing reaction between –COOH and H_2O or –OH and H_2O with the crosslinking group, apart from the fact that many of these chemistries have been mainly used with water soluble or dispersible

oligomers, which are under scrutiny due to CLP labelling and REACH. Furthermore, these formulations tend to be usually two packs systems.

Several ways have been presented in literature such as the use of unsaturation crosslinking to produce one pack crosslinking waterborne systems. Based on the alkyd oxidative curing of solventborne coatings, several approaches have been made to obtain unsaturation in waterborne latexes, which will lead to oxidative crosslinking in the presence of O_2 and eventually metal catalysts. For instance, Tillson [79] used allyl methacrylate to increase the amount of pendant double bonds at the end of the emulsion polymerization reaction, and Taylor *et al.*[80] included styrene in their formulations to enhance the survival of the pendant double bonds for the subsequent oxidation reactions.

Eastman Chemical Co. introduced acetoacetoxyethyl methacrylate (AAEMA) in the market in the late 1980s, and since then its use for crosslinking reactions of waterborne latexes has been widely explored. AAEMA is preferred because it provides environmentally friendly coatings which are less toxic and able to cure at room temperature.[81]

1.5. Crosslinking with acetoacetoxy ethyl methacrylate (AAEMA)

AAEMA monomer has two reactive sites, the polymerizable methacrylate group and carbonyl group in the acetoacetoxy moiety (Figure 1.7). It is capable to react with various functional groups such as (poly)isocyanates and (poly)ketamines.[82] However, the crosslinking chemistry of AAEMA with diamines has been widely studied for coating applications. The functional monomer AAEMA can easily be incorporated in an acrylic latex and can be used for crosslinking with diamines at room temperature.[83] In this sense, the AAEMA functionality offers unique versatility for the latex coating application. From the early studies by Noomen in two pack

systems with AAEMA functionalized latexes and water soluble polyamine crosslinkers, [84] and the first trials of two-pots one-pack systems by Geurink et al. [85] to the multiple patents presenting their use for the crosslinking of waterborne polymeric dispersions,[86,87] the use of AAEMA functionalized latexes has been extensive.

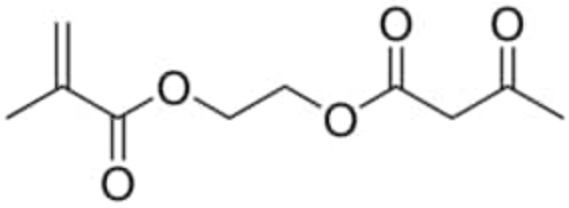

Figure 1.7. Acetoacetoxy ethyl methacrylate.

The acetoacetoxy moieties attached to waterborne particles cannot survive at high temperatures, therefore to protect the stability, the latex should be stored at low temperature.[88] Several approaches have been tried to improve the stability of acetoacetoxy moieties, the most commonly used approach being the formation of enamine by reacting it with ammonia. Bors and Lavoie studied the stability of enamines prepared by reacting ammonia with acetoacetoxy based latex. The authors found that enamines are more hydrolytically stable than acetoacetoxy moieties.[89]

Feng *et al.* investigated the relative rate of crosslinking and interdiffusion in the film prepared by poly(butyl methacrylate) and poly(2-ethylhexylmethacrylate) latexes with 10 wt% of AAEMA as a co-monomer. 1,6 hexanediamine was used as crosslinker and it was found that the reaction between latex particles and crosslinker occurred rapidly. The final film had a good integrity and excellent solvent resistance. From the interdiffusion study, the authors found that polymer diffusion was still possible in the system.[90] U.S Patent 5,998,543 claims the formation of water based acetoacetoxy functional particles that can coexist with stable water based amino

functional particles in a two-pots one-pack system.[91] Both polymer particles are prepared by seeded emulsion polymerization and are identical in terms of particle size and zeta potential. Both polymer particles are mixed and during the film formation ammonia is released, acetoacetoxy regenerated and made available for crosslinking.[91]

1.6. Crosslinking and interdiffusion during film formation.

As it has been mentioned earlier, chemical crosslinking will provide strong linkages in the final film. This crosslinking can be achieved in the main polymerization step or after it, called post-crosslinking.[92] The main difference between crosslinking and post-crosslinking is the way the material is being processed afterwards.[92] The major problem of crosslinking occurring during the main polymerization step is the hindrance of particle-particle coalescence during film formation. If the crosslinking occurs during the main polymerization step, a highly crosslinked structure is formed inside each polymer particle, which provides no chance to chains for diffusion during film formation. This is how weak films, with low cohesive strength, can be obtained from highly crosslinked polymers.

However, if crosslinking occurs after or during polymer diffusion, a strong film can be prepared. Geurts et al. found this problem for polymer particles containing epoxy moieties, when they tried to crosslink them with diamines. As the initial polymer particles already had a high gel content, the reaction between epoxy groups and diamines was not favored.[93] In fact, in order to quantify the relative rates of both processes, i.e. diffusion and crosslinking, a parameter has been proposed, as the ratio between the characteristic time for polymer chain diffusion (t_{diff}) and the time required to observe one crosslink reaction per chain in the system (t_{rxn}); $\alpha = t_{diff} / t_{rxn}$.[94] If α is very high (very little time needed to produce crosslinking compared to the time needed for

diffusion), the film will be weak, while if diffusion is fast enough so that crosslinking reactions can occur between polymer chains from neighboring particles ($\alpha << 1$), the film will be much stronger. In this sense, Winnik et al. proved for melamine crosslinked latex that diffusion increased more rapidly with temperature than crosslinking reactions, and as a result, α was decreased for higher curing temperatures.[95] When both interdiffusion and crosslinking rates are comparable to each other, there is the possibility that crosslinking occurs at the interface and restricts the interdiffusion between the polymer particles. In order to investigate the polymer interdiffusion, three methods are commonly used. Two method use fluorescence technique i.e., Fluorescence Resonance Energy Transfer (FRET) and Pyrene Excimer Fluorescence (PEF) [35], while the third method is Small Angle Neutron Scattering (SANS).[33,96]

SANS experiment is based on the difference of the neutron scattering between hydrogen and deuterium. Therefore, a small fraction of deuterium is used for labelling the polymeric dispersions. Before the interdiffusion happens, the labelling agent (deuterium) has a certain radius of gyration (Rg), which increases after diffusion when the film is formed. Therefore, the scattering of neutrons can be used to quantify the diffusion of polymer chains.[97] In the case of FRET, analogous polymer particles containing donor dyes or acceptor dyes are initially synthesized, and then blended. When the film starts to form, and interdiffusion between donor labelled and acceptor labelled particles starts to occur, an energy transfer is produced from donor to acceptor monomer. As the polymer particles diffusion progresses, the extent of energy transfer further increases and as a result, there is a clear effect on the fluorescence profile decay. Therefore, the interdiffusion can be calculated by following the evolution of fluorescence decay of the donor dye.[34,98] In comparison to FRET, PEF is a relatively new fluorescence method to measure the interdiffusion. It is based on the fact that excited molecules emit light at different wavelengths if they are isolated or in close contact, forming an excimer.[99] Pyrene is the most

often used labelling molecule in this technique because it can be excited by UV-light.[100] Therefore, two latexes are prepared, one containing labelled monomer and another without it. Once both latexes are blended, the fluorescence spectrum of the blend contains two peak areas, one corresponding to the excited pyrene monomer and the second one corresponding to the excimer (due to a region with high pyrene concentration). When the latex blend film starts to dry, the local concentration of pyrene decreases as it interdiffuses to neighbouring polymer particles free of pyrene, and as a result the fluorescence coming from the excimer decreases. The diffusion speed of the polymer can be deduced by calculating the excimer/ monomer ratio. [99,101]

On the other hand, in order to measure the crosslinking rate, the improvement on the strength of the film and the decrease of the flow behavior of final polymer can be followed. When we consider the rheological behavior in viscoelastic polymers, the storage modulus E' stores the elastic portion and loss modulus E" characterizes the viscous portion of polymers. The flow is affected by molecular motion. Therefore, when crosslinking increases in the polymer system, the elasticity in the material will increase (E'>E") due to the formation of crosslinked joints, and the flow behavior of polymer will decrease.[102] When covalent crosslinks are formed the free volume is reduced and T_G will also increase. Furthermore, the chemical structural changes occurring as a consequence of crosslinking can also be followed by the NMR or FTIR.

1.7. Objective and outline of the thesis

The position of the functional group in the dispersion classifies the crosslinking system into two classes. In the first class, the polymer particles are crosslinked with water soluble or dispersable crosslinkers (2K systems). The high reactivity of the functional group can produce

premature crosslinking in the wet state and decrease the shelf life in this case. Therefore, both components can only be mixed just before application in epoxy/amine [93], melamine/formadehyde [103], hydroxyl/isocyanate [104,105] acetoacetoxy/amine[90], and carboxyl/amine[106] systems. The second type of crosslinking systems is a one pack system (1K). In this class, self-curing dispersions are prepared by using both functional groups in the same dispersion, being alkoxy silane[107] and Upy containing functional particles[107] examples of this crosslinking type. In this PhD, the first type of crosslinking system (2K) will be studied.

Due to concerns with CLP labelling and REACH, low molecular weight crosslinkers dissolved or dispersed in water are under scrutiny. One alternative would be to go to a non-oligomeric two-component system. In this case, the functional groups would be attached to two different, higher molecular weight, polymer particles. Therefore, the approach not only fulfils environmental restriction but also would enhance the shelf life of the system by preparing a second set of polymer particles that stop the reaction by ionic or steric repulsion.

In this PhD, the acetoacetoxy based crosslinking chemistry has been studied, functionalizing the polymer particles with acetoacetoxy ethyl methacrylate (AAEMA). These particles have also served as the base to produce amine functionalized particles. Therefore, the films produced by mixing acetoacetoxy functionalized polymer particles and amino functionalized particles have been studied. The chemical crosslinking between AAEMA and amines has been studied previously in the literature, [90,108] but most of the times, just the solution reactions has been studied. Very limited studies have been reported to follow the crosslinking reaction after the incorporation of these functional monomers in latex particles.[74] Therefore, in this PhD the kinetics of the crosslinking chemistry between AAEMA functionalized polymer particles and amines functionalized polymer particles in two pack waterborne latexes have been studied,

together with the effect it has on interdiffusion of polymer chains and on the final properties of the produced films. The thesis has the following structure.

Chapter 2 is devoted to study the crosslinking kinetics between acetoacetoxy ethylmethacrylate (AAEMA) functionalized particles and hexamethylenediamine functionalized polymer particles. The effect of temperature and time on the crosslinking reaction between these moieties will be discussed, together with the properties of the resulting crosslinked films.

In **Chapter 3** the amine functionality was changed from linear hexamethylenediamine to multifunctional polyethyleneimine (PEI). This chapter presents the kinetic study of the crosslinking between AAEMA based polymer particles and PEI based polymer particles and the interdiffusion study between polymer particles (by FRET and PEF).

In **Chapter 4** the crosslinking chemistry between AAEMA based functionality and PEI based functionality has been further investigated by preparing systems with different main monomer composition, with different particles size and with different T_G polymers. The properties of the produced films and the comparison with the films prepared in the previous Chapter, are also shown.

The work presented in **Chapter 5** was carried out in BASF SE (Ludwigshafen, Germany) under the supervision of Dr. Nico Velling. In this chapter, the incorporation of the polymer resin into a paint formulation was studied. The potential benefits of the incorporation of a crosslinkable polymer resin into paint were analyzed by studying the film formation, hardness development, chemical resistance and blocking performance.

Finally, in **Chapter 6** the most relevant conclusions of the thesis are summarized.

1.8. References

[1] K.D. Weiss, Paint and coatings: A mature industry in transition, Prog. Polym. Sci. 22 (1997) 203–245. https://doi.org/10.1016/S0079-6700(96)00019-6.

[2] J.L. Adgate, L.E. Eberly, C. Stroebel, E.D. Pellizzari, K. Sexton, Personal, Indoor, and Outdoor VOC Exposures in a Probability Sample of Children, J. Expo. Sci. Environ. Epidemiol. 2004 141. 14 (2004) S4–S13. https://doi.org/10.1038/sj.jea.7500353.

[3] J. Sherman, B. Chin, P.D.T. Huibers, R. Garcia-Valls, T.A. Hatton, Solvent replacement for green processing, Environ. Health Perspect.106 (1998) 253–271. https://doi.org/10.1289/EHP.98106S1253.

[4] R.A. Webster.D.C. Ryntz, Handbook of Industrial Chemistry and Biotechnology, 13th ed., Springer International Publishing, 2017. https://doi.org/10.1007/978-3-319-52287-6.

[5] European Commission, Screening study to identify reductions in VOC emissions due to the restrictions in the VOC content of products, 2002.

[6] European Commission, Report on the implementation and review of Directive 2004/42/EC of the European Parliament and of the Council on the limitation of emissions of volatile organic compounds due to the use of organic solvents in certain paints and varnishes and vehicle refin, 2011.

[7] R. Joseph, High-Solids, Low-VOC, Solvent-Based Coatings, Met. Finish. 97 (1999) 117–126. https://doi.org/10.1016/S0026-0576(99)80769-7.

[8] Z. Zhu, R. Li, C. Zhang, S. Gong, Preparation and properties of high solid content and low viscositywaterborne polyurethane-acrylate emulsion with a reactive emulsifier, Polymers (Basel). 10 (2018) 154. https://doi.org/10.3390/polym10020154.

[9] Z. Ai, R. Deng, Q. Zhou, S. Liao, H. Zhang, High solid content latex: Preparation methods and application, Adv. Colloid Interface Sci. 159 (2010) 45–59. https://doi.org/10.1016/J.CIS.2010.05.003.

[10] I. de F.A. Mariz, J.R. Leiza, J.C. De la Cal, Competitive particle growth: A tool to control the particle size distribution for the synthesis of high solids content low viscosity latexes, Chem. Eng. J. 168 (2011) 938–946. https://doi.org/10.1016/J.CEJ.2011.02.023.

[11] I. de F.A. Mariz, I.S. Millichamp, J.C. de la Cal, J.R. Leiza, High performance water-borne paints with high volume solids based on bimodal latexes, Prog. Org. Coatings. 68 (2010) 225–233. https://doi.org/10.1016/J.PORGCOAT.2010.01.008.

[12] S.H. Moayed, S. Fatemi, S. Pourmahdian, Synthesis of a latex with bimodal particle size distribution for coating applications using acrylic monomers, Prog. Org. Coatings. 60 (2007) 312–319. https://doi.org/10.1016/J.PORGCOAT.2007.07.023.

[13] J.M. Asua, Polymer Reaction Engineering, 1st ed., John Wiley and Sons, 2008. https://doi.org/10.1002/9780470692134.

[14] J.M. Asua, Emulsion polymerization: From fundamental mechanisms to process developments, J. Polym. Sci. Part A Polym. Chem. 42 (2004) 1025–1041. https://doi.org/10.1002/pola.11096.

[15] A. Penlidis, S.R. Ponnuswamy, C. Kiparissides, K.F. O'Driscoll, Polymer reaction engineering: Modelling considerations for control studies, Chem. Eng. J. 50 (1992) 95–107. https://doi.org/10.1016/0300-9467(92)80013-Z.

[16] S.C. Thickett, R.G. Gilbert, Emulsion polymerization: State of the art in kinetics and mechanisms, Polymer (Guildf). 48 (2007) 6965–6991. https://doi.org/10.1016/J.POLYMER.2007.09.031.

[17] W. V. Smith, R.H. Ewart, Kinetics of Emulsion Polymerization, J. Chem. Phys. 16 (2004) 592. https://doi.org/10.1063/1.1746951.

[18] W.D. Harkins, A General Theory of the Mechanism of Emulsion Polymerization, J. Am. Chem. Soc. 69 (1947) 1428–1444. https://doi.org/10.1021/ja01198a053.

[19] W.J. Priest, Particle growth in the aqueous polymerization of vinyl acetate, J. Phys. Chem. 56 (1952) 1077–1082. https://doi.org/10.1021/j150501a010.

[20] I.A. Maxwell, B.R. Morrison, D.H. Napper, R.G. Gilbert, Entry of free radicals into latex particles in emulsion polymerization, Macromolecules. 24 (2002) 1629–1640. https://doi.org/10.1021/MA00007A028.

[21] J.W. Vanderhoff, E.B. Bradford, W.K. Carrington, Transport of water through latex films., J Polym Sci, Part C, Polym Symp. 41 (1973) 155–174. https://doi.org/10.1002/polc.5070410116.

[22] P.A. Steward, J. Hearn, M.C. Wilkinson, Overview of polymer latex film formation and properties, Adv. Colloid Interface Sci. 86 (2000) 195–267. https://doi.org/10.1016/S0001-8686(99)00037-8.

[23] J.L. Keddie, Film formation of latex, Mater. Sci. Eng. R Reports. 21 (1997) 101–170. https://doi.org/10.1016/S0927-796X(97)00011-9.

[24] S.G. Croll, Drying of latex paint, J. Coatings Technol. 58 (1984) 41–49.

[25] D.P. Sheetz, Formation of films by drying of latex, J. Appl. Polym. Sci. 9 (1965) 3759–3773. https://doi.org/10.1002/app.1965.070091123.

[26] J. Keddie, A.F. Routh, Fundamentals of Latex Film Formation, Springer Netherlands, 2010.

[27] A.F. Routh, W.B. Russel, Horizontal drying fronts during solvent evaporation from latex films, AIChE J. 44 (1998) 2088–2098. https://doi.org/10.1002/AIC.690440916.

[28] J. Mallégol, G. Bennett, P.J. McDonald, J.L. Keddie, O. Dupont, Skin development during the film formation of waterborne acrylic pressure-sensitive adhesives containing tackifying resin, J. Adhes. 82 (2006) 217–238. https://doi.org/10.1080/00218460600646461.

[29] M. Ma, K. Jiang, G. Qiu, D. Wang, X. Hu, X. Jin, Z.G. Chen, Fundamental study on electro-reduction of solid titania in molten calcium chloride, J. Rare Earths. 23 (2005) 46–49. https://doi.org/10.1016/j.porgcoat.2004.07.023.

[30] F. Dobler, M. Lambla, Y. Holl, Coalescence mechanisms of polymer colloids, in: Trends Colloid Interface Sci. VII, Steinkopff, 2008: pp. 51–52. https://doi.org/10.1007/bfb0118471.

[31] A.F. Routh, W.B. Russel, Deformation mechanisms during latex film formation: Experimental evidence, Ind. Eng. Chem. Res. 40 (2001) 4302–4308. https://doi.org/10.1021/ie001070h.

[32] G.L. Brown, Formation of films from polymer dispersions, J. Polym. Sci. 22 (1956) 423–434. https://doi.org/10.1002/pol.1956.1202210208.

[33] G.D. Wignall, A. Klein, G.A. Miller, L.H. Sperling, Film Formation from Latex: Hindered Initial Interdiffusion of Constrained Polystyrene Chains Characterized by Small-Angle Neutron Scattering, J. Macromol. Sci. Part B. 27 (1988) 217–231. https://doi.org/10.1080/00222348808245763.

[34] Y. Wang, M.A. Winnik, Polymer diffusion across interfaces in latex films, J. Phys. Chem. 97 (1993) 2507–2515. https://doi.org/10.1021/j100113a008.

[35] E.M. Boczar, B.C. Dionne, Z. Fu, A.B. Kirk, P.M. Lesko, A.D. Koller, Spectroscopic Studies of Polymer Interdiffusion during Film Formation, Macromolecules. 26 (1993) 5772–5781. https://doi.org/10.1021/ma00073a035.

[36] S.T. Eckersley, A. Rudin, The film formation of acrylic latexes: A comprehensive model of film coalescence, J. Appl. Polym. Sci. 53 (1994) 1139–1147. https://doi.org/10.1002/app.1994.070530902.

[37] D.P. Jensen, L.W. Morgan, Particle size as it relates to the minimum film formation temperature of latices, J. Appl. Polym. Sci. 42 (1991) 2845–2849. https://doi.org/10.1002/app.1991.070421024.

[38] S. Piçarra, A. Fidalgo, A. Fedorov, J.M.G. Martinho, J.P.S. Farinha, Smart Polymer Nanoparticles for High-Performance Water-Borne Coatings, Langmuir. 30 (2014) 12345–12353. https://doi.org/10.1021/la502826r.

[39] J. V. Barbosa, J. Moniz, A. Mendes, F.D. Magalhães, M.M.S.M. Bastos, Incorporation of an acrylic fatty acid derivative as comonomer for oxidative cure in acrylic latex, J. Coatings Technol. Res. 11 (2014) 765–773. https://doi.org/10.1007/S11998-014-9582-Y.

[40] M. Lahtinen, E. Glad, S. Koskimies, F. Sundholm, K. Rissanen, Synthesis of novel reactive coalescing agents and their application in a latex coating, J. Appl. Polym. Sci. 87 (2003) 610–615. https://doi.org/10.1002/app.11336.

[41] Y. Liu, W. Schroeder, M. Soleimani, W. Lau, M.A. Winnik, Effect of hyperbranched poly(butyl methacrylate) on polymer diffusion in poly(butyl acrylate- co -methyl methacrylate) latex films, Macromolecules. 43 (2010) 6438–6449.

[42] J.G. Tsavalas, D.C. Sundberg, Hydroplasticization of polymers: Model predictions and application to emulsion polymers, Langmuir. 26 (2010) 6960–6966.

[43] S.M. Dron, M. Paulis, Tracking Hydroplasticization by DSC: Movement of Water Domains Bound to Poly(Meth)Acrylates during Latex Film Formation, Polymers (Basel). 12 (2020) 2500. https://doi.org/10.3390/POLYM12112500.

[44] S.M. Dron, S.J. Bohorquez, D. Mestach, M. Paulis, Reducing the amount of coalescing aid in high performance waterborne polymeric coatings, Eur. Polym. J. 170 (2022) 111175. https://doi.org/10.1016/J.EURPOLYMJ.2022.111175.

[45] S.T. Eckersley, B.J. Helmer, Mechanistic considerations of particle size effects on film properties of hard/soft latex blends, J. Coatings Technol. 69 (1997) 97–107. https://doi.org/10.1007/BF02696096.

[46] A. Tzitzinou, J.L. Keddie, J.M. Geurts, A.C.I.A. Peters, R. Satguru, Film Formation of Latex Blends with Bimodal Particle Size Distributions: Consideration of Particle Deformability and Continuity of the Dispersed Phase, Macromolecules. 33 (2000) 2695–2708. https://doi.org/10.1021/MA991372Z.

[47] Ş. Uğur, S. Sunay, Ö. Pekcan, Film formation of nano-sized hard latex (PS) in soft polymer matrix (PBA): An excimer study, Polym. Compos. 31 (2010) 1611–1619. https://doi.org/10.1002/PC.20950.

[48] D. Colombini, H. Hassander, O.J. Karlsson, F.H.J. Maurer, Influence of the Particle Size and Particle Size Ratio on the Morphology and Viscoelastic Properties of Bimodal Hard/Soft Latex Blends, Macromolecules. 37 (2004) 6865–6873. https://doi.org/10.1021/MA030455J.

[49] D.C. Sundberg, A.P. Casassa, J. Pantazopoulos, M.R. Muscato, B. Kronberg, J. Berg, Morphology development of polymeric microparticles in aqueous dispersions. I. Thermodynamic considerations, J. Appl. Polym. Sci. 41 (1990) 1425–1442. https://doi.org/10.1002/APP.1990.070410706.

[50] E. Limousin, N. Ballard, J.M. Asua, Soft core–hard shell latex particles for mechanically strong VOC-free polymer films, J. Appl. Polym. Sci. 136 (2019) 47608. https://doi.org/10.1002/APP.47608.

[51] J. Feng, M.A. Winnik, R.R. Shivers, B. Clubb, Polymer Blend Latex Films: Morphology and Transparency, Macromolecules. 28 (1995) 7671–7682. https://doi.org/10.1021/MA00127A013/ASSET/MA00127A013.FP.PNG_V03.

[52] J. Feng, E. Odrobina, M.A. Winnik, Effect of Hard Polymer Filler Particles on Polymer Diffusion in a Low-Tg Latex Film, Macromolecules. 31 (1998) 5290–5299. https://doi.org/10.1021/MA980117W.

[53] D. Juhué, J. Lang, Film Formation from Dispersion of Core-Shell Latex Particles, Macromolecules. 28 (1995) 1306–1308. https://doi.org/10.1021/MA00108A070/ASSET/MA00108A070.FP.PNG_V03.

[54] K. Price, W. Wu, K. Wood, S. Kong, A. McCormick, L. Francis, Stress development and film formation in multiphase composite latexes, J. Coatings Technol. Res. 11 (2014) 827–839. https://doi.org/10.1007/S11998-014-9606-7.

[55] J. Geurts, J. Bouman, A. Overbeek, New waterborne acrylic binders for zero VOC paints, J. Coatings Technol. Res. 5 (2008) 57–63. https://doi.org/10.1007/S11998-007-9036-X.

[56] J.R. Rogers, Coating composition comprising a terpolymer, an alkali soluble resin, and a zirconyl-fugitive ligand compound. US3320196A, 2006.

[57] S. Tungchaiwattana, R. Groves, P.A. Lovell, O. Pinprayoon, B.R. Saunders, Tuning the mechanical properties of nanostructured ionomer films by controlling the extents of covalent crosslinking in core-shell nanoparticles, J. Mater. Chem. 22 (2012) 5840–5847. https://doi.org/10.1039/C2JM16223G.

[58] M. Argaiz, F. Ruipérez, M. Aguirre, R. Tomovska, Ionic Inter-Particle Complexation Effect on the Performance of Waterborne Coatings, Polym. 13 (2021) 3098. https://doi.org/10.3390/POLYM13183098.

[59] M.S. Musa, A.H. Milani, P. Shaw, G. Simpson, P.A. Lovell, E. Eaves, N. Hodson, B.R. Saunders, Tuning the modulus of nanostructured ionomer films of core–shell nanoparticles based on poly(n-butyl acrylate), Soft Matter. 12 (2016) 8112–8123. https://doi.org/10.1039/C6SM01563H.

[60] L. Voorhaar, R. Hoogenboom, Supramolecular polymer networks: hydrogels and bulk materials, Chem. Soc. Rev. 45 (2016) 4013–4031. https://doi.org/10.1039/C6CS00130K.

[61] T.P. Huynh, P. Sonar, H. Haick, Advanced Materials for Use in Soft Self-Healing Devices, Adv. Mater. 29 (2017) 1604973. https://doi.org/10.1002/adma.201604973.

[62] K.J. Lee, Y.W. Kim, J.H. Koh, J.H. Kim, Supramolecular polymer/metal salt complexes containing quadruple hydrogen bonding units, J. Polym. Sci. Part B Polym. Phys. 45 (2007) 3181–3188. https://doi.org/10.1002/POLB.21316.

[63] L.S. Shimizu, Perspectives on main-chain hydrogen bonded supramolecular polymers, Polym. Int. 56 (2007) 444–452. https://doi.org/10.1002/PI.2198.

[64] F.E. Bailey, R.D. Lundberg, R.W. Callard, Some factors affecting the molecular association of poly(ethylene oxide) and poly(acrylic acid) in aqueous solution, J. Polym. Sci. Part A Gen. Pap. 2 (1964) 845–851. https://doi.org/10.1002/POL.1964.100020221.

[65] N. Jiménez, N. Ballard, J.M. Asua, Hydrogen Bond-Directed Formation of Stiff Polymer Films Using Naturally Occurring Polyphenols, Macromolecules. 52 (2019) 9724–9734. https://doi.org/10.1021/acs.macromol.9b01694.

[66] G.B. Kauffman, Charles Goodyear (1800-1860), American Inventor, on the Bicentennial of His Birth, Chem. Educ. 6 (2001) 50–54. https://doi.org/10.1007/s00897000443a.

[67] M. Luther, C. Heuck, Products of Latex Character and a Process for Producing the Same. US1864078A, 1932.

[68] J.W. Taylor, M.A. Winnik, Functional latex and thermoset latex films, J. Coatings Technol. Res. 1 (2004) 163–190. https://doi.org/10.1007/s11998-004-0011-5.

[69] C.A. Córdoba, L.I. Ronco, M.C.G. Passeggi, R.J. Minari, L.M. Gugliotta, Waterborne acrylic-melamine latexes with controlled film microstructure, Prog. Org. Coatings. 136 (2019). https://doi.org/10.1016/j.porgcoat.2019.105239.

[70] D.J. Merline, S. Vukusic, A.A. Abdala, Melamine formaldehyde: Curing studies and reaction mechanism, Polym. J. 45 (2013) 413–419. https://doi.org/10.1038/PJ.2012.162.

[71] M.H. Fischer, The toxic effects of formaldehyde and formalin, J. Exp. Med. 6 (1905) 487–518. https://doi.org/10.1084/jem.6.4-6.487.

[72] R.. Roesler, K. Danielmeier, Tris-3-(1-aziridino)propionates and their use in formulated products, Prog. Org. Coatings. 50 (2004) 1–27. https://doi.org/10.1016/J.PORGCOAT.2003.09.004.

[73] J.K. Mistry, M.R. Van De Mark, Aziridine cure of acrylic colloidal unimolecular polymers (CUPs), J. Coatings Technol. Res. 10 (2013) 453–463. https://doi.org/10.1007/S11998-013-9489-Z.

[74] I. Dahlquist, S. Freigert, L. Truison, Contact allergy to trimethylolpropane triacrylate (TMPTA) in an aziridine plastic hardener, Contact Dermatitis. 9 (1983) 122–124. https://doi.org/10.1111/j.1600-0536.1983.tb04317.x.

[75] H.H. Pham, J.P.S. Farinha, M.A. Winnik, Cross-linking, miscibility, and interface structure in blends of poly(2-ethylhexyl methacrylate) copolymers. An energy transfer study, Macromolecules. 33 (2000) 5850–5862. https://doi.org/10.1021/ma991832o.

[76] H.H. Pham, M.A. Winnik, Polymer interdiffusion vs cross-linking in carboxylic acid-carbodiimide latex films. Effect of annealing temperature, reactive group concentration, and carbodiimide substituent, Macromolecules. 39 (2006) 1425–1435.

[77] M. Okubo, Y. Nakamura, T. Matsumoto, Studies on suspension and emulsion. XXXV. Effect of epoxy groups at the surface layer of ethyl acrylate–glycidyl methacrylate copolymer emulsion particles on its crosslinking reactivity, J. Polym. Sci. Polym. Chem. Ed. 18 (1980) 2451–2459. https://doi.org/10.1002/pol.1980.170180804.

[78] S. Magnet, J. Guillot, A. Guyot, C. Pichot, Crosslinking ability of styrene—butyl acrylate copolymer latices functionalized with glycidyl methacrylate, Prog. Org. Coatings. 20 (1992) 73–80. https://doi.org/10.1016/0033-0655(92)85005-G.

[79] H.C. Tillson, Coating composition comprising a terpolymer of an alkyl acrylate, an alkyl methacrylate and an ester of a beta,gamma-unsaturated alcohol with methacrylic acid. US3219610A, 1961.

[80] J.W. Taylor, M.J. Collins, M.D. Clark, Waterborne polymers having pendant allyl groups. EP0820478B1, 1996.

[81] I. González, Waterborne acrylic latex for direct to metal coatings: from process conditions to final product. PhD, University of Basque Country, 2006.

[82] M. Ooka, H. Ozawa, Recent developments in crosslinking technology for coating resins, Prog. Org. Coatings. 23 (1994) 325–338. https://doi.org/10.1016/0033-0655(94)87002-0.

[83] K. Beshah, W. Devonport, A study of acetoacetoxyethyl methacrylate hydrolysis in acrylic latex polymers as a function of pH, J. Coatings Technol. Res. 10 (2013) 821–828. https://doi.org/10.1007/s11998-013-9512-4.

[84] A. Noomen, The chemistry and physics of low-emission coatings. Part 2. Waterborne two-pack coatings, Prog. Org. Coatings. 17 (1989) 27–39. https://doi.org/10.1016/0033-0655(89)80011-1.

[85] P.J.A. Geurink, L. Van Dalen, L.G.J. Van Der Ven, R.R. Lamping, Analytical aspects and film properties of two-pack acetoacetate functional latexes, Prog. Org. Coatings. 27 (1996) 73–78. https://doi.org/10.1016/0300-9440(95)00522-6.

[86] Bartman, Acetoacetate functionalized polymers and monomers useful for crosslinking formulations. US 4408018 A, 1982.

[87] D.A. Bors, W.D. Emmons, S.S. Edwards, Method for light-assisted curing of coatings. US5296530A, 1996.

[88] T. James Wayne Taylor, Kingsport, Functional latexes resistant to hydrolysis. US5962556A, 1997.

[89] D.A. Bors, A.C. Lavoie, W.D. Emmons, Air curing polymer composition. US5484849A, 1996.

[90] J. Feng, H. Pham, P. Macdonald, M.A. Winnik, J.M. Geurts, H. Zirkzee, S. Van Es, A.L. German, Formation and crosslinking of latex films through the reaction of acetoacetoxy groups with diamines under ambient conditions, J. Coatings Technol. 70 (1998) 57–68. https://doi.org/10.1007/BF02730151.

[91] M.J. Collins, J.W. Taylor, Stable amino-containing polymer latex blends. US5998543., 1997.

[92] G. Tillet, B. Boutevin, B. Ameduri, Chemical reactions of polymer crosslinking and post-crosslinking at room and medium temperature, Prog. Polym. Sci. 36 (2011) 191–217. https://doi.org/10.1016/j.progpolymsci.2010.08.003.

[93] J.M. Geurts, J.J.G.S. Van Es, A.L. German, Latexes with intrinsic crosslink activity, Prog. Org. Coatings. 29 (1996) 107–115. https://doi.org/10.1016/S0300-9440(96)00623-6.

[94] A. Aradian, E. Raphaël, P.G. De Gennes, Strengthening of a polymer interface: interdiffusion and cross-linking, Macromolecules. 33 (2000) 9444–9451. https://doi.org/10.1021/ma0010581.

[95] M.A. Winnik, Interdiffusion and crosslinking in thermoset latex films, J. Coatings

Technol. 74 (2002) 49–63. https://doi.org/10.1007/bf02720150.

[96] K. Hahn, G. Ley, H. Schuller, R. Oberthür, On particle coalescence in latex films, Colloid Polym. Sci. 264 (1986) 1092–1096. https://doi.org/10.1007/BF01410329.

[97] E. Odrobina, M.A. Winnik, Influence of Entanglements on the Time Dependence of Mixing in Nonradiative Energy Transfer Studies of Polymer Diffusion in Latex Films, Macromolecules. 34 (2001) 6029–6038. https://doi.org/10.1021/MA0014618.

[98] Y.S. Liu, J. Feng, M.A. Winnik, Study of polymer diffusion across the interface in latex films through direct energy transfer experiments, J. Chem. Phys. 101 (1998) 9096. https://doi.org/10.1063/1.468488.

[99] R. Casier, M. Gauthier, J. Duhamel, Using Pyrene Excimer Fluorescence To Probe Polymer Diffusion in Latex Films, Macromolecules. 50 (2017) 1635–1644. https://doi.org/10.1021/ACS.MACROMOL.6B02726.

[100] S. Farhangi, J. Duhamel, Probing Side Chain Dynamics of Branched Macromolecules by Pyrene Excimer Fluorescence, Macromolecules. 49 (2015) 353–361. https://doi.org/10.1021/ACS.MACROMOL.5B02476.

[101] G.P.C. Drummen, Fluorescent probes and fluorescence (microscopy) techniques-illuminating biological and biomedical research, Molecules. 17 (2012) 14067–14090. https://doi.org/10.3390/molecules171214067.

[102] J. Lu, A.J. Easteal, N.R. Edmonds, Crosslinkable poly(vinyl acetate) emulsions for wood adhesive, Pigment & Resin Technol. 40 (2011) 161–168. https://doi.org/10.1108/03699421111130423.

[103] X. Liu, C. Zhang, T. Xiong, D. Chen, A. Zhong, Rheological and curing behavior of aqueous ambient self-crosslinkable polyacrylate emulsion, J. Appl. Polym. Sci. 106 (2007) 1448–1455. https://doi.org/10.1002/APP.25534.

[104] J.W. Taylor, S.L. Renner, Isocyanate crosslinked waterborne coatings. US 6,646,091, 2003.

[105] T. Nabuurs, W.J. Soer, R. Peters, Isocyanate crosslinking in two-component waterborne coatings, Polym. Int. 68 (2019) 856–861. https://doi.org/10.1002/PI.5681.

[106] W.T. Brown, Effect of crosslinker reaction rate on film properties for thermoset coatings, J. Coatings Technol. 72 (2000) 63–70. https://doi.org/10.1007/bf02698021.

[107] S. Parvate, P. Mahanwar, Advances in self-crosslinking of acrylic emulsion: what we know and what we would like to know, J. Dispers. Sci. Technol. 40 (2019) 519–536. https://doi.org/10.1080/01932691.2018.1472012.

[108] A. Mori, T. Kitayama, M. Takatani, T. Okamoto, A honeymoon-type adhesive for wood products based on acetoacetylated poly(vinyl alcohol) and diamines: Effect of diamines and degree of acetoacetylation, J. Appl. Polym. Sci. 91 (2004) 2966–2972. https://doi.org/10.1002/app.13491.

Chapter 2.

Crosslinking kinetics in acetoacetoxy - diamine based waterborne system.

2.1. Introduction

As it has been mentioned in the Introduction, waterborne polymeric binders, latexes, represent a more environmentally friendly alternative than their solventborne counterparts do. However, the process to obtain a solid film from a solution of polymer chains differs significantly from the process needed to form a film from a dispersion of polymer particles in water. Therefore, the film formation process of waterborne latexes requires polymers with T_G below the application temperature, in order to be soft enough to favour the coalescence and interdiffusion between polymer particles.[1] However, low T_G polymers will produce soft films that may not be efficient for coating applications. Such film forming paradox of waterborne latexes has been overcome in different ways as explained in the previous chapter, being interparticle crosslinking during film formation, one of the methods employed to obtain hard and resistant films from waterborne latexes.[2] Among the different chemistries used in these crosslinking reactions, the reaction between acetoacetoxy and amine moieties has attracted much attention, since the first reports in late 80's.[3,4]

The most used monomer to provide the acetoacetoxy functionality is acetoacetoxy ethyl methacrylate (AAEMA), as it has a methacrylate moiety that can easily react by radical polymerization and an acetoacetoxy moiety that can give crosslinking reactions with various functional groups such as diamines or isocyanates.[5,2] Such crosslinking reactions provide films with improved mechanical strength, chemical resistance and durability.[6-8] Furthermore, it is claimed that one of the main benefits of the crosslinking reaction between acetoacetoxy moieties and diamines, is their occurrence at room temperature.[8-13] This statement seems to be true for monomeric AAEMA and diamines dissolved in tetrahydrofurane (THF).[12] However, when AAEMA is attached to a polymer chain and the diamine moiety is either dissolved in the continuous phase or attached to another polymer chain, things start to change. On one hand, some authors have admitted that it is not easy to follow the crosslinking reaction between both moieties by NMR or FTIR, and they have used model systems at higher concentrations or in solution to mimic the reaction.[10,8] In these situations, the mobility of both reactants is favoured, and they cannot fully describe the crosslinking reaction rate in a film being formed from a waterborne latex. In fact, Geurts *et al.* [14] suggested for a similar crosslinking reaction between polymeric epoxy and hexamethylenediamine (HDMA) moieties, during the film formation from a solution polymer, that the crosslinking was fast as long as the solvent was present and the polymer was movable due to plasticization. However, the crosslinking rate decreased significantly when the solvent was evaporated and the polymer became rigid due a T_G higher that room temperature. They saw that the problem was decreased when a lower T_G polymer was used from solution, and it increased for waterborne polymers, where no solvent is present for the plasticization.

On the other hand, it has been reported that the acetoacetoxy moiety is not fully stable in water, and it is prone to suffer hydrolysis upon storage of the latex, mainly at low pH. Due to the

hydrolysis, hydroxyl methacrylate (HEMA) and beta keto acid are formed.[10,15] Therefore, the acetoacetoxy moiety is usually converted to the more stable enamine form by reaction with ammonia, and this enamine can then exchange with the diamine crosslinking agent. This exchange reaction has been seen to be an equilibrium reaction that is favoured towards the diamine crosslinking when the ammonia is released from the films. However, this release needs some high temperature to occur, as seen by Esser *et al.,*[10] who reported the need of three days annealing at 60 °C to fully eliminate the NH_3 and complete the crosslinking reaction. In any case, the kinetics of AAEMA based crosslinking with diamines in waterborne polymeric systems has not been explored in detail in the literature.

In order to analyse such kinetics, in this chapter, waterborne polymer particles containing AAEMA functional moieties and polymer particles containing amine functional moieties, prepared from HDMA, were synthesized and blended. First, the kinetics study of the crosslinking reaction was carried out in the films formed from such blends by FTIR spectroscopy and rheological measurements. Then, the effect of the crosslinking reactions was further investigated at different temperatures by mechanical and water absorption test. The results demonstrate the rate of crosslinking at room temperature may not be the desired one for industrial applications.

2.2. Experimental Part

2.2.1. Synthesis of MMA/BA/AAEMA latex

For the production of the latexes, a seeded semibatch emulsion polymerization procedure was used.[13] Table 2.1 presents the formulation used to prepare the seed by batch emulsion polymerization (all the materials have been included in Appendix I).

Table 2.1. Formulation of the seed produced by batch emulsion polymerization

Ingredients	Charge (g)
Methyl methacrylate	31.29
Butyl acrylate	31.34
Water	250.31
SLS	1.255
$NaHCO_3$	0.326
$K_2S_2O_8$	0.31

This seed was used to produce the final latexes by seeded emulsion polymerization with two feeding steps. We used 10 to 90 ratio of seed monomer to monomer used in the next two feeding stages. 42.78 g of seed were introduced in the reactor, where the first stage feeding (Table 2.2) was added at a feed rate of 0.442 g/min. Once the stage-1 feeding was completed, the second feeding was started to the same reactor. In the second stage of feeding, 31.5 g of extra water was added to maintain the solids content at 50% and a feeding rate of 0.23 g/min was used (see formulation in Table 2.2). AAEMA functional monomer was included in the recipe in this second feeding stage. We named this latex as component-0 (C-0).

Table 2.2. Formulation used in the two steps of growing of the seed by semibatch emulsion polymerization for the synthesis of MMA/BA/AAEMA latex

Ingredients	Feed (1) Growth of the seed (g)	Feed (2) Addition of functional monomer (g)
Methyl methacrylate	24.76	12.23
Butyl acrylate	24.51	12.15
Water	27.92	14.24
SLS	0.99	0.4915
Disponil A3065	1.34	0.662
Methacrylic Acid	0.467	0.20
$K_2S_2O_8$	0.2	0.1
Acetoacetoxy ethyl methacrylate (AAEMA)		4.4

Once C-0 latex was prepared, the emulsion was cooled and ammonium hydroxide (NH_4OH) (28%) was added in 5 min under continuous stirring. The NH_4OH was added in a mol ratio of 2:1 in NH_4OH: AAEMA. This way AAEMA functionalized and protected component-1 (C-1) latex was prepared. For the preparation of amine functionalized component-2 (C-2) latex, C-0 latex was reacted with HMDA instead of with ammonium hydroxide, in a 1:1 mol ratio between acetoacetoxy group and HMDA. From these two latexes, C-1 and C-2, a blend latex was prepared with equal weight ratio of both components by mechanical stirring at room temperature (Blend).

2.2.2. Latex and film characterization

The solids content of the seed and the latex was obtained gravimetrically, and it was used to analyse the evolution of the conversion during the polymerization reaction. The particle size of polymer particles was measured by Dynamic Light Scattering Spectroscopy, DLS (Malvern® Zetasier Nano). For the analysis, samples were diluted to such a low concentration that it can safely be assumed that no monomer was present in the polymer particles, namely that the unswollen particle sizes were measured. The gel content of the synthesized polymers was determined by soxhlet extraction of the dried latex film using tetrahydrofuran (THF) under reflux conditions for 24 h. The separated insoluble fraction recovered is considered gel and the ratio between its mass and the initial dried latex mass is the gel content.

In order to analyse the water absorption of the films, they were prepared from the casting of the latex or blends at room temperature and at 60 °C. Polymer films with thickness of 0.5 mm were prepared and then immersed in deionized high-purity water. For the analysis, the samples were weighted after different time intervals, and the relative weight increase to the initial film weight was calculated. Tensile tests of the films dried at room temperature and at 60 °C were

performed on Universal testing machine TA.HD plus Texture Analyser at a crosshead speed of 0.42 mm/s. Samples with approximate length of 3.55 mm and 0.55 mm of thickness were used. Dynamic Mechanical Thermal Analysis (DMTA) were carried out using a dynamic mechanical thermal analyser Triton 2000 DMA, Triton Technology Ltd with Single cantilever bending geometry. We investigated the rheological properties by calculating the E', E" and tan delta at 2°C heating rate/min. On the other hand, we performed time sweeps at 60 °C for 240 min for HMDA containing system. After the time sweep, another temperature sweep was carried out to compare with the initial sample.

For the kinetic analysis of the evolution of the crosslinking reaction, FTIR spectra were recorded using a Nicolet is-50 equipment. The spectra were registered with the resolution of 4 cm^{-1} with scan number 32. The samples were prepared by casting over CaF_2 support.

2.3. Results and discussion

Component-0 (C-0) latex was successfully obtained with a final solids content of 47 % and a conversion of 96 %, with an average particle size of 129 ± 1 nm. There was no significant change in the average particle size during the formation of component-1 (129 ± 1 nm), and neither by the formation of component-2 (130 ± 1 nm) or the Blend (131 ± 1 nm). The gel content of C-0 measured by Soxhlet extraction in THF was 54 %, while it increased to 78.5 % in the Blend dried at room temperature, and to 81.5 % in the Blend dried at 60 °C. From this result, it is clear that gel content is high in C-0, even in the absence of HMDA. The gel content of the latex containing AAEMA was likely due to the presence of divinyl species as impurities in the AAEMA.[13] Nevertheless, that gel content increased significantly in the Blend film dried at room temperature. As the HDMA is not soluble in THF, this increase of the gel, or fraction of polymer insoluble in THF, can be attributed to polymer chains linked to HDMA, apart from the pre-existing

gel. This insoluble amount is further increased when increasing the film annealing temperature to 60 °C, suggesting that more chains are linked to HDMA at this temperature, or that the crosslinking reaction between moieties of different particles has proceeded further.

2.3.1. FTIR characterization

In order to follow the chemical structural changes produced during the synthesis of C-1, C-2 and the Blend, a FTIR analysis of the films produced from the different latexes was carried out. Figure 2.1 presents the whole FTIR spectra of C-0, C-1, C-2 and Blend films dried at room temperature. There are two regions that present the most significative changes between the different samples: the region from 3000 cm^{-1} to 4000 cm^{-1}, named as N-H stretching region and the region from 1500 cm^{-1} to 1800 cm^{-1}, named as carbonyl stretching region. Both regions have been analysed separately for the formation of C-1 (Figure 2.3), C-2 (Figure 2.5) and Blend (Figure 2.6).

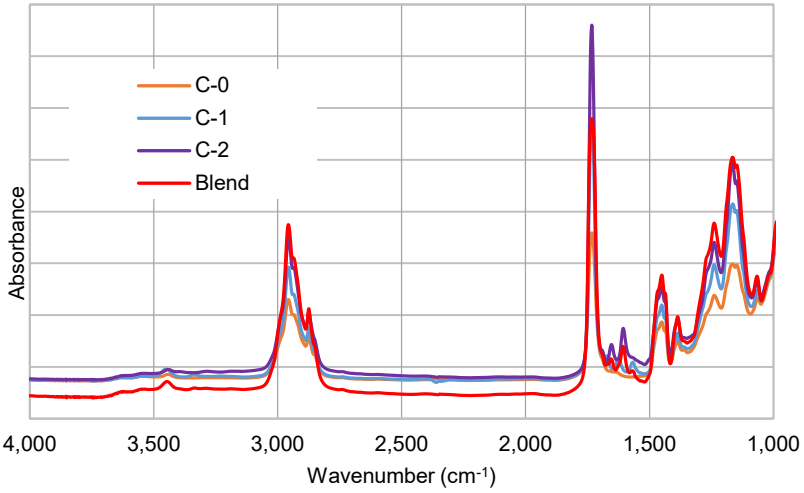

Figure 2.1. FTIR spectra of the pure components (C-0, C-1 and C-2) and Blend at RT (1 day drying) in HMDA based crosslinking chemistry.

During the formation of C-1, primary amines were formed as shown in Figure 2.2, deduced from the primary enamine stretching bands that appeared around 3336 cm^{-1} and 3430 cm^{-1} (overlapped with the carbonyl harmonic stretching) (Figure 2.3 a). In the carbonyl stretching region, three new bands appeared at 1670, 1624 and 1570 cm^{-1} related to carbonyl stretching of the primary enamines, C=C stretching and N-H bending as shown in Figure 2.3 (b). All these new absorptions confirmed the formation of the enamine when the latex C-0 reacted with ammonium hydroxide.

Figure 2.2. Scheme of reaction for the preparation of C-1 in HDMA based crosslinking system.

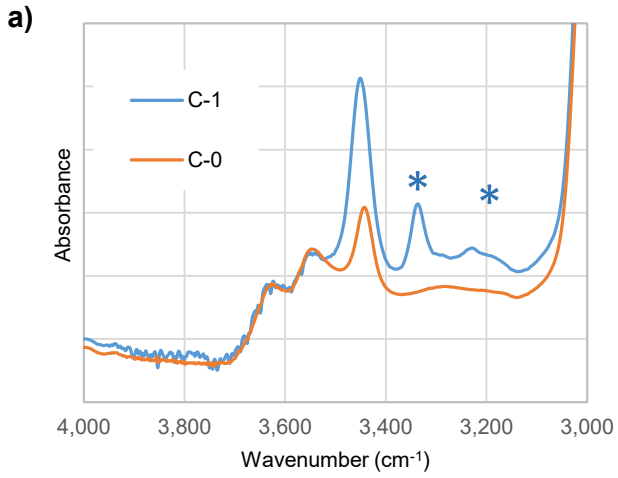

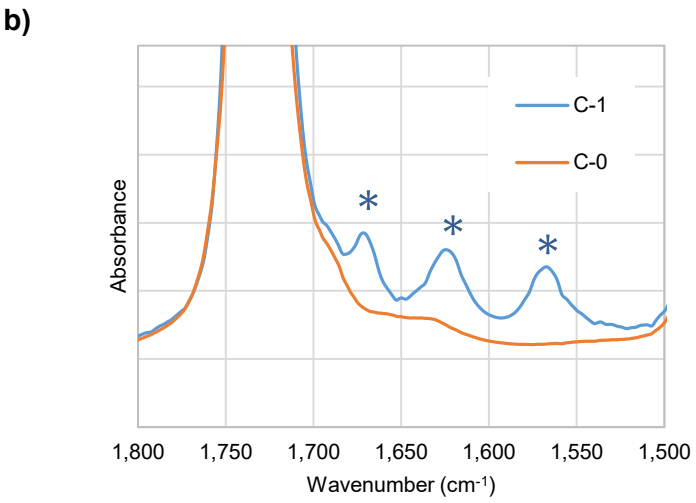

Figure 2.3. FTIR spectra of component-1 dried at RT for 1 day. Image (a) shows N-H stretching region and image (b) represents carbonyl stretching region.

During the formation of component-2 as presented in Figure 2.4, secondary enamines were formed. The signal of secondary enamine in N-H stretching region appeared around 3200 cm^{-1} while the signals corresponding to remaining primary amine stretching of HDMA appeared at 3395 and 3285 cm^{-1} (Figure 2.5 a). In case of carbonyl stretching region, three signals were observed related to carbonyl stretching (1690 cm^{-1}), C=C stretching + NH bending of the secondary enamine (1654 cm^{-1}) and NH_2 bending (1606 cm^{-1}) of the remaining HDMA (Figure 2.5 b). All these new absorptions were related to the formation of secondary enamine groups.

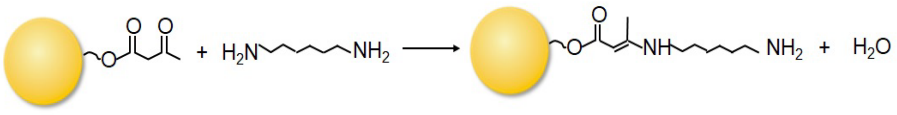

Figure 2.4. Scheme of reaction for the preparation of C-2 in HDMA based crosslinking system.

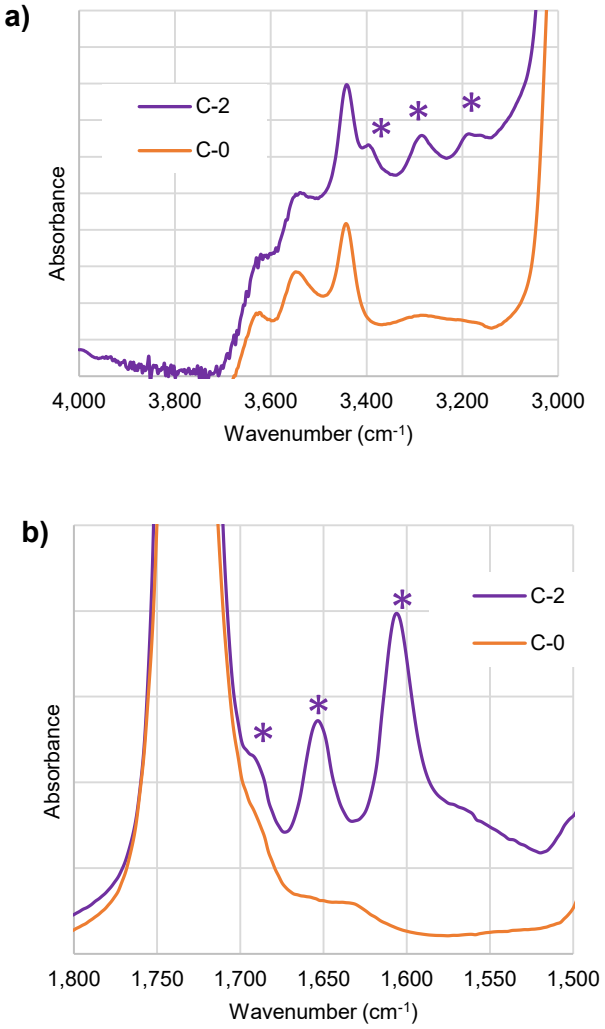

Figure 2.5. FTIR spectra of component-2 dried at RT for 1 day. a) image shows N-H stretching region and b) image represents carbonyl stretching region.

Finally, the FTIR spectra recorded during the blend formation are shown in Figure 2.6. In the NH region of the Blend, five absorptions were observed related to primary amine stretching (3395+3285 cm^{-1}), primary enamine stretching (3336+3430 cm^{-1}) and secondary enamine

stretching (3200 cm^{-1}). In the carbonyl stretching region of the Blend, six contributions were observed. 1690 cm^{-1}, carbonyl stretching of secondary enamine, 1670 cm^{-1}, carbonyl stretching of primary enamine, 1654 cm^{-1}, C=C stretching of secondary enamine + NH bending of secondary enamine, 1624 cm^{-1}, C=C stretching of primary enamine, 1606 cm^{-1}, NH bending of primary amine, and 1570 cm^{-1}, NH bending of primary enamine. Ideally, [3] the crosslinking reaction between the protected acetoacetoxy group of C-1 and the amine functionalized C-2 should produce the complete transformation of primary enamines to secondary ones (see scheme in Figure 2.7). However, the infrared results showed that in the Blend, bands related to primary enamine remained in the infrared spectrum and accordingly, full conversion was not obtained at room temperature.

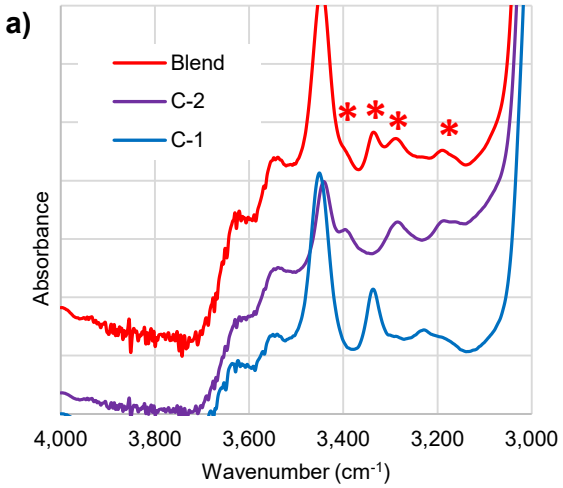

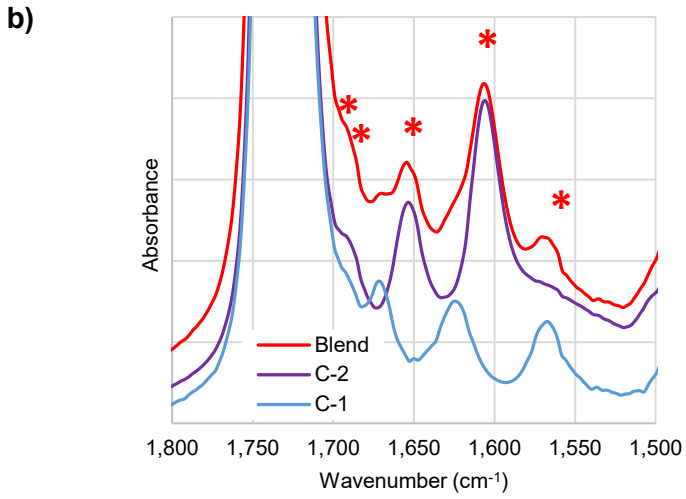

Figure 2.6. FTIR spectra of Blend after 1 day drying at RT. a) image shows N-H stretching region and b) image represents carbonyl stretching region in HMDA based crosslinking system.

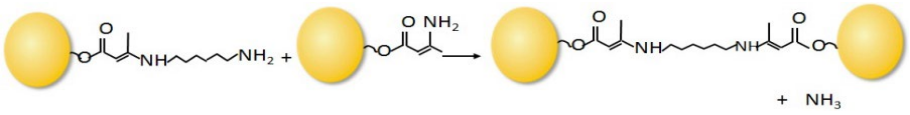

Figure 2.7. Scheme of crosslinking reaction between C-1 and C-2 during Blend formation in HDMA based crosslinking system.

As the complete disappearance of primary enamine moieties was not obtained after drying the film at room temperature for one day as predicted by literature,[8-10,12,13,16] it was decided to follow the crosslinking reaction quantitatively by FTIR. Therefore, Blend film dried at room temperature for one, two and three days was analysed, before drying it at 60 °C for one more day and analysing it again. Figure 2.8 presents the high wavenumber region for such analysis. In this region, three main absorptions were observed: 3336 cm^{-1}, 3285 cm^{-1} and 3200 cm^{-1} related to primary enamine, primary amine and secondary enamine respectively. As

observed, the absorbance of the band related to the primary enamines decreased in the drying process.

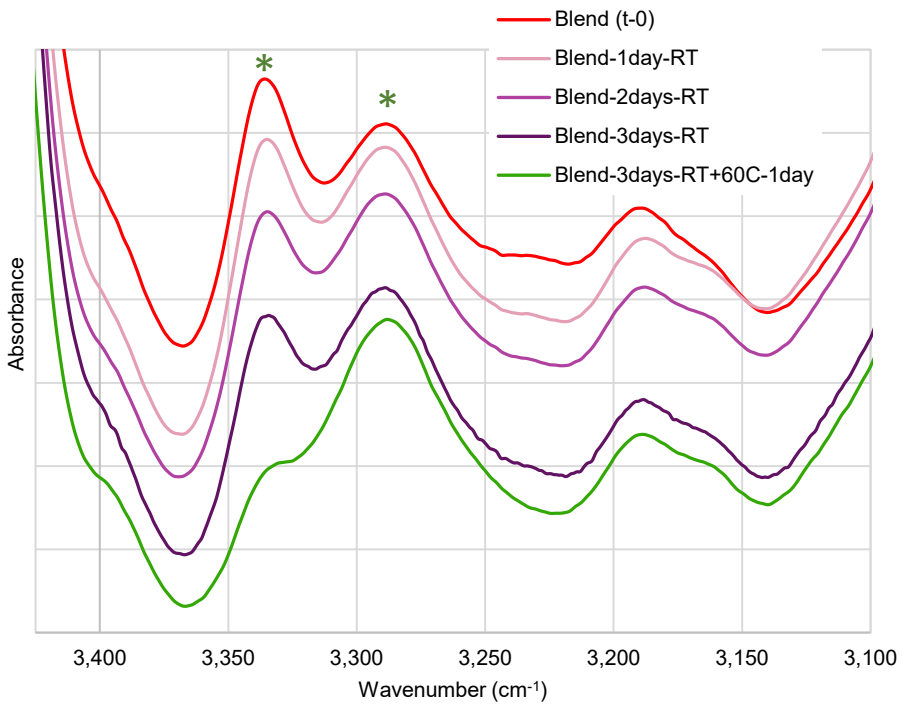

Figure 2.8. FTIR spectra of N-H stretching region after drying the Blend at RT for 1, 2 and 3 day and then 3 days + 1 day at 60 °C in HMDA based crosslinking system.

In order to quantify the crosslinking, we chose N-H stretching region as shown in Figure 2.8. The primary enamine peak area (N-H stretching region) was normalized with the carbonyl harmonic peak from MMA and BA (around 3430 cm^{-1}). Then we calculated the conversion of the crosslinking reaction by following the evolution of primary enamines, considering that the conversion was negligible at time 0. Figure 2.9 presents the crosslinking percentage obtained during drying time at room temperature and after one day at 60 °C. It was noticed that the reaction proceeded continuously for 3 days at RT drying condition, but after 3 days only 30 % of

conversion was achieved. It was needed one day of annealing at 60 °C to complete the crosslinking reaction as shown in Figure 2.9. The slow kinetics of crosslinking between AAEMA and diamine moieties could probably have been deduced from the long drying times (four weeks) proposed by some authors to prepare fully crosslinked films.[12] On the other hand, the ambient condition crosslinking between acetoacetoxy functionalized natural rubber latex and glutaraldehyde presented by Thongnuanchan et al. could be mentioned.[17] They observed a great increase of the tensile strength after having dried the samples at 30 °C for 7 days. The lower time needed by these authors to produce a fully crosslinked material may be related to the lower T_G of natural rubber, which shows higher mobility to be crosslinked at room temperature, and to the excess of glutaraldehyde, that may act as plasticizer to improve the mobility as well.

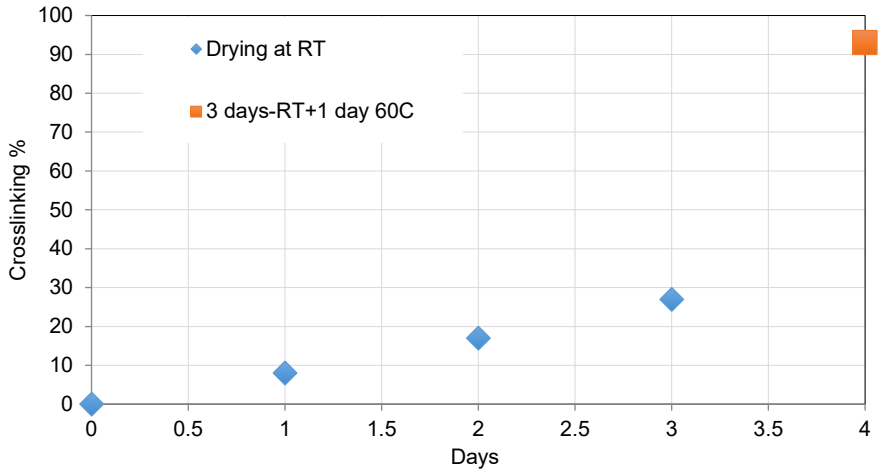

Figure 2.9. Crosslinking degree studied via FTIR analysis with time and temperature in HMDA based crosslinking system.

2.3.2. Rheological measurements

Once the kinetics of the crosslinking reaction was followed by FTIR, its evolution at 60°C was also assessed by DMTA. In order to check the evolution of moduli value with time, a time sweep test was performed at constant temperature of 60°C, as presented in Figure 2.10. It was found that the moduli (both E' and E") increased very slightly for around 100 min, and then it remained constant.

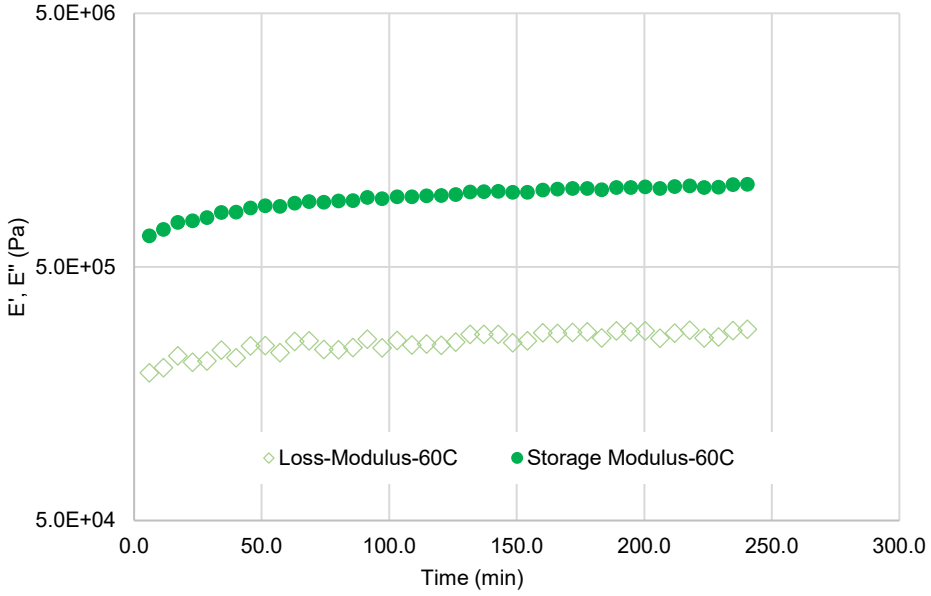

Figure 2.10. Time sweep at 60 °C and 0.1 Hz for Blend-HDMA film initially dried at RT.

From the evolution of the storage modulus (E') located within the rubbery plateau region, the evolution of the average molecular weight between crosslinking joints (Mc) can be approximated using the following equation based on the theory of rubber elasticity;[18]

$$Mc = \frac{3RT\rho}{E'}$$

Where R is the ideal gas constant, T is the temperature, ρ the polymer density (ρ = 1.1 g / cm^{-3}), and E' the storage modulus. The model assumes that each crosslinked chain contributes RT to the modulus, and therefore, the rubber modulus is proportional to the density of crosslinked chains.[19] The proportionality contains, however, some uncertainties, because some defects on the network such as dangling and free chains are not considered, and could leave to some deviation. Figure 2.11 presents the evolution of Mc during the time sweep at 60 °C of the Blend film initially dried at room temperature.

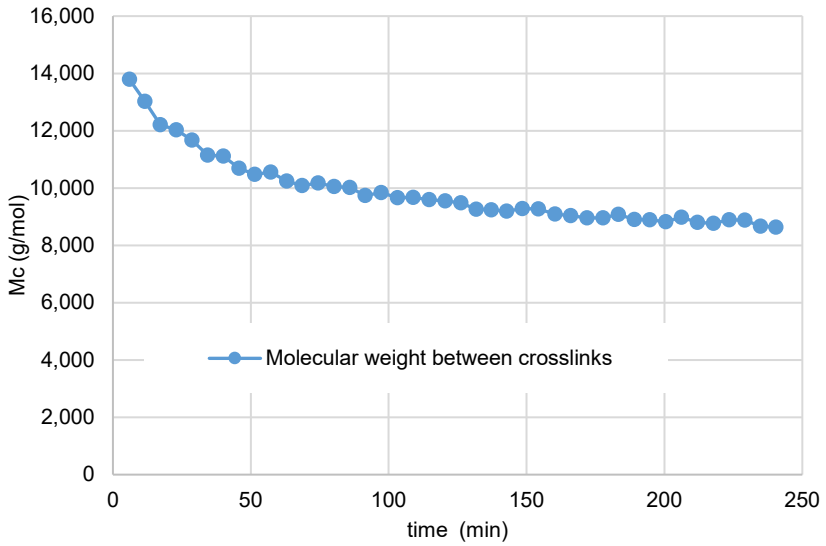

Figure 2.11. Evolution of molecular weight between crosslinking joints (Mc) at 60 °C, for Blend-HDMA film initially dried at RT.

The Mc decreases from the initial 13,790 g/mol to 8,600 g/mol after 4 hours of annealing at 60 °C. If we consider the ratio of total monomer units to AAEMA moieties in the latex formulation, this could give us an estimation of the average molecular weight between crosslinks in a fully crosslinked system. For our formulation, this estimation would be 4215 g/mol, which is

slightly lower than the value estimated in Figure 2.11. However, taking into account that the AAEMA will only be located in the outer shell of C-1 polymer particles, and that it would only produce crosslinking reactions with the amine moieties present in the shell of C-2 particles, it seems reasonable to predict that the inner particles polymer chains in C-1 and C-2 would not be crosslinked and would therefore decrease the E' of the material, increasing its estimated average Mc.

Once the time sweep at 60 °C was finished after 240 minutes, the sample was cooled down again, and a temperature sweep was performed. The results of this experiment was compared with the one that had been carried out before the time sweep at 60 °C (Figure 2.12).

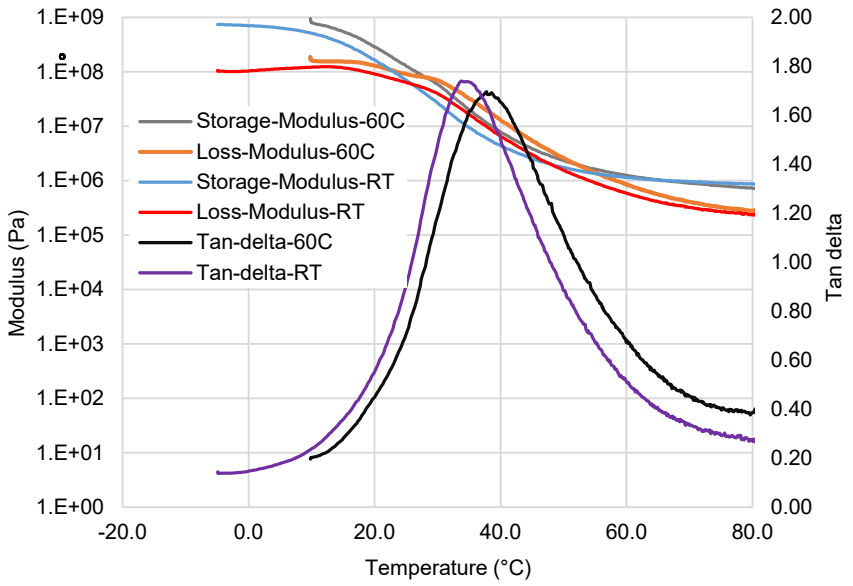

Figure 2.12. Comparison of moduli (E' and E") and tan delta value at for Blend-HDMA after being dried at RT and after being annealed at 60 °C for 240 minutes.

It was found that there was a slight decrease in the intensity of tan delta peak and the peak slightly moved toward higher temperature (from 34 to 37 °C) for the sample after being

annealed at 60°C for 240 minutes. The peak height of tan delta is related to the segmental mobility of the network. Therefore, the height decrease observed in the annealed film can be a result of the decreased segmental mobility or increased crosslinking density, which together with the increase in T_G would show that a more crosslinked film was formed after annealing at 60 °C. In general, these results would confirm what was already seen by FTIR quantification, that after one day of annealing at 60 °C, most crosslinking reactions had already taken place.

2.3.3. Tensile test

Therefore, it was decided to analyse the tensile test properties of Blend films dried at room temperature for three days and compare them to the ones of the Blend films annealed additionally for one day at 60 °C (Figure 2.13).

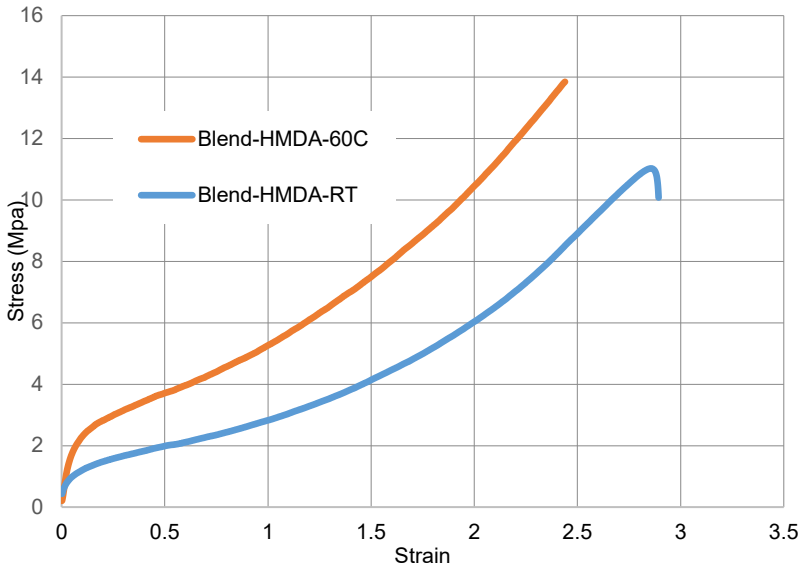

Figure 2.13. Comparison of tensile test performed for Blend films prepared at room temperature and 60 °C in HMDA based crosslinking chemistry.

The annealing temperature effect could be clearly seen, as the Young's modulus increased and elongation to break slightly decreased for the film annealed at 60 °C compared to the film dried at room temperature. Both properties could be explained by the increase in the crosslinking between polymer particles already detected by FTIR and rheological measurements.

2.3.4. Water absorption test

The swelling of the films will definitely be affected by the presence of crosslinked structure in the final film. In this case, we studied the absorption of films using water as solvent. Figure 2.14 presents the results found for water absorption tests, for C-0 film and Blend films dried at RT and at 60 °C, respectively.

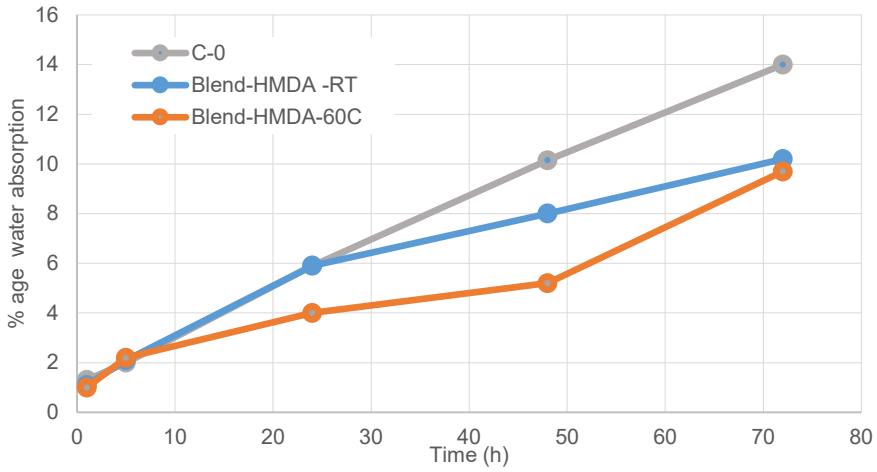

Figure 2.14. Comparison of water absorption behaviour of Blend films prepared at room temperature and 60°C in HMDA based crosslinking chemistry.

A decrease in the absorption of the water can be seen from C-O film (without HDMA crosslinking moieties) to Blend films. Therefore, the presence of the HDMA crosslinking moiety

did effectively increase the crosslinking density, decreasing the water swellability. This decrease is more evident in the first 48 hours of immersion in water for the Blend film annealed at 60 °C than for the Blend film dried at room temperature for 3 days. Therefore, the increased crosslinking density observed by FTIR, rheology and mechanical properties in the film annealed at 60 °C had a positive effect on the reduced water absorption. Nevertheless, it was seen that the difference between the water absorbed by the Blend dried at RT for 3 days and the one annealed at 60 °C was reduced for longer absorption times.

2.4. Conclusions

This chapter describes the evolution of interparticle crosslinking reaction with time and temperature in the HMDA–AAEMA based crosslinking system. Two separate waterborne latexes were prepared with AAEMA and HDMA functionality, respectively. The acetoacetoxy-diamine crosslinking chemistry proceeds fast in solution at room temperature, but the crosslinking evolution between such moieties attached to different polymer particles had not been studied in depth before. It was found by FTIR that the crosslinking reaction evolves slowly with time at room temperature, and it requires higher temperature (annealing at 60 °C) to get fully crosslinked film. Rheological measurements also confirmed it, as the time sweep test showed how the moduli evolved fast at 60 °C. The increase in T_g after annealing at 60 °C, together with improved mechanical and water resistance properties, strengthen the conclusion that a more crosslinked structure was formed when annealing at 60°C.

2.5. References

[1] A.F. Keddie, Joseph, Routh, Fundamentals of Latex Film Formation, in: Fundam. Latex Film Form., 2010: pp. XVIII, 308.

[2] J.W. Taylor, M.A. Winnik, Functional latex and thermoset latex films, JCT Res. 2004 13. 1 (2004) 163–190. https://doi.org/10.1007/S11998-004-0011-5.

[3] F. del Rector, W.W. Blount, D.R. Leonard, Applications for acetoacetyl chemistry in thermoset coatings, J. Coatings Technol. 61 (1989) 31–37.

[4] A. Noomen, The chemistry and physics of low-emission coatings. Part 2. Waterborne two-pack coatings, Prog. Org. Coatings. 17 (1989) 27–39. https://doi.org/10.1016/0033-0655(89)80011-1.

[5] M. Ooka, H. Ozawa, Recent developments in crosslinking technology for coating resins, Prog. Org. Coatings. 23 (1994) 325–338. https://doi.org/10.1016/0033-0655(94)87002-0.

[6] S. Magnet, J. Guillot, A. Guyot, C. Pichot, Crosslinking ability of styrene—butyl acrylate copolymer latices functionalized with glycidyl methacrylate, Prog. Org. Coatings. 20 (1992) 73–80. https://doi.org/10.1016/0033-0655(92)85005-G.

[7] P.J.A. Geurink, L. Van Dalen, L.G.J. Van Der Ven, R.R. Lamping, Analytical aspects and film properties of two-pack acetoacetate functional latexes, Prog. Org. Coatings. 27 (1996) 73–78. https://doi.org/10.1016/0300-9440(95)00522-6.

[8] J. Feng, H. Pham, P. Macdonald, M.A. Winnik, J.M. Geurts, H. Zirkzee, S. van Es, A.L. German, Formation and crosslinking of latex films through the reaction of acetoacetoxy groups with diamines under ambient conditions, J. Coatings Technol. 1998 70881. 70 (1998) 57–68. https://doi.org/10.1007/BF02730151.

[9] N. Moszner, U. Salz, V. Rheinberger, Reaction behaviour of monomeric β-ketoesters, Polym. Bull. 1994 324. 32 (1994) 419–426. https://doi.org/10.1007/BF00587883.

[10] R.J. Esser, J.E. Devona, D.E. Setzke, L. Wagemans, Waterbased crosslinkable surface coatings, Prog. Org. Coatings. 36 (1999) 45–52. https://doi.org/10.1016/S0300-9440(99)00019-3.

[11] A. Mori, T. Kitayama, M. Takatani, T. Okamoto, A honeymoon-type adhesive for wood products based on acetoacetylated poly(vinyl alcohol) and diamines: Effect of diamines and degree of acetoacetylation, J. Appl. Polym. Sci. 91 (2004) 2966–2972. https://doi.org/10.1002/app.13491.

[12] Y.J. Park, M.J. Monteiro, S. Van Es, A.L. German, Effect of ambient crosslinking on the mechanical properties and film morphology of PSTY-P(BA-co-AAEMA) reactive composite latexes, Eur. Polym. J. 37 (2001) 965–973. https://doi.org/10.1016/S0014-3057(00)00206-8.

[13] I. González, J.M. Asua, J.R. Leiza, Crosslinking in Acetoacetoxy Functional Waterborne Crosslinkable Latexes, Macromol. Symp. 243 (2006) 53–62. https://doi.org/10.1002/MASY.200651106.

[14] J.M. Geurts, J.J.G.S. Van Es, A.L. German, Latexes with intrinsic crosslink activity, Prog. Org. Coatings. 29 (1996) 107–115. https://doi.org/10.1016/S0300-9440(96)00623-6.

[15] K. Beshah, W. Devonport, A study of acetoacetoxyethyl methacrylate hydrolysis in acrylic latex polymers as a function of pH, J. Coatings Technol. Res. 10 (2013) 821–828. https://doi.org/10.1007/S11998-013-9512-4/FIGURES/11.

[16] J. Lu, A.J. Easteal, N.R. Edmonds, Crosslinkable poly(vinyl acetate) emulsions for wood adhesive, Pigment & Resin Technol. 40 (2011) 161–168. https://doi.org/10.1108/03699421111130423.

[17] B. Thongnuanchan, Rattanawadee Ninjan, C. Nakason, Acetoacetoxy functionalized natural rubber latex capable of forming cross-linkable film under ambient conditions, Iran. Polym. J. 26 (2017) 41–53. https://doi.org/10.1007/s13726-016-0497-6.

[18] D.H. Campbell, Calculation of crosslink density of thermoset polymers a simpler method, PCI-Paint Coatings Ind. 34 (2018) 33–38.

[19] C. Li, A. Strachan, Evolution of network topology of bifunctional epoxy thermosets during cure and its relationship to thermo-mechanical properties: A molecular dynamics study, Polymer. 75 (2015) 151–160. https://doi.org/10.1016/J.POLYMER.2015.08.037.

Chapter 3.

Crosslinking kinetics and interdiffusion during film formation in acetoacetoxy - polyethyleneimine functionalized latexes.

3.1. Introduction

As it has been pointed out, the primary purpose of crosslinking of polymer chains is to enhance their final properties such as the solvent resistance, durability and mechanical performance of the materials.[1] Moreover, the crosslinking can be achieved during the main polymerization step or after it, as a post-crosslinking.[2] The main difference between crosslinking and post-crosslinking is the way the materials are being processed afterwards, as a too early crosslinking may hinder a correct processing of the polymeric material.[2,3]

This basic concept also applies to polymeric coatings made from waterborne latexes. In these waterborne systems, the film formation process plays a vital role on defining the final properties of the film. More specifically, the relative rate of diffusion of polymer chains between polymer particles and crosslinking between polymer chains are key variables playing a crucial role on the development of the final film properties.[4,5] Three possible scenarios could occur. Firstly, if the rate of crosslinking is faster than diffusion, or crosslinking occurs during the main polymerization step, a highly crosslinked structure is formed inside each polymer particle, which

provides no chance to chains for diffusion during film formation. This is how weak films, with low cohesive strength, can be obtained from highly crosslinked polymers.[3,5,6] Geurts et al. found this problem for polymer particles containing epoxy moieties, when they tried to crosslink them with diamines. As the initial polymer particles already had a high gel content, the reaction between epoxy groups and diamines was not favored.[7] Secondly, if the rate of diffusion is faster than crosslinking a strong film can be prepared, as the crosslinks will occur on a fully diffused system.[8-10] Finally, if the rate of crosslinking is comparable to diffusion rate, the polymer particles diffuse to some extent to the boundaries and then crosslinking may occur in the interface, restricting the full diffusion of polymer chains between polymer particles.

Therefore, in order to design hard and solvent resistant coatings from waterborne latexes, it is not only important to follow crosslinking reactions during the production of the films but also the interdiffusion of polymer chains. There are basically three methods to measure the polymer chain interdiffusion during film formation. Two of them use fluorescence i.e., Flourescence Energy Transfer (FRET) and Pyrene Excimer Flourescence (PEF).[11] The third method is small angle neutron scattering (SANS).[12,13]

FRET is a quantitative technique to measure polymer interdiffusion among particles. For the measurement, two latexes are synthesized; one containing a donor monomer (e.g. 9-Ph (9-Phenanthryl) methyl methacrylate (Phe-MMA)) and the other containing an acceptor monomer (e.g. 1-(4-nitrophenyl)-2-pyrrolidinmethyl)-acrylate (NNP-A)). Then, both latexes are mixed together, in such a way that donor and acceptor moieties are present in different particles. During the film formation process, these polymers diffuse across the particles boundaries, they bring donor and acceptor dyes into proximity, allowing the extent of energy transfer to increase and leading to a faster decrease in the fluorescence decay profile. Therefore, following the evolution

of the fluorescence decay profile, the fraction of mixing between polymer particles can be calculated.[14,15] PEF is a relatively new fluorescence method to measure the interdiffusion. It is based on the fact that excited molecules emit light at different wavelengths if they are isolated or in close contact, forming an excimer.[16] Pyrene is the most often used molecule in this technique because it can be excited by UV-light.[17] To carry out PEF measurements, two equivalent latexes are prepared, one labelled with the compound that forms the excimer and the other unlabelled. Then both latexes are blended and the film formation is followed by fluorescence. When the latex blend film starts to dry, the local concentration of pyrene decreases, as it will diffuse to the surrounding particles, not containing pyrene, and as a result the fluorescence coming from the excimer decreases. The diffusion speed of the polymer can be deduced by calculating the excimer/monomer ratio.[16,18]

In the previous chapter, we reported the kinetic study of the crosslinking between hexamethylenediamine (HMDA) functionalized polymer particles and AAEMA functionalized polymer particles, in a two-pot one pack system.[19] This way, the use of water soluble amine crosslinkers was avoided, favouring the REACH implementation of the crosslinking coating system. The kinetic study showed that crosslinking reaction evolves slowly at room temperature, as opposed to what seemed to be widely supposed and that temperature had a significant effect on driving the crosslinking degree to its completeness. Nevertheless, the functionalization of the amine bearing particles with longer polyethylenimine (PEI) groups, instead that with short diamines (such as HDMA), seems to produce better final properties in the two-pot one-pack system.[20]

Therefore, the objective of this work is to follow the evolution of crosslinking and interdiffusion in two-pot one pack binder system, pot-1 (component-1) prepared by AAEMA

functional polymer particles and pot-2 (component-2) by PEI based functional polymer particles. Two different PEI (LUPASOL G-20, 1300 g/mol and LUPASOL G-35, 2000 g/mol) were used in the study To follow the kinetics of the crosslinking reaction, FTIR spectroscopy and rheological measurements were carried out, analysing also the effect of temperature. On the other hand, the interdiffusion of polymer chains was followed by FRET and PEF experiments, while the crosslinking reaction was also occurring. Film morphology was analysed by TEM of the cryossectioned films with different PEI contents. All this information was used to justify the mechanical properties of the crosslinked films obtained with different amine functionality contents and at different annealing conditions.

3.2. Experimental part

3.2.1. Synthesis of MMA/BA/AAEMA latex

For the production of the latexes, a seeded semibatch emulsion polymerization procedure was used. The detailed recipe for the synthesis of C-0 has been mentioned in section 2.2.1. In that recipe, C-0 was prepared with 5 % weight based on total monomer (wbtm) of AAEMA. Furthermore, C-0 with 10 % wbtm of AAEMA was also prepared.

Once C-0 latex was prepared, the emulsion was cooled and ammonium hydroxide (NH_4OH) (28%) was added in 5 min under continuous stirring to one fraction of it. The NH_4OH was added in a mol ratio of 2:1 in NH_4OH : AAEMA. This way AAEMA functionalized and protected component 1 (C-1) latex was prepared.

For the preparation of amine functionalized component 2 (C-2) latex, a fraction of C-0 latex was reacted with polyethyleneimine (PEI). The Mw of the PEI used in the main body of this work, LUPASOL G-20, was 1300 g/mol. PEI is composed of $–CH_2\text{-}CH_2\text{-}N(H)_x\text{-}$ repeating units,

x being 0, 1 or 2. In case of LUPASOL G-20, considering an average molecular weight of 43 g for this repeating unit, it can be estimated that this PEI will be composed of 30 of these repeating units. Assuming an even distribution of N, NH and NH_2 groups, it can be said that each PEI molecule will have 20 amine groups able to react with AAEMA moieties. In order to prepare C-2 latex, we selected a molar ratio of 7.7 reactive amine groups per AAEMA functional groups, or one PEI molecule per 2.6 AAEMA molecules in the C-0 latex. Component-2 was prepared by adding slowly C-0 latex into PEI solution. From these components, C-1 and C-2, a blend latex was prepared with equal weight ratio of both components (Blend-PEI-7.7). For comparison purposes, a lower and higher amine/AAEMA ratios were also selected, namely 0.2, 4 and 15. These component-2 were named C-2_0.2ratio, C-2_4ratio, and C-2_15ratio. In the final part of the chapter, the mechanical properties of the Blend obtained using a longer PEI in the production of C-2 (LUPASOL G-35, 2000 g/mol) will also be presented.

In order to study the interdiffusion of the polymer chains by FRET, latexes labelled with donor monomer and with acceptor monomer were prepared. Seeded semibatch emulsion polymerization was used in both cases including the donor monomer 9-Phenanthryl methyl methacrylate (Phe MMA) or the acceptor monomer 1-(4-nitrophenyl)-2 pyrrolidin methyl)-acrylate in the first or in the second feeding stage. Therefore, four latexes were prepared (by following the recipe mentioned in Table 3.1), two of them contained the labelled monomers in first shell and two contained the labelled monomers in the second shell. The quantity chosen for both donor and acceptor monomers were 0.010 g (1 % in weight based on the total monomer of the recipe presented in Table 3.1).

Once latexes with labelled donor monomer and labelled acceptor monomer were prepared, three blends were prepared from them, one control blend (named as

Blank Blend-FRET) and the other two were crosslinked blends. Blank Blend-FRET contained 50:50 of C-0 containing labelled donor monomer and C-0 containing acceptor monomer, in which the crosslinking moiety had not been included. For the preparation of the crosslinked blends for FRET analysis, first C-1 from C-0 with donor monomer and C-2 from C-0 containing acceptor monomer were prepared. For the preparation of labelled C-1, the mol ratio of 2:1 between NH_4OH to AAEMA was used. During the preparation of C-2, we prepared two different C-2 by using different amounts of PEI. The polyethyleneimine was added to maintain a mol ratio of 0.2 and 7.7 between N-H of PEI and acetoacetoxy groups respectively. Therefore, two blends were prepared by mixing equal amounts of component-1 and 2. First blend was named as "PEI-0.2-FRET" having C-2 with 0.2 NH to AAEMA ratio and second blend was named as "PEI-7.7-FRET" having a ratio of 7.7.

Table 3.1. Formulation used to produce the seed by batch emulsion polymerization and the first and second feeding for the semibatch emulsion polymerization for the synthesis of labelled latexes for FRET experiment.

Ingredients	Seed (g)	First feeding (g)	Second feeding (g)
Methyl methacrylate (MMA)	1.78	10.25	5.04
Butyl acrylate (BA)	1.78	10.25	5.04
SLS	0.07	0.414	0.20
$NaHCO_3$	0.017	-	-
$K_2S_2O_8$	0.017	0.083	0.048
Disponil A3065	-	0.561	0.27
Water	14.29	11.65	5.73
Methacrylic acid (MAA)	-	0.159	0.08
Acetoacetoxy ethyl methacrylate (AAEMA)	-	-	1.83
(9-Phenanthryl) methyl methacrylate (Phe MMA)		0.01 In first or second feeding	
1-(4-nitrophenyl)-2 pyrrolidin methyl)- acrylate		0.01 In first or second feeding	

In order to study the interdiffusion of the polymer chains by PEF, fluorescent labelled and unlabelled latexes were also prepared. Batch emulsion polymerization was used for the preparation of the seeds, in which 1-pyrenemethyl methacrylate was introduced in the case of the labelled latex. Then the shell was prepared by semibatch emulsion polymerization by using the whole seed. The formulation used for both seed and shell formation for the preparation of labelled and unlabelled latexes is presented in Table 3.2.

Table 3.2. Formulation used to produce the seed by batch emulsion polymerization and the final latex by semibatch emulsion polymerization for the synthesis of labelled and unlabelled latexes for PEF study.

Ingredients	Seed (g) (labelled latex)	Seed (g) (unlabelled latex)	Feed (g)
Methyl methacrylate (MMA)	2.19	2.19	6.025
Butyl Acrylate (BA)	2.19	2.19	6.025
SLS	0.087	0.087	0.245
$NaHCO_3$	0.0217	0.0217	-
$K_2S_2O_8$	0.0217	0.0217	0.064
Disponil A3065	-	-	0.33
Water	17.57	17.57	6.9
Methacrylic acid (MAA)	-	-	0.096
Acetoacetoxy ethyl methacrylate (AAEMA)	-	-	0.88
1-Pyrenemethyl methacrylate	0.887	-	

Once the two latexes (labelled and unlabelled) were prepared, three blends were prepared from them, one control blend (named as Blank Blend-PEF) and the other two were crosslinked blends. For the preparation of Blank Blend-PEF, a ratio of 5:95 between labelled to unlabelled latex was used, without the addition of any PEI. So Blank Blend-PEF contained to C-0 like latexes, in which the crosslinking moiety had not been included. For the preparation of the crosslinked blends for PEF analysis, first C-1 and C-2 components from both unlabelled and labelled latexes were prepared. For the preparation of unlabelled C-1, the mol ratio of 2:1 between NH_4OH to AAEMA was used. During the preparation of labelled and unlabelled C-2,

we prepared two different C-2 by using different amounts of PEI. The polyethyleneimine was added to maintain a mol ratio of 0.2 and 7.7 between N-H of PEI and acetoacetoxy groups respectively. Therefore, two blends were prepared by mixing equal amounts of component-1 and 2. First blend was named as “PEI-0.2-PEF” having C-2 with 0.2 NH to AAEMA ratio and second blend named as “PEI-7.7-PEF” having a ratio of 7.7. The following weight ratio of components was selected for the preparation of the crosslinked blends: 5 % of labelled C-2, 45 % of unlabelled C-2 and 50 % of unlabelled C-1. This way the total ratio of labelled to unlabelled latexes was 5/95, as in the Blank Blend-PEF.

Table 3.3 presents the codes used along the work to define the samples studied.

Table 3.3. Samples code used.

Sample code	**Definition of samples**	
	Single latexes	**Two pot**
C-0	Latex functionalized with AAEMA	
C-1	C0 + NH_4OH	Blend-PEI-7.7 (C-1+C-2_7-7 ratio)
C-2	C0 + PEI (7.7 NH/AAEMA)	
C-2_0.2 ratio	C0 + PEI (0.2 NH/AAEMA)	Blend PEI-0.2 (C-1+C-2_0.2 ratio)
C-2_4 ratio	C0 + PEI (4 NH/AAEMA)	Blend PEI-4 (C-1+C-2_4 ratio)
C-2_15 ratio	C0 + PEI (15 NH/AAEMA)	Blend PEI-15 (C-1+C-2_15 ratio)
Labelled C-0-FRET	C-0 labelled latex with donor and acceptor monomer	Blank Blend-FRET (50% Labelled C-0 with donor + 50% Labelled C-0 with acceptor)
Labelled C-2_0.2 ratio-FRET	Labelled C-0+PEI (0.2 amine/ AAEMA)	PEI-0.2-FRET (50% Labelled C-1 with donor + 50% Labelled C-2_0.2 ratio with acceptor).
Labelled C-2_7.7 ratio-FRET	Labelled C-0+PEI (7.7 amine/ AAEMA)	PEI-7.7-FRET (50% Labelled C-1 with donor + 50% Labelled C-2_7.7 ratio with acceptor).
Labelled C-0-PEF	C-0 labelled with pyrene	Blank Blend-PEF (5% Labelled C-0 + 95% C-0)

Labelled C-2_0.2 ratio-PEF	Labelled C-0+PEI (0.2 amine/ AAEMA)	PEI-0.2-PEF (5% Labelled C-2_0.2 ratio + 45% C-2_0.2 ratio + 50% C-1)
Labelled C-2_7.7 ratio-PEF	Labelled C-0+PEI (7.7 amine/ AAEMA)	PEI-7.7-PEF (5% Labelled C-2_7.7 ratio + 45% C-2_7.7 ratio + 50% C-1)

3.2.2. Latex and film characterization

The solids content of the seed and the latex was obtained gravimetrically, and it was used to analyse the evolution of the conversion during the polymerization reaction. The particle size of polymer particles was measured by Dynamic Light Scattering, DLS (Malvern® Zetasier Nano). For the analysis, samples were diluted to such a low concentration that it can safely be assumed that no monomer was present in the polymer particles, namely that the unswollen particle sizes were measured.

For the kinetic analysis of the evolution of the crosslinking reaction, FTIR spectra were recorded using a Nicolet iS50 equipment. The spectra were registered with the resolution of 4 cm^{-1} with scan number 32. The samples were prepared by casting over CaF_2 support. The RT film formation was carried out at 23 °C with relative humidity of 55 % and for high temperature treatment, the film was place in an oven with static air at 60 °C. Dynamic Mechanical Thermal Analysis (DMTA) were carried out using a dynamic mechanical thermal analyser Triton 2000 DMA, Triton Technology Ltd with Single cantilever bending geometry. We investigated the rheological properties by calculating the E', E" and tan delta at 2 °C heating rate /min heating rate. On the other hand, we performed time sweeps at 60 °C for 1500 min for PEI containing system. After the time sweep, another temperature sweep was carried out to compare with the initial sample.

FRET measurements were conducted by employing a FS920 single photon counting spectroflourimenter from Edinburgh Instruments (Edinburgh, Scotland, UK) equipped with a 450 W Xenon arc lamp and lifetime decays were acquired using time-correlated single-photon counting (TCSPC) accessory with 340 nanometer excitation wavelength. To perform this study, mixtures of 1:1 weight based total donor and acceptor labelled latex were prepared and few drops of the mixture were spread on a small quartz plate (25 x 25 mm) to form a film. The films were allowed to dry at 23 ± 2 °C and 50 ± 5 % relative humidity. The time at which the films appeared dry and transparent was considered as time zero (within 35 minutes in the samples of this work). After this period, two different drying protocols were followed; room temperature drying (RT) and RT + higher temperature annealing at 60 °C. The area under each standardized fluorescence decay profile is equal to the total fluorescence intensity from the sample, which is proportional to the quantum efficiency of fluorescence. One could calculate the quantum efficiency of energy transfer (ϕ_{ET}) from the changes in the area under the decay profiles. Thus, ϕ_{ET} can be related to the fraction of molecular mixing in a system of labelled particles and it is defined as shown in Equation 3.1. In our analysis of donor fluorescence decay data, we assume that all deviations from a strictly exponential donor decay profile are due to energy transfer.

$$\phi_{ET}(t) = 1 - \frac{\int_0^\infty I_D(t)dt}{\int_0^\infty I_D^0(t)dt} \qquad \text{(Eq. 3.1)}$$

PEF measurements were conducted by using Flouromax-4 apparatus (Horiba Jobin-Yvon) equipped with 450 W Xenon arc lamp. Thin blend latex films were applied on quartz crystal by spin coating (8000 rpm, without diluting the latex). The samples were deposited in the equipment, excited with 340 nm and measured in the range of 360 nm to 600 nm. The signal was collected at 45° orientation to the beam. The measurements were carried out after annealing the film during different times at room temperature and at 60 °C.

The morphology of films was studied by means of Transmission Electron Microscopy (TEM). TEM analysis was carried out with a TecnaiTM G2 20 Twin device at 200 kV (FEI Electron Microscopes). The films were cryosectioned with a Leica EMUC6 cryoultramicrotome at 30 °C below the T_G of the sample, with a Diatome 45° diamond 30 knife, and the observations were made in the microscope (TEM), after RuO_4 staining. Tensile tests of the free standing films annealed at room temperature (23 °C with relative humidity of 55 %) and at 60 °C were performed on Universal testing machine TA.HD plus Texture Analyser at a crosshead speed of 0.42 mm/s. Samples with approximate length of 55 mm and 0.55 mm of thickness were used.

3.3. Results and discussions

3.3.1. Kinetics of crosslinking reaction

In case of C-0, prepared from 5 wbtm % of AAEMA, the particle size achieved was 130 nm and the latex had a solids content of 47 wt % with 95 % of monomer conversion. There was no change in solids content during the formation of C-1 by the addition of NH_4OH. However, it decreased to 40 wt % solids content during the formation of C-2. The particle sizes of C-1 and C-2 measured right after their preparation were 130 and 134 nm respectively. However, in case of C-0 prepared from 10 wbtm % of AAEMA, it was not possible to prepare stable C-2 dispersion, therefore it was not possible to follow the study with this system.

FTIR spectroscopy analysis was used to study the chemical structural changes during the synthesis of C-1, C-2 and the crosslinked Blend-PEI-7.7. The FTIR spectra of C-0, C-1, C-2 and Blend film casted at room temperature will be presented in the two regions that present the most significant changes: the region from 3800 cm^{-1} to 3000 cm^{-1}, named as N-H stretching

region and the region from 1800 cm^{-1} to 1500 cm^{-1}, named as carbonyl stretching region. Both regions have been analysed separately for the formation of C-1, C-2 and Blend in Figure 3.1.

In the NH stretching vibration region, in addition to the band due to the carbonyl harmonic at 3430 cm^{-1}, two bands around 3336 cm^{-1} and 3430 cm^{-1} could be observed for C-1, assigned to the NH_2 stretching of the primary enamine. These two bands did not appear in the spectrum of C-2 that was characterized by a broad absorption centred at 3290 cm^{-1}. This band was assigned to the secondary enamine stretching that was overlapped with the NH_2 and NH stretching and the Polyethyleneimine. Finally, in the Blend, the bands of primary and secondary enamine stretching could be found.

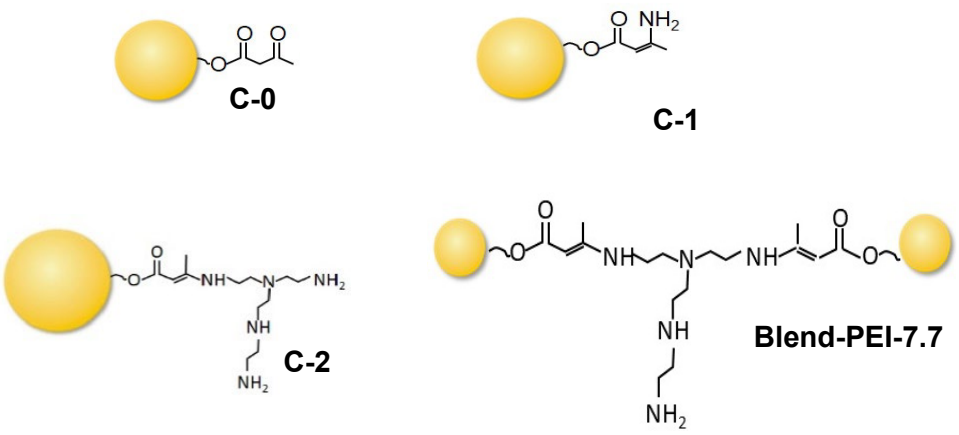

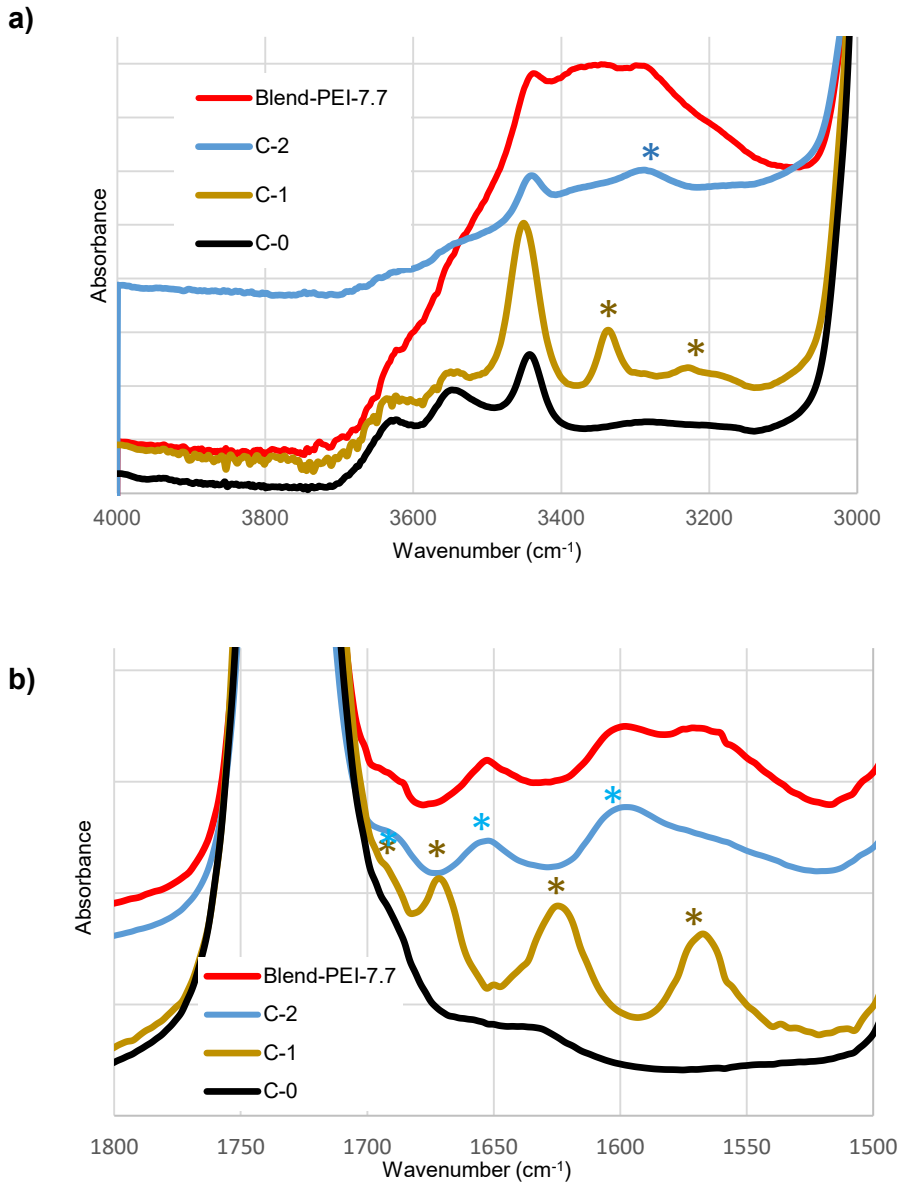

Figure 3.1. Model chemical structures of C-0, C-1, C-2 and crosslinked Blend particles and FTIR spectra of a) N-H stretching region and b) carbonyl stretching region of C-0, C-1, C-2 and Blend films prepared at RT (1 day).

In the carbonyl stretching region of C1, three bands appeared at 1670, 1624 and 1562 cm^{-1} related to carbonyl stretching next to the primary amine, C=C stretching and NH_2 bending of the primary enamine respectively. However, the spectrum of C-2 was characterized by the bands related to the secondary enamine (1690 cm^{-1} C=O stretching and 1654 cm^{-1} C=C stretching and NH bending) and to the remaining Polyethyleneimine bending at 1606 cm^{-1}. In the Blend-PEI-7.7, bands related to primary and secondary enamine and to the remaining Polyethyleneimine could be found.

Ideally, the crosslinking reaction between the protected acetoacetoxy group of C-1 and the amine functionalized C-2 should be complete, when all the primary amines coming from the protection of acetoacetoxy by NH_4OH in C-1 disappear due to the reaction with PEI amines. However, the infrared results (Figure 3.1) showed that the bands related to primary enamine from C-1 at 1562 cm^{-1} remained in the spectrum and accordingly full conversion was not obtained after one day of film formation at room temperature. Therefore, it was decided to follow the crosslinking reaction quantitatively by FTIR for different times and annealing temperatures. Thus the FTIR spectra of the Blend-PEI-7.7 film annealed at room temperature for one, two and three days was analysed, and then after annealing at 60 °C for 1 h, 3 h and 24 h. Figure 3.2 presents the low wavenumber region for such analysis. In this region, the evolution of primary amines absorption at 1562 cm^{-1} was followed for the quantification of the crosslinking.

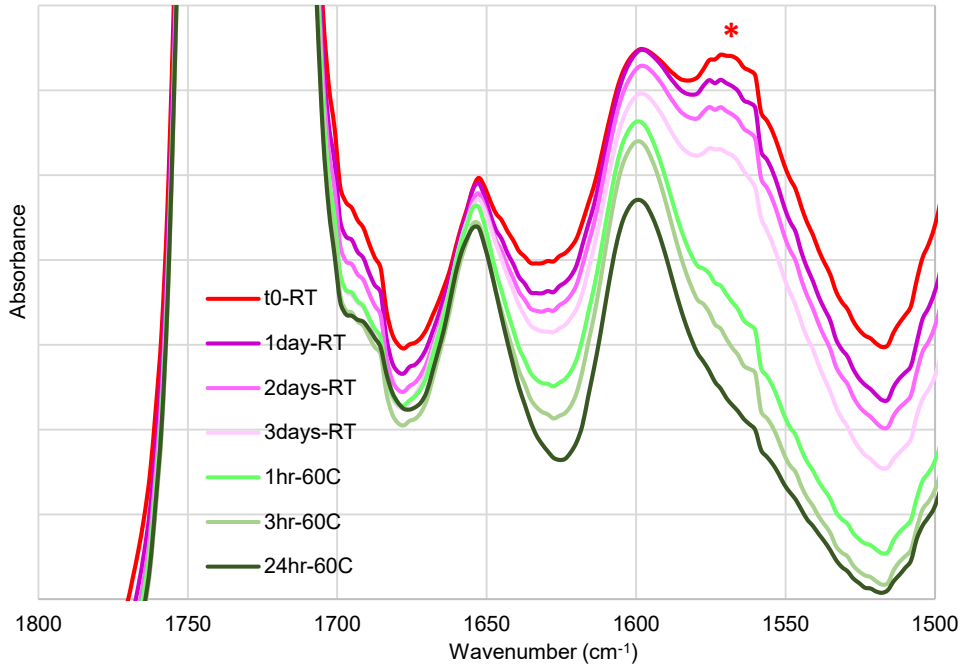

Figure 3.2. FTIR spectra in the carbonyl stretching region after annealing the Blend-PEI-7.7 film at RT for 1, 2 and 3 days and then 1, 3 and 24 h at 60 °C.

For the quantification study, the area of the primary amine peak coming from C-1 at 1562 cm^{-1} at different crosslinking times was measured and the conversion was calculated according to Equation 3.2, considering that the conversion was negligible at time 0.

$$\%Croslinking = (1 - \frac{A1566(t)}{A1562(0days)}) * 100 \qquad \text{(Eq. 3.2)}$$

Figure 3.3 presents the crosslinking percentage obtained during annealing at room temperature for three days and for 1, 3 and 24 hours at 60 °C. It was noticed that the reaction proceeded slowly for 3 days at RT and only 20 % of conversion was achieved in this time. The annealing at 60 °C speeded up the process, as around 70 % conversion was already achieved

after 1 hour, 74 % conversion 3 hours and almost 100 % conversion after 24 hours, to complete the crosslinking reaction as shown in Figure 3.3.

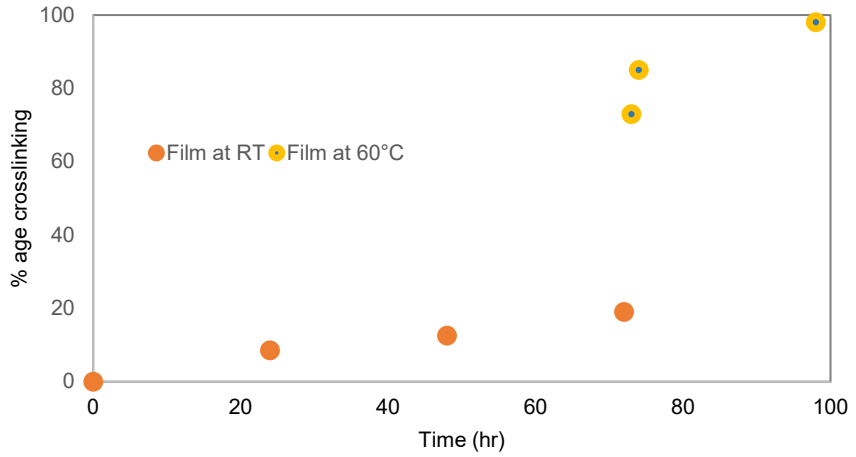

Figure 3.3. Evolution of crosslinking degree in Blend-PEI-7.7 film calculated via FTIR analysis with time and temperature.

The crosslinking reaction kinetics were also studied by rheological measurements. Figure 3.4 presents the evolution of moduli value with time, performed by a time sweep test at constant temperature of 60 °C. We found that the moduli (both E' and E") values initially increased significantly and then reached a certain plateau. The significant increase of moduli with time was due to the crosslinking reactions occurring between C-1 and C-2 components in the film. These data match the crosslinking degree calculated by FTIR, where it was also seen that crosslinking reaction evolved rapidly in the initial hours of annealing at 60°C, but around 24 hours were required to fully convert the reaction. In these rheological measurements, it can be seen that around 1500 minutes are needed to reach to the plateau of the moduli, very similar to the 24 hours (1440 min) observed by FTIR. In the previous chapter, hexamethylenediamine (HDMA) was used as amine moiety in C-2, instead of oligomeric PEI.[19] In that case, the full crosslinking reaction took just 100 minutes at 60 °C, suggesting that the smaller size of HDMA in the amine

functionalized C-2 particles favoured the crosslinking reaction with the AAEMA functionalized C- 1 particles, compared to the larger PEI functionalized C-2 particles.

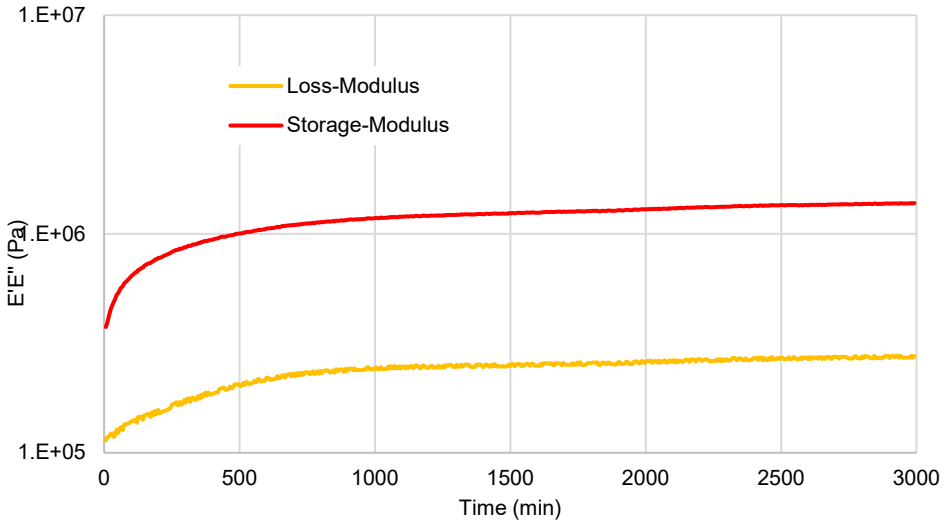

Figure 3.4. Time sweep at 60 °C and 0.1 Hz for Blend-PEI-7.7 film initially annealed at RT.

Moreover, it has also been seen in previous chapter that the average molecular weight between crosslinking joints (Mc) in HMDA based system decreased from 13,800 g/mol to 8,600 g/mol after 100 min of annealing at 60 °C. If we repeat the calculations for the current system, where PEI is used as amine moiety source, Mc is initially 18,500 g/mol and it decreases to 5,400 g/mol after 1500 min of annealing at 60 °C. Therefore, even if initially the average molecular weight between crosslinks is higher (due probably to the higher molecular weight of PEI compared to HDMA), once all the amine groups of PEI react, the net gets more tight and the average length between crosslinking points decreases more than for the case of HDMA, which only has two amine groups per molecule.

However, taking a look to the crosslinking % at RT derived from FTIR, it could be noticed that the rate was low, but steady. Therefore, the Blend film casted at RT was left at that temperature for 30 days, and its rheological properties were analysed by DMTA. Figure 3.5 presents the tan delta curves of Blend-PEI-7.7 film annealed at RT for 3 days and 30 days, and the same films annealed for 1 day more at 60 °C.

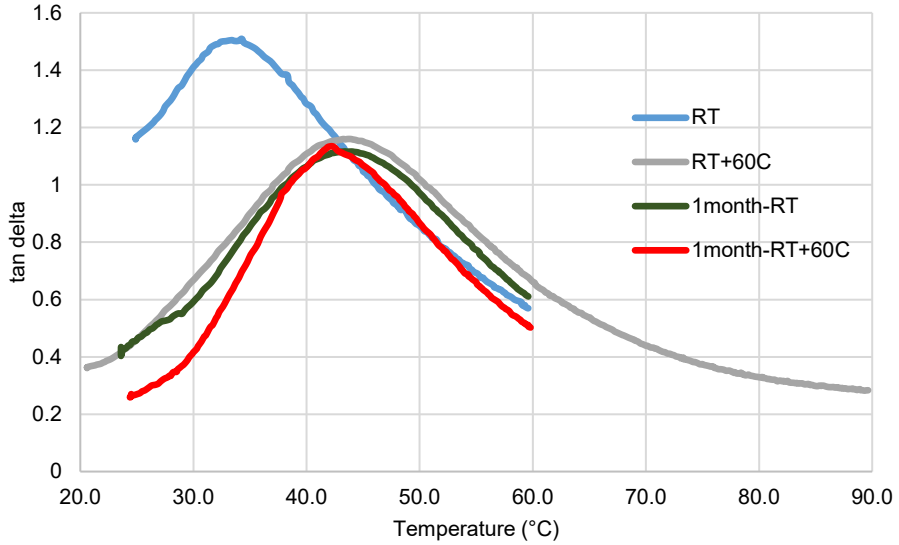

Figure 3.5. Comparison of tan delta curves of the Blend-PEI-7.7 film annealed at different T and time conditions.

Two main changes were found in tan delta curve of the Blend-PEI-7.7 annealed at RT 3 days and that of the film further annealed at 60 °C for one day. First, there was a decrease in the intensity of tan delta peak and the second change was the shift of the peak towards higher temperature (from 33 to 44 °C). The first change might appear because after annealing at 60 °C for 1 day full crosslinking was achieved, leaving a lower amount of amorphous phase and decreasing the segmental chain mobility, and the intensity of the peak. The reason for the second change was the formation of more crosslinked joints that increases the T_G value for sample

annealed at 60 °C. However, it can be noticed that the Blend-PEI-7.7 film annealed at RT for 30 days, presented the same tan delta curve as the film annealed at 60 °C for one day. And the curve was not further changed, when the Blend-PEI-7.7 films annealed for 30 days at RT was further annealed at 60 °C for one more day. Therefore, it can be concluded that full crosslinking can also be achieved at RT for this system, but with much longer drying times.

3.3.2. Evolution of polymer interparticle diffusion

FRET experiments were initially performed to measure the interdiffusion of polymer chains in the film formation process of crosslinked films. Two-labelled C-0 latexes were synthesized, one containing the labelled donor monomer and the second one containing the labelled acceptor monomer. In both cases, an average particle size of around 128-130 nm was achieved in the 42-44 % solids content latexes.

In order to follow the kinetics of the interdiffusion by FRET experiment, the first step was to find the position where the labelled monomer should be introduced. As it has been explained in the experimental section, the labelled monomers were fed in the first feeding stage (localizing the labelled monomers ideally in the first shell) or in the second feeding stage (localizing the labelled monomer in the second shell). Figure 3.6 presents a comparative study of the fluorescence decay in Blank-Blend-FRET system containing the labelled monomers in first shell with the system containing the labelled monomers in second shell. The fluorescence decay profile of Blank-Blend-FRET film (not containing any crosslinking moieties) containing the labelled monomer in second shell was similar both for the film dried at RT and for the annealed film, showing almost complete interdiffusion even at RT. The reason might be the presence of both labelled donor and acceptor monomers located very close to each other. However, in the case of labelled monomers located in the first shell of the polymer particles, the decay profile in

the film dried at RT and 60 °C differ, as it is slower at RT and faster when we annealed the film. It seems that in that case, both donor and acceptor are present far from each other in the film initially and therefore, we will be able follow the kinetics of the interdiffusion between the polymer particles if we locate the labelled monomers in the first shell.

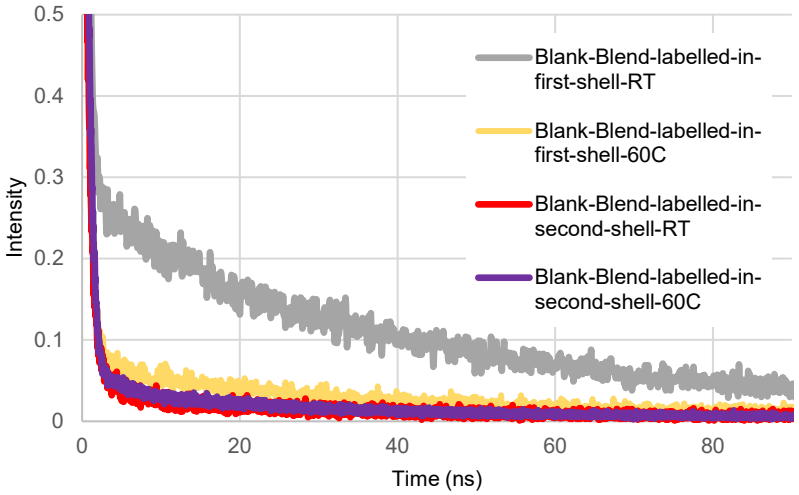

Figure 3.6. FRET experiment of blank blend film containing both donor and acceptor in the first and second shell.

Once the non-crosslinked films was analyzed, the crosslinked films were analyzed by FRET. Figure 3.7 presents the fluorescence decay profile of the blend films prepared by using different ratios of PEI (crosslinked films). It has been seen that the decay is fast and there is no difference in the decay profile while choosing different ratios of PEI. This fast decay would mean a high quantum efficiency energy transfer, and high interdiffusion of polymer chains even in the presence of crosslinking between polymer particles. However, in order to check if PEI itself can be affecting FRET experiment, a latex was prepared containing the donor monomer and PEI in the shell (without any acceptor in the film).

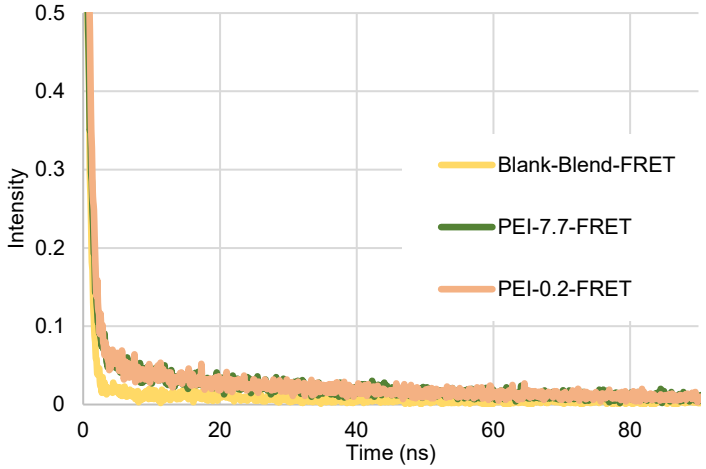

Figure 3.7. FRET experiment of crosslinked blend film (PEI-7.7-FRET and PEI-0.2-FRET) and Blank-Blend-FRET film.

Figure 3.8 presents the comparison of the fluorescence decay profile of the latex film prepared with only donor monomer, with the latex film containing donor monomer and PEI. In principle, the presence of PEI should not affect the decay profile, as it is not an acceptor monomer. However, it can be seen that PEI is accelerating the decay profile. If comparison is made with the blend films containing crosslinking moieties (Figure 3.9), it has been noticed that in all the systems the decay profile is almost same. Therefore, it can be concluded that the presence of PEI is affecting the flourescence decay of the donor monomer, and we cannot use FRET technique with these monomers to analyse the interdiffusion of polymer chains in this crosslinking system.

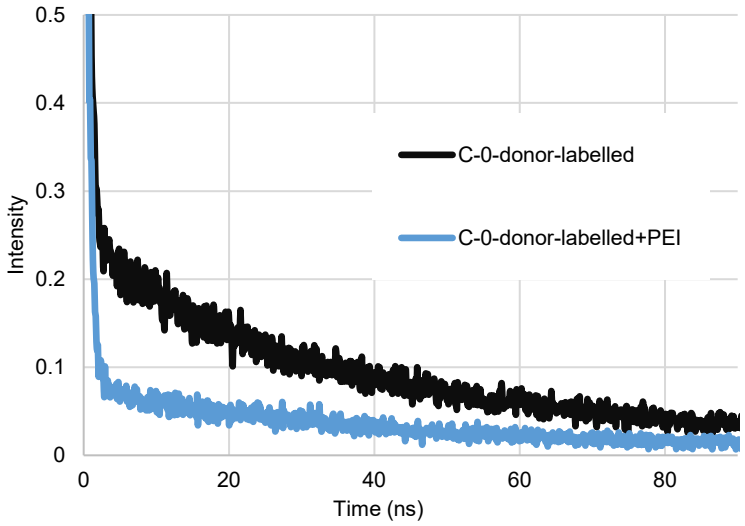

Figure 3.8. FRET experiment of a latex containing donor monomer in the absence and presence of PEI.

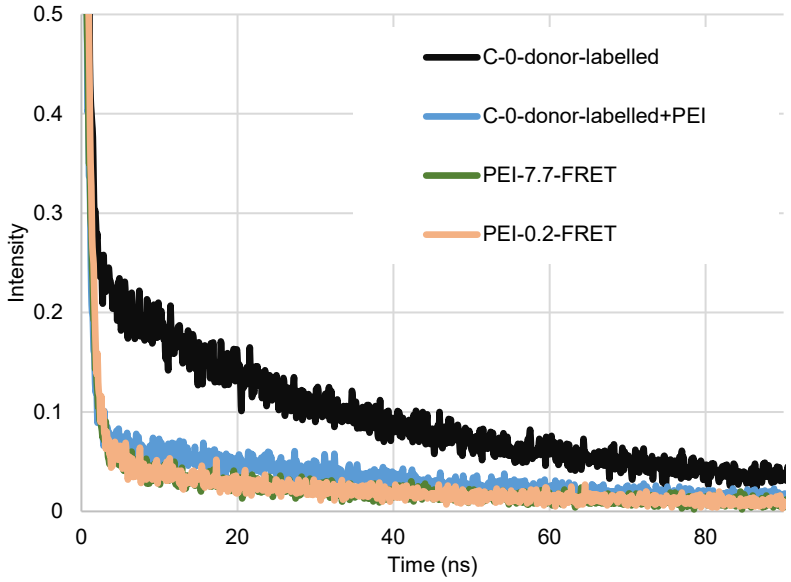

Figure 3.9. FRET experiment of latex containing donor monomer + PEI in the shell and crosslinked blends i.e, PEI 7.7-FRET and PEI-0.2-FRET.

Therefore, PEF approach was used to measure the interdiffusion. PEF experiments used 1-pyrene methyl methacrylate monomer for labelling the latexes. Labeled and unlabeled C-0 latexes were synthesized, with a particle size of 73 nm and a solids content of 37 wt % for the labelled latex and 90 nm particle size and 38 wt % solids content for the unlabelled latex. First, the interdiffusion was studied by PEF in a control non-crosslinked system. Therefore, a non-crosslinked control blend containing a 5/95 weight ratio of labelled C-0 latex to unlabelled C-0 latex was prepared, in the absence of any amine crosslinking moiety. Figure 3.10 shows the fluorescence spectra of this control film prepared at different temperature and annealing times.

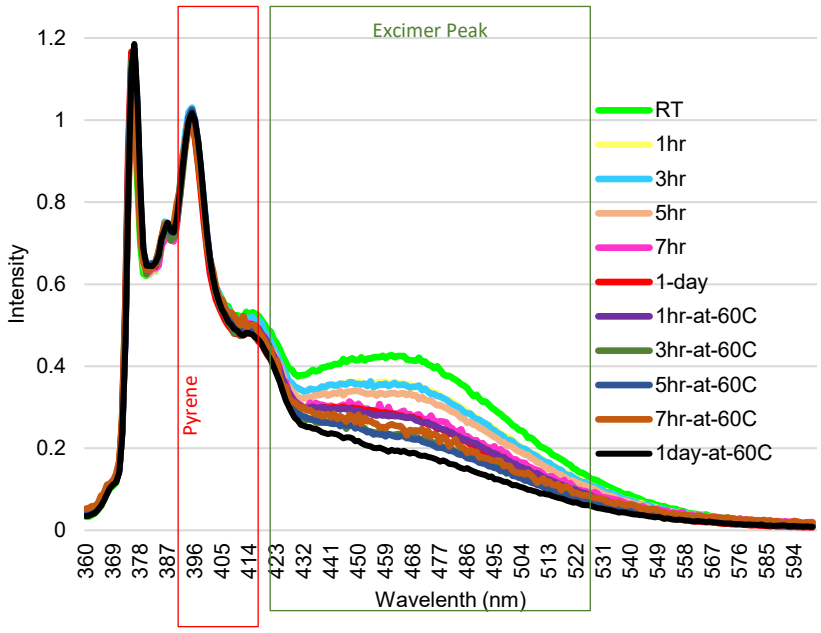

Figure 3.10. Fluorescence spectra of the uncrosslinked control blend latex film (Blank Blend-PEI) containing 5 % of labelled C-0 latex and 95 % of unlabelled C-0 latex, annealed at RT and 60 °C for different times.

The pyrene monomer fluorescence peak *(I_M)* appears in the region from 392 to 398 nm. The excimer emission (I_E) is located between 450 and 540 nm. The spectra in Figure 3.10 have

been normalized to the pyrene monomer fluorescence peak. It can be seen that during the film annealing process, the ratio between the intensity of the band associated to the excimer, and that of the monomer ($R = I_E/I_M$) decreases. The decrease in the excimer band can be explained by the decrease of the local concentration of pyrene containing polymer chains, as they diffuse out of the labelled particles into adjacent unlabelled ones. Then, the same procedure was applied to crosslinked blends, in which the labelled latex was surface modified with different PEI contents to produce C-2 labelled compounds. Figure 3.11 and 3.12 present the evolution of the fluorescence spectrum with time and temperature in the blend film 0.2-PEI-PEF and 7.7-PEI-PEF respectively. The spectra have been normalized to the pyrene monomer fluorescence peak.

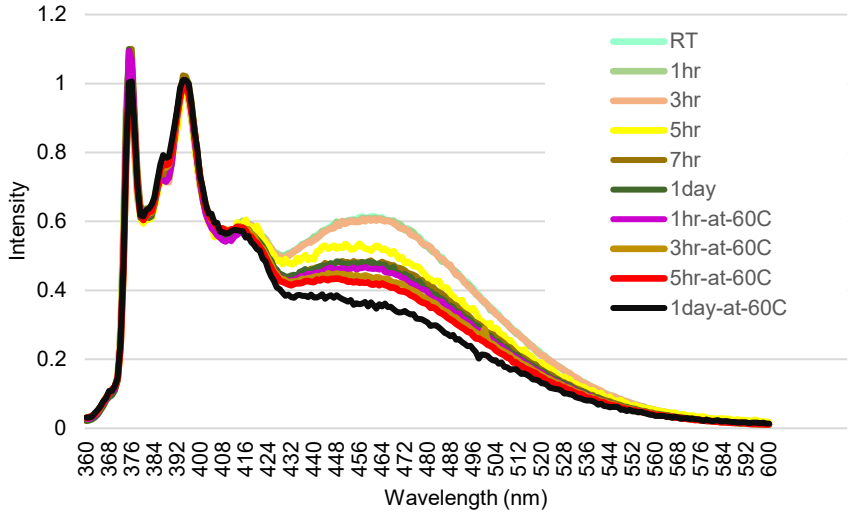

Figure 3.11. Evolution of interdiffusion by fluorescence (PEF) experiment of the crosslinked film 0.2-PEI-PEF dried at RT and 60 °C for different times.

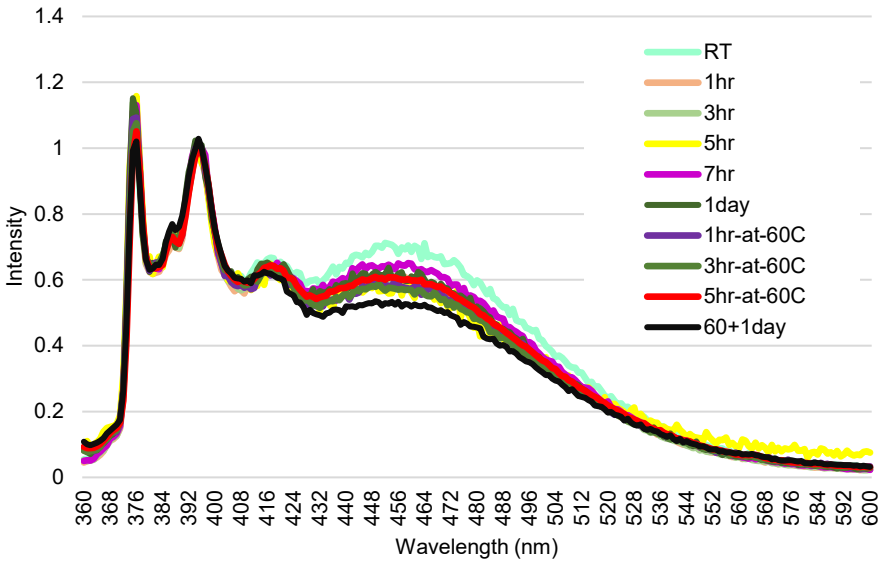

Figure 3.12. Evolution of interdiffusion by fluorescence (PEF) experiment of the crosslinked film7.7-PEI-PEF dried at RT and 60 °C for different times.

Figure 3.13 presents the evolution of I_E/I_M ratio with time and temperature in the non-crosslinked Blank-Blend-PEF film and in the crosslinked blend films. In the case of the Blank-Blend-PEF film, as seen in Figure 3.13, the I_E/I_M ratio decreases slowly at room temperature, to reach some kind of plateau after 24 hours, but it decreases further on annealing at 60 °C, to keep almost the same I_E/I_M ratio for further annealing at 60 °C. Therefore, it can be seen that polymer chains interdiffuse at RT (even if slowly) and there is a clear effect of temperature on speeding up the interdiffusion of polymer chains in this control system without crosslinking moieties. When crosslinking is included in the film, the interdiffusion extent changes depending on the PEI/AAEMA ratio. In case of blend “0.2-PEI-PEF”, the interdiffusion trend is similar to the non-crosslinked Blank-Blend-PEF, showing a first low interdiffusion extent at room temperature that is enhanced at 60 °C. However, the initial I_E/I_M values are higher for the “0.2-PEI-PEF” blend as compared to Blank-Blend-PEF, suggesting some kind of hindrance to

interdiffusion given by water molecules that could be retained by the hydrophilic PEI moieties. However, once those molecules would evaporate, the I_E/I_M ratio presents a sudden decrease, due to the interdiffusion of polymer chains among polymer particles. However, in case of the crosslinked "7.7-PEI-PEF" blend, the I_E/I_M ratio was maintained almost constant at RT and there was just a slight decrease while annealing at 60 °C, suggesting a negligible interdiffusion of polymer chains between polymer particles for this crosslinked system. According to Narayanaswami et al., the excimer to monomer intensity ratio (I_E/I_M) is reduced three fold when the distance between pyrene units goes from 5 Å to 20 Å.[21] Considering the values that are presented in Figure 3.13, it can be said that such reduction is observed for the Blank-Blend-PEF sample (when no crosslinking PEI was included in the sample). However, when a significant number of PEI moieities are inserted in "7.7-PEI-PEF" blend, the I_E/I_M ratio only reduced from 2.5 to 2.08 at the end on the annealing at 60 °C. Therefore, a movement of the pyrene having chains of less than 1 nm could be expected.

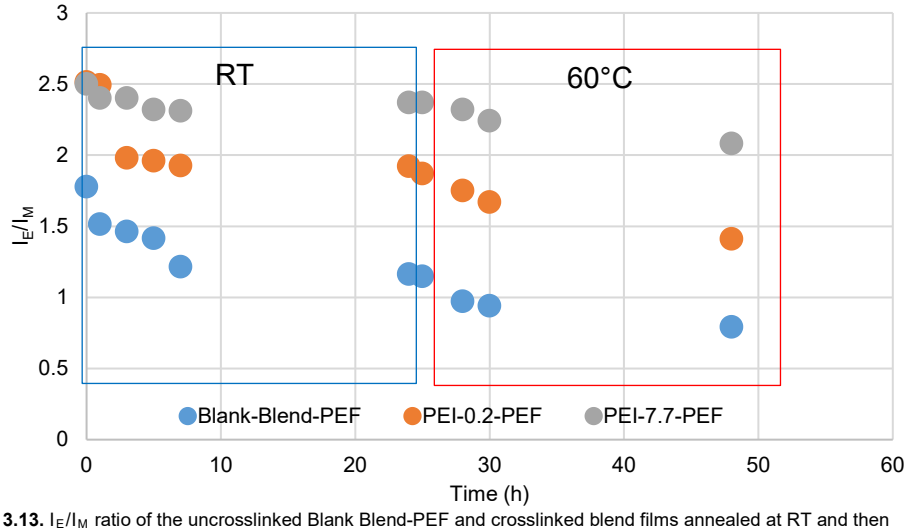

Figure 3.13. I_E/I_M ratio of the uncrosslinked Blank Blend-PEF and crosslinked blend films annealed at RT and then annealed at 60 °C for different times.

TEM analysis was carried out in order to see if the crosslinked Blend films (PEI-7 and PEI-0.2) presented defects or holes in its structure, as a consequence of this lack of polymer interdiffusion between polymer particles, or between C-1 and C-2 particles in the final film. Figure 3.14 shows the TEM images of the Blend film (PEI-7.7) annealed at RT and annealed at 60 °C, cryosectioned and stained with RuO_4. The amines moieties are stained with RuO_4 and appear dark in the interparticle spaces. Apparently, there is no difference in the TEM images of the film annealed at RT and that of the film annealed at 60 °C, but in a closer look it seems that boundaries are not that sharp in the annealed film as in the RT dried film. Figure 3.15 shows the TEM images of the Blend film (PEI-0.2) annealed at RT, cryosectioned and stained with RuO_4. The presence of slightly visible honeycomb structure indicated the presence of a lower amount of amines in the interparticle spaces, compared to PEI-7.7 blend.

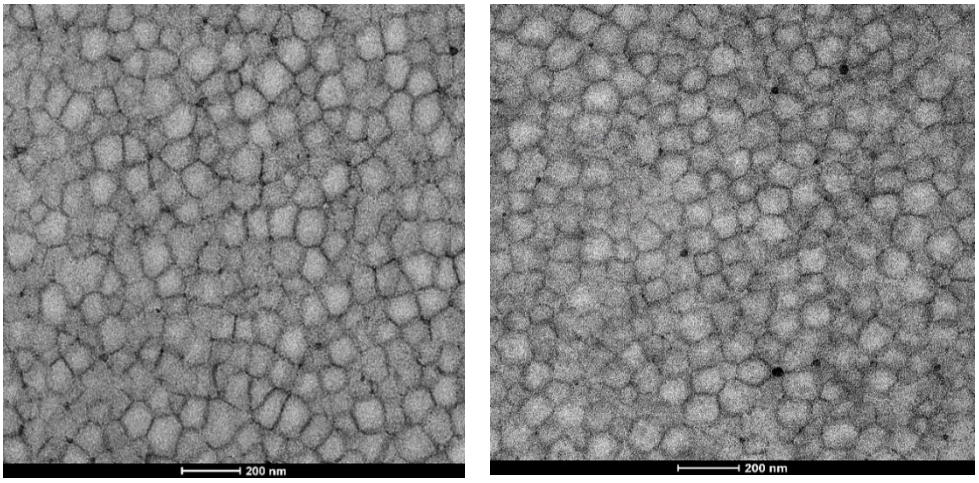

Figure 3.14. TEM images for Blend film (7.7 PEI) cryosectioned and stained for 5 min with RuO_4. The image on left was taken from the RT annealed film and right image from the film annealed at 60 °C.

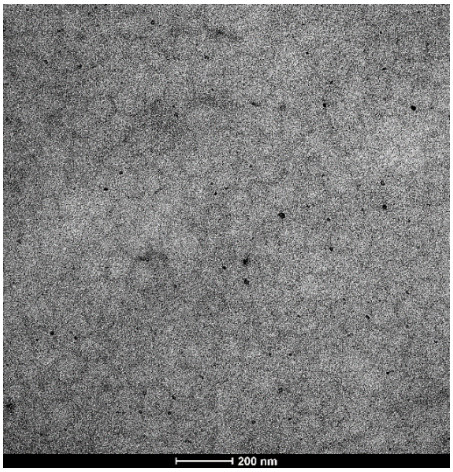

Figure 3.15. TEM images for Blend film (0.2-PEI) annealed at RT, cryosectioned and stained for 5 min with RuO_4.

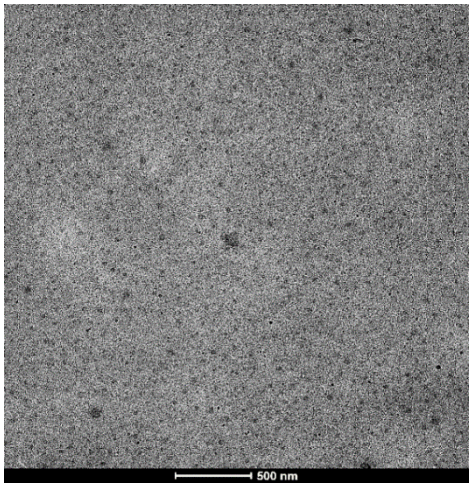

Figure 3.16. TEM image of Component-0 dried at RT, cryosectioned and stained for 5 min with RuO_4.

In order to confirm the presence of amines on the interparticle spaces, the TEM images of component-0 (Figure 3.16) has also been analysed. In that case it was seen that films were homogenous and there was no presence of any honeycomb structure as the one seen in Figure 3.16. Therefore, this image supported the presence of amines moieties in the interparticle

spaces of crosslinked blend films and moreover the formation of this honeycomb structure due to the crosslinking reaction of between C-1 and C-2 particles, which could hinder the interdiffusion of polymer chains between adjacent particles.

3.3.3. Mechanical properties

The effect of crosslinking and interdiffusion has also been studied by measuring the mechanical strength of films annealed 3 days at RT or with an extra annealing at 60 °C for another day. Figure 3.17 presents the mechanical properties of a non-crosslinked film (C-0), of the Blend containing 0.2 amine to AAEMA ratio in C-2 and of the Blend containing 7.7 ratio.

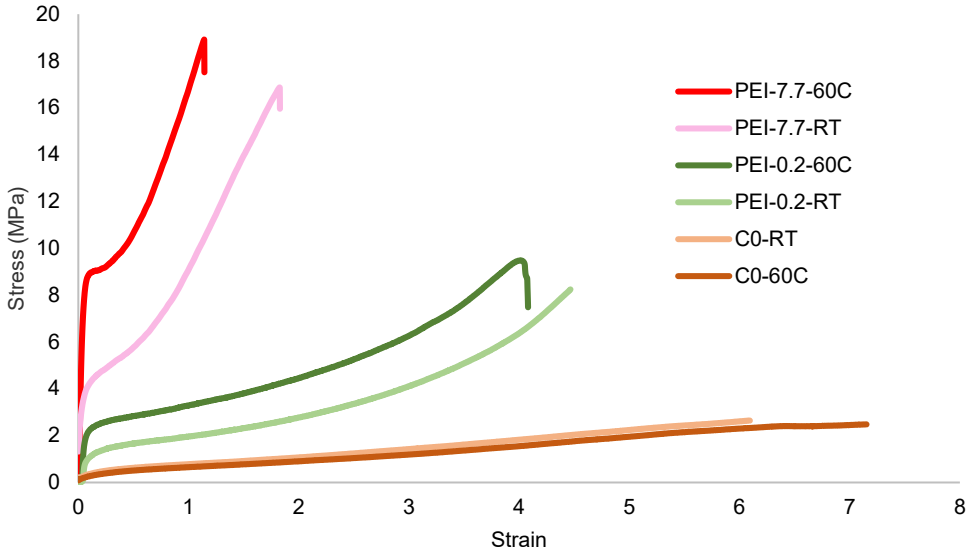

Figure 3.17. Comparison of tensile test for Blend films prepared at room temperature and 60 °C.

For the non-crosslinked C-0 film, the mechanical properties did not significantly vary when the film was annealed at RT or at 60 °C. Figure 3.13 showed that the interdiffusion was just

slightly further increased when annealing the non-crosslinked film at 60 °C, which could be the reason for the slightly higher elongation (from 6 to 7 %) at break for the annealed film. However, annealing at 60 °C had a significant effect on the films when the crosslinking PEI moiety attached to C-2 was included. The Young's modulus of the films increased significantly (modulus increased from 54 (±5) MPa to 206 (±10) MPa) when annealing the films at 60°C. As shown previously by FTIR and rheological measurements, full crosslinking was only achieved after annealing the films at 60 °C for 24 hours, which would be the reason for the increase of the Young's modulus and decrease of the elongation at break of the films annealed at those conditions. Furthermore, a significant effect of the amount of PEI used to produce C-2 can also be detected. 0.2 ratio of amine/AAEMA produces some crosslinking points between polymer particles, producing stronger films (modulus increased from 11 (±3) MPa to 32 (±5) MPa) than non-crosslinked C-0 film, but 7.7 ratio increases even more the strength of the films. Therefore, the higher interdiffusion between particles produced in 0.2 PEI film cannot compensate the higher crosslinking degree of 7.7 PEI film.

In order to check if higher PEI ratios could lead to higher mechanical properties, a NH-AAEMA ratio of 15 was also tried to prepare C-2. A ratio of 4 NH-AAEMA was also included in the study. In Figure 3.18, the comparison between the tensile test of the blend films having different ratio of amine / AAEMA is presented. It has been seen that modulus increases from 0.2-PEI to 4-PEI and it further increases in case of PEI-7.7. However, when we use PEI-15 (that contained almost double amine as compared to PEI-7.7), the modulus decreased. The results indicate that the presence of more amount of PEI acted negatively in developing the stiffness of the film. The reason might be the presence of the extra amount of PEI acting as a softener of the film. Therefore, it has been concluded that there is a limit in using the PEI with reference to AAEMA in this system and if the limit is crossed, the film becomes soft.

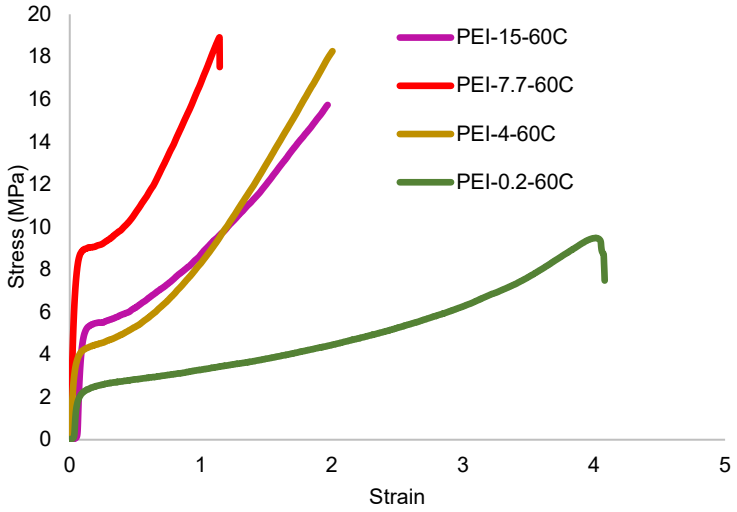

Figure 3.18. Comparison of tensile test for blend films annealed at 60°C having different amine / AAEMA ratio.

Until now, the PEI used in the system was LUPASOL G-20, with an average molecular weight of 1300 g/mol. In this investigation, we also used PEI with larger molecular weight i.e., LUPASOL G-35, with average molecular weight of 2000 g/mol. Figure 3.19 presents the comparative study of the tensile test in both systems (G-20 and G-35) dried at RT and 60°C, together with the films crosslinked with linear HMDA. We can infer from the comparison that in the three cases, some activation energy in the form of temperature was required for the full crosslinking of the systems. However, in case of G-35, the difference between RT (less stiff as compared to G-20) and annealed film is more, meaning that RT dried film has to overcome a higher barrier to achieve crosslinking as compared to films using G-20.The reason was the chemical structure of G-35, that is more bulky as compared to G-20. However, after annealing both films showed similar stiffness. If we compare these mechanical properties with the ones obtained with HDMA instead of with PEI, it can be seen that the mechanical properties have been greatly improved by the PEI containing multiple amine groups, and therefore favoring a more 3D crosslinked network.

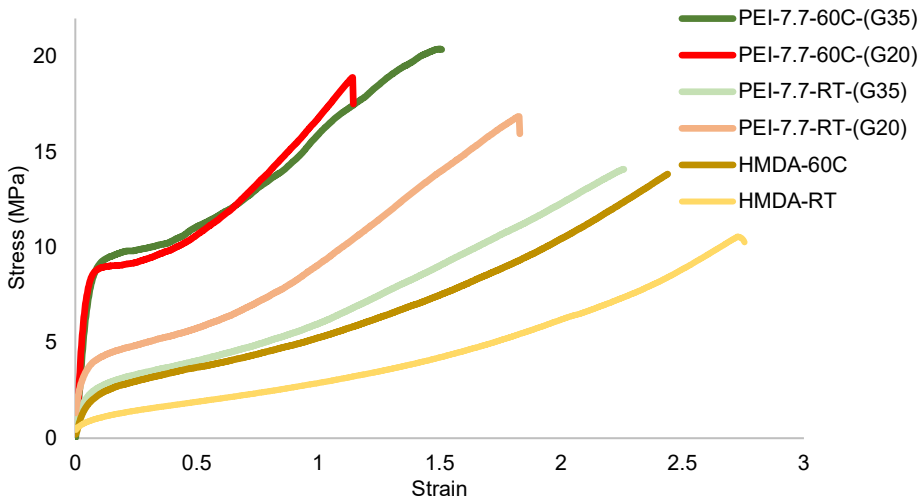

Figure 3.19. Tensile tests results of blend films dried at RT and 60ºC for PEI-LUPASOL G20, PEI-LUPASOL G35 and HMDA crosslinked films.

Therefore, taking into consideration the crosslinking and the interdiffusion studies carried out, it seems that the crosslinking reaction is occurring on the shell and it is occurring before interdiffusion of the polymer chains between particles to produce a strong film (Figure 3.20).

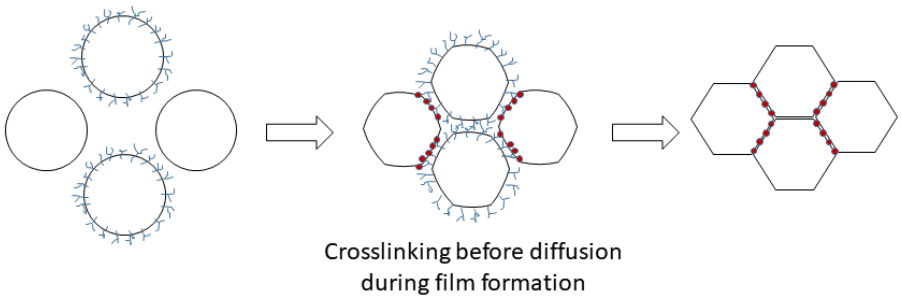

Figure 3.20. Film formation route for polymers presenting interparticle crosslinking reactions.

3.4. Conclusions

In this chapter, latex particles functionalized with acetoacetoxy moieties have been blended with latex particles functionalized by the amine moieities provided by Polyethyleneimine, in order to provide strong films by interparticle crosslinking during film formation. Therefore, the reacting species were linked to different particles and not solubilized in the aqueous phase. It has been proved by FTIR and rheological measurements that once the two-pot-one-pack latex is cast, crosslinking reactions between amine and acetoacetoxy moieities start to occur at room temperature, but they evolve very slowly at this temperature, needing one month to get full crosslinking. However, annealing at 60 °C speeds up the crosslinking reactions, being completed after 24 hours. On the other hand, in order to study the interdiffusion of polymer chain during film formation, FRET experiment has been performed. The approach cannot be used in this crosslinked system because the presence of polyethyleneimine in the crosslinked blends affect the flourescence decay profile of the donor monomer. Therefore, PEF experiments were performed. PEF experiments have shown that the interdiffusion between particles is negligible when crosslinking between particles occur at high amine concentration on the surface of the particles. Nevertheless, the lack of interdiffusion did not prevent from obtaining strong films for the highest crosslinked Blend film. In fact, the crosslinked Blend in which more interdiffusion was obtained at the expense of reducing the crosslinking density, by including a lower amount of amine moieties in component-2, did not present so high mechanical properties. There is also a limit of using amine moities in the preparation of component-2, the film becoming soft when excess amount of amine was used. Moreover, the size of amines used for the preparation of component-2, also plays an important role, as amines with larger chain size i.e., G-35 with Mw of 2000 g/mol, presented lower mechanical properties after being dried at room temperature, as

compared to PEI with smaller chain length i.e., G-20 (1300 g/mol). Nevertheless, similar properties were obtained when both films were annealed at 60 ºC.

3.5. References

[1] M. Ooka, H. Ozawa, Recent developments in crosslinking technology for coating resins, Prog. Org. Coatings. 23 (1994) 325–338. https://doi.org/10.1016/0033-0655(94)87002-0.

[2] J. Feng, H. Pham, P. Macdonald, M.A. Winnik, J.M. Geurts, H. Zirkzee, S. Van Es, A.L. German, Formation and crosslinking of latex films through the reaction of acetoacetoxy groups with diamines under ambient conditions, J. Coatings Technol. 70 (1998) 57–68. https://doi.org/10.1007/bf02730151.

[3] A. Zosel, G. Ley, Influence of Cross-Linking on Structure, Mechanical Properties, and Strength of Latex Films, Macromolecules. 26 (1993) 2222–2227. https://doi.org/10.1021/ma00061a013.

[4] F. Tronc, R. Liu, M.A. Winnik, S.T. Eckersley, G.D. Rose, J.M. Weishuhn, D.M. Meunier, Epoxy-functionalized, low glass-transition temperature latex. I. Synthesis, characterizations, and polymer interdiffusion, J. Polym. Sci. Part A Polym. Chem. 40 (2002) 2609–2625. https://doi.org/10.1002/POLA.10319.

[5] M.A. Winnik, Interdiffusion and crosslinking in thermoset latex films, J. Coatings Technol. 74 (2002) 49–63. https://doi.org/10.1007/BF02720150.

[6] C. Pichot, Recent developments in the functionalization of latex particles, Makromol. Chemie. Macromol. Symp. 35–36 (1990) 327–347. https://doi.org/10.1002/masy.19900350120.

[7] J.M. Geurts, J.J.G.S. Van Es, A.L. German, Latexes with intrinsic crosslink activity, Prog. Org. Coatings. 29 (1996) 107–115. https://doi.org/10.1016/S0300-9440(96)00623-6.

[8] A. Aradian, E. Raphaël, P.G. De Gennes, Strengthening of a Polymer Interface: Interdiffusion and Cross-Linking, Macromolecules. 33 (2000) 9444–9451. https://doi.org/10.1021/MA0010581.

[9] C.A. Córdoba, S.E. Collins, M.C.G. Passeggi, S.E. Vaillard, L.M. Gugliotta, R.J. Minari, Crosslinkable acrylic-melamine latex produced by miniemulsion polymerization, Prog. Org. Coatings. 118 (2018) 82–90. https://doi.org/10.1016/J.PORGCOAT.2018.01.013.

[10] E.C. Galgoci, P.C. Komar, J.D. Elmore, High performance waterborne coatings based on dispersions of a solid epoxy resin and an amine-functional curing agent, J. Coatings Technol. 71 (1999) 45–52. https://doi.org/10.1007/BF02697895.

[11] E.M. Boczar, B.C. Dionne, Z. Fu, A.B. Kirk, P.M. Lesko, A.D. Koller, Spectroscopic Studies of Polymer Interdiffusion during Film Formation, Macromolecules. 26 (1993) 5772–5781. https://doi.org/10.1021/ma00073a035.

[12] G.D. Wignall, A. Klein, G.A. Miller, L.H. Sperling, Film Formation from Latex: Hindered Initial Interdiffusion of Constrained Polystyrene Chains Characterized by Small-Angle Neutron Scattering, J. Macromol. Sci. Part B. 27 (1988) 217–231. https://doi.org/10.1080/00222348808245763.

[13] K. Hahn, G. Ley, H. Schuller, R. Oberthür, On particle coalescence in latex films, Colloid Polym. Sci. 264 (1986) 1092–1096. https://doi.org/10.1007/BF01410329.

[14] Y. Wang, M.A. Winnik, Polymer diffusion across interfaces in latex films, J. Phys. Chem. 97 (2002) 2507–2515. https://doi.org/10.1021/J100113A008.

[15] Y.S. Liu, J. Feng, M.A. Winnik, Study of polymer diffusion across the interface in latex films through direct energy transfer experiments, J. Chem. Phys. 101 (1998) 9096. https://doi.org/10.1063/1.468488.

[16] R. Casier, M. Gauthier, J. Duhamel, Using Pyrene Excimer Fluorescence To Probe Polymer Diffusion in Latex Films, Macromolecules. 50 (2017) 1635–1644. https://doi.org/10.1021/ACS.MACROMOL.6B02726.

[17] S. Farhangi, J. Duhamel, Probing Side Chain Dynamics of Branched Macromolecules by Pyrene Excimer Fluorescence, Macromolecules. 49 (2015) 353–361. https://doi.org/10.1021/ACS.MACROMOL.5B02476.

[18] G.P.C. Drummen, Fluorescent probes and fluorescence (microscopy) techniques-illuminating biological and biomedical research, Molecules. 17 (2012) 14067–14090. https://doi.org/10.3390/molecules171214067.

[19] S. Tariq, L. Irusta, M. Fernández, M. Paulis, Kinetic study of crosslinking between acetoacetoxy and hexamethylene diamine functionalized waterborne latexes in two-pack systems, Prog. Org. Coatings. 165 (2022) 106732. https://doi.org/10.1016/J.PORGCOAT.2022.106732.

[20] M.J. Collins, J.W. Taylor, Stable amino-containing polymer latex blends. US5998543., (1997).

[21] G.K. Bains, S.H. Kim, E.J. Sorin, V. Narayanaswami, The extent of pyrene excimer fluorescence emission is a reflector of distance and flexibility: Analysis of the segment linking the LDL receptor-binding and tetramerization domains of apolipoprotein E3, Biochemistry. 51 (2012) 6207–6219. https://doi.org/10.1021/bi3005285.

Chapter 4.

Effect of different particle size and T_G on acetoacetoxy-amine based crosslinking.

4.1. Introduction

In Chapter 3, the acetoacetoxy and amines based crosslinking chemistry between latexes having the same copolymer composition and particle size has been presented, as a way to overcome the film formation dilemma of waterborne coatings. As it was presented in the Introduction to this PhD, there have been different approaches to beat this dilemma, and in this chapter one of them, namely the use of blends of hard and soft particles with the same or with different particles, will be combined with the interparticle crosslinking approach. It has been extensively reported that the use of blends of hard and soft particles presents advantages from the film formation and final properties point of view, and it is a simpler approach compared to the production of hybrid particles containing both polymer phases. [1,2] The idea lying behind the blend is the reinforcement offered by the hard phase polymer, to the film forming soft phase polymer, which allows at the end the production of harder films with lower plasticizer contents. [3-9]

Apart from the different T_G of the latexes contained in the blend, the effect of using different particle sizes has also been studied by different researchers. Therefore, while for blends of latexes having similar particle size but different T_G phases, the minimum film formation

temperature (MFFT) starts increasing above volume fractions of the hard phase above 55 %,[10] or 70 % in case of semycrystalline hard phase, [11] this volume fraction limit changes when the particle sizes of each polymer phase are not the same. In fact, it has been reported that the MFFT increases as the ratio between the particle size of the soft phase and that of the hard phase (d_{soft}/d_{hard}) increases for a given volume fraction of hard particles.[6,12] This can be explained by the lower fraction of hard particles needed to create a hard phase network when d_{soft}/d_{hard} is high.

The main aim when it comes to use different particle sizes is to maximize the packing of particles in the film, leaving the minimum interstitial spaces as possible. It has been reported that maximum packing can be achieved by using five or more size particles, as a void fraction of just 0.0384 could be achieved in this case.[13] However, this approach seems to be unrealistic in some of the application areas. An alternative approach was proposed by the Kusy by introducing the concept of phase continuity.[14] According to Kusy, the optimal packing can be achieved when small particles act as a continuous phase around the big particles. The concept has been applied by Eckersley and Helmer in bimodal blends.[6] In this strategy, the minimum volume required to provide maximum packing is considered as the critical volume, V_c. Figure 4.1 presents the critical volume calculation based on the Kusy assumption, where it can be seen that the value of V_c depends on the size ratio between large and small particles.

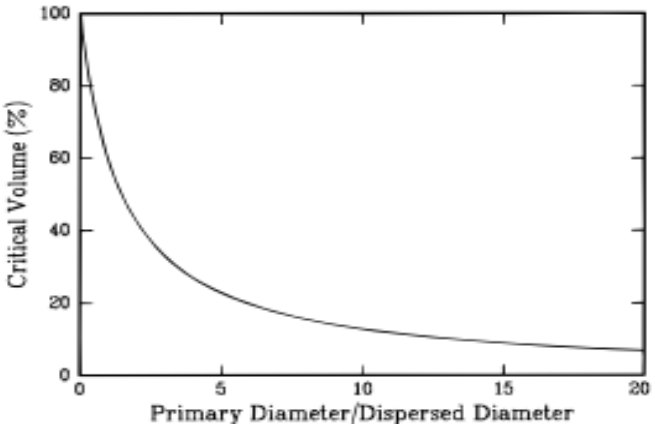

Figure 4.1. Critical volume (%) required to achieve closed packing for system containing different particle size.[15] The critical volume percentage has been prepared by using Kusy equation.[14]

Tzitzinou and coworkers applied a similar strategy of critical volume fraction calculation to prepare minimum void containing films with a bimodal system.[15] The authors prepared different blends containing different sizes and different hardness of polymer particles for the preparation of polymer films. When a ratio of 6:1 for large-soft to small-hard particles size was used, the volume fraction of small-hard particles (V_c) was around 0.18. In fact, for volume fractions of 0.18 of hard phase small particles, continuous and crack free films were produced. However, at hard particles volume fractions above this value, voids and nanocracks could be observed in the films.[15] A similar ratio of 80/20 of volume fraction in large particles to small particles was also observed by Peters and coworkers, when blending particles of 350 and 50 nm ($dp_{large}/dp_{small}=7$) for the best performance in terms of particles packing, reduced water absorption and better mechanical properties of the films.[5] Similar improvements in mechanical properties, blocking resistance and elastic modulus have been found by other authors when blending hard and soft particles with the adequate volume fractions in order to obtain a percolating network of hard particles around the soft particles.[6,16,17] Pedraza and Soucek presented an interesting study on the effect of particle size in melamine-formaldehyde

crosslinked latex system.[18] They made blends of small (around 50 nm) and large particle (around 350 nm) latexes with and without hydroxyl functionality on their surface, before mixing them with the melamine-formaldehyde crosslinker. They saw that the tensile properties were mainly increased when the small particles contained the hydroxyl functionalities, as the phase continuity of crosslinked small particles was much easier in this way.

Nevertheless, the risk of stratification should not be forgotten when latexes with different particle sizes are blended.[19,20] This problem is more acute when low solids content latex blends are being dried, as the time needed for the final film formation is higher, allowing more time for particle segregation by size. In any case, it should not be neglected in high solids content latexes too, as small segregation effects may lead to the separation from the optimum packing situation.

Therefore, this chapter comprises two main parts. In the first part, preliminary studies of the AcAc-Amine based crosslinking chemistry have been carried out in blends of latexes with different particle sizes and T_G. In this preliminary study, the mechanical properties and the water resistance properties have been compared to the system with similar particle size and T_G, and the stratification or phase segregation has been analyzed by microscopic techniques. After seeing the potential of this preliminary study, in the second part of the chapter, the different blends produced at a larger scale will be presented. These latex blends will be used as binders for a coating formulation in Chapter 5. Nevertheless, their behavior as binders is presented in this Chapter 4.

4.2. Experimental

4.2.1. Preliminary experiments

4.2.1.1. Synthesis of large and soft particles latex

To prepare large and soft particles, we have followed the recipe shown in Tables 4.1 and 4.2.

Table 4.1. Formulation used to produce the seed by batch emulsion polymerization for the preparation of large and soft particles latex.

Ingredients	Seed Formation
Methyl methacrylate	11.42
Butyl acrylate	11.42
Water	76.47
Dowfax 2A1	0.46
$K_2S_2O_8$	0.23

Table 4.2. Formulation used for the synthesis of MMA/BA/AAEMA latex with large and soft particles by semibatch emulsion polymerization.

Ingredients	Initial Charge (g)	Stream-1 Growth of the seed (g)	Stream-2 (g)
Seed amount	28.8		
Methyl methacrylate	1.46	140.5	
Butyl acrylate	1.46	140.5	
Acetoacetoxy ethyl methacrylate (AAEMA)		15.6	
Water	240	50	50
Dowfax 2A1		2.4	
Methacrylic Acid		2.78	
$K_2S_2O_8$	0.5		1

First, the seed was synthesized by batch emulsion polymerization (Table 4.1). Then, the growth of the seed was carried out by semi continuous emulsion polymerization. The initial charge of 28 g of seed latex, water and small amount of monomers were added to the reactor. The initial charge was purged with nitrogen for 15 minutes, after that a fraction of initiator was added. When a small increase of the temperature was observed, which meant the reaction began, the rest of the ingredients were added in two different streams. The feeding rate for the first stream was 2.65 g/min and for second one 0.22 g/min. When 50 % of feeding was completed, 15.6 g of AAEMA was added in the preemulsion of stream 1 (Table 4.2). This way a latex with a solids content of 47 % and 273 nm particle size was achieved, with a T_G of 22 ºC.

Component-2 was prepared from this latex by reacting it with polyethyleneinimine (PEI) by using the mol ratio of 7.7: 1 between N-H of PEI: AAEMA. Component-1 was also prepared from this latex by mixing it with NH_4OH (2:1, NH_4OH: AAEMA ratio).

4.2.1.2. Synthesis of small and soft particles latex

For the preparation of the seed, we used the recipe presented in Table 4.3. The seed quantity used for the following feeding stage was 62.1 g, which is 30 to 70 ratio of seed to feed monomers used in next stage. The formulation used for feeding is also presented in Table 4.3. The feeding rate was 0.23 g/min.

Table 4.3. Formulation used to produce the seed by batch emulsion polymerization and the final latex by semibatch emulsion polymerization for the synthesis of MMA/BA/AAEMA latex having small soft particles.

Ingredients	Seed (g)	Feed (g) Addition of functional monomer
Methyl methacrylate	31.29	12.23
Butyl acrylate	31.34	12.15
Water	250.31	14.24
SLS	1.255	0.492
$NaHCO_3$	0.326	
Disponil A3065		0.662
Methacrylic Acid		0.20
$K_2S_2O_8$	0.31	0.1
Acetoacetoxy ethyl methacrylate (AAEMA)		2

This way a latex with a solids content of 37 % with 87 nm particle size was achieved. The component-1 was prepared from this latex by mixing it with NH_4OH with the mol ratio of 2:1 between NH_4OH and AAEMA.

4.2.1.3. Synthesis of small and hard particles latex

First, a batch emulsion polymerization was used for the preparation of the seed (Table 4.4). 42.78 g of this seed was used for the subsequent growing by semibatch emulsion polymerization, with a 10 to 90 ratio of seed to monomers used in next two stages. The formulation used for next two feedings is also presented in the Table 4.4. The feeding rate for first and second stage of feeding was 0.442 g/min and 0.23 g/min respectively. A latex with a solids content of 43.5 % and 130 nm particle size was achieved with a T_G of 44.5°C. The prepared latex was used to prepare component-2 by reacting the latex with PEI.

Table 4.4. Formulation used to produce the seed by batch emulsion polymerization and the final latex by semibatch emulsion polymerization for the synthesis of MMA/BA/AAEMA with small particle size and high T_G latex.

Ingredients	Seed (g)	First Shell (g) Growth of the seed	Second Shell (g) Addition of functional monomer
Methyl methacrylate	43.7	34.31	17.06
Butyl acrylate	18.7	14.07	7.31
Water	250.31	27.92	45.74
SLS	1.255	0.99	0.49
$NaHCO_3$	0.326		
Disponil A3065		1.34	0.662
Methacrylic Acid		0.467	0.20
$K_2S_2O_8$	0.31	0.2	0.1
Acetoacetoxy ethyl methacrylate (AAEMA)			4.4

4.2.1.4. Blend Formation

Two different blends were prepared from these preliminary latexes. Initially a blend with latexes having different particles size and same co-monomer composition (same T_G) was prepared. In this case, as the particle size difference between big and small particles was around 3.3, the critical volume of 30% was chosen, following the work of Kusy.[14] Therefore, 30 % of component-1 polymer phase (small soft particles latex) and 70 % of component-2 polymer phase (large soft particles latex) were chosen for the preparation of the blend to get a maximum packed film.

On the other hand, in order to prepare a system having different particle size and T_G, as the particle size difference was not high, equal amounts of both components were selected to prepare the blend film.

4.2.2. Higher scale latex synthesis

Once the potential of blending different particle size and T_G latexes was assessed in the preliminary studies, a broader study of such systems was planned, with the aim to later formulate them in BASF. Four latexes were synthesized in a higher scale as shown in Appendix I, following the seeded semibatch emulsion polymerization technique, namely:

- Latex with larger particle size and softer particles: Latexes 1_LS and 2_LS
- Latex with smaller particle size and softer particles: Latexes 3_SS and 4_SS
- Latex with larger particle size and harder particles: Latex 5_LH
- Latex with smaller particle size and harder particles: Latex 6_SH

4.2.2.1. Blend Formation

Based on the experience with the preliminary experiments, four different blends were prepared from these latexes. In the first one, the effect of different particle size was only considered in the blend, so the blend LS-SS was prepared. In the next two, both particle size and T_G were different in the blend, so blends LS-SH and LH-SS were prepared. Finally, in blend SS-SH, both latexes had the same particle size but different T_G. Table 4.5 presents the different blends prepared, showing as well which latex was used as component-1 and component-2 in each case.

Table 4.5. Compositions of the different blends produced based on latexes with different particle size and T_G.

System	Composition		Non-crosslinkable dispersion	Crosslinkable dispersion
	Component-1	Component-2		
LS-SS	1_LS (73 %)	3_SS (27%)	Ref_blend LS-SS	Blend LS-SS
LS-SH	2_LS (73 %)	6_SH (27 %)	Ref_blend LS-SH	Blend LS-SH
LH-SS	5_LH (50%)	4_SS (50 %)	Ref_blend LH-SS	Blend LH-SS
SS-SH	6_SH (50 %)	3_SS (50%)	Ref_blend SH-SS	Blend SH-SS

It should be noted that when different particle sizes were used in the blends, the initial idea was to have a 73 % / 27 % of polymer in the large and in small particles respectively, in

order to be close to the maximum packing condition. However, when system LH-SS was tried with a ratio 73/27, the minimum film formation temperature (MFFT) was above 30 ºC, which was not interesting from the application point of view. Therefore, in this case, a 50/50 ratio was selected, which produced a MFFT below room temperature. Furthermore, for the case in which similar particle sizes were mixed (SH-SS), equal amounts of both components were used.

Furthermore, Ref_blend and Blend samples were prepared. In the case of the reference blends, they were prepared just blending the two latexes, without converting them into component-1 and component-2 by reacting them with the NH_4OH or the PEI. Therefore, these blends are reference non-crosslinkable blends. On the other hand, component-1 and component-2 were prepared before producing the Blends, in the crosslinkable systems.

4.2.3. Latex and film characterization

The solids content of the seed and the latex was obtained gravimetrically, and it was used to analyse the evolution of the conversion during the polymerization reaction. The particle size of polymer particles was measured by Dynamic Light Scattering, DLS (Malvern® Zetasier Nano). For the analysis, samples were diluted to such a low concentration that it can safely be assumed that no monomer was present in the polymer particles, namely that the unswollen particle sizes were measured.

Tensile tests of the free standing films annealed at room temperature (23 °C with relative humidity of 55 %) and at 60 °C were performed on Universal testing machine TA.HD plus Texture Analyser at a crosshead speed of 0.42 mm/s. Samples with approximate length of 55 mm and 0.55 mm of thickness were used.

The morphology of films was studied by means of Transmission Electron Microscopy (TEM). TEM analysis was carried out with a TecnaiTM G2 20 Twin device at 200 kV (FEI Electron

Microscopes). The films were cryosectioned with a Leica EMUC6 cryoultramicrotome at 30 °C below the T_G of the sample, with a Diatome 45° diamond 30 knife, and the observations were made in the microscope (TEM), after RuO_4 staining.

To carry out the surface analysis of the film by drop casting and morphology analysis of the cross-section of the film, Atomic Force Microscopy (AFM) measurements were performed. AFM images were obtained using a Bruker dimension icon atomic force microscope equipped with the Nano Scope V Controller (Bruker), operating in Tapping mode. An integrated silicon tip/cantilever (TESP-V2, Bruker) with a resonance frequency of 320 kHz and nominal constant of 37 N/m was used. To determine the cross-section, samples were cut on a Leica FC6 cryoultramicrotome, at -25 °C.

In order to study the chemical resistance, first MEK double rub test was performed by following ASTM D4752-03 standard pattern. Latex films were cast on black panels with constant wet thickness of 250 µm. The films were dried for one day at RT and then annealed for one day at 60 °C. Once the films were prepared, a cheese cloth was folded in the index finger and then soaked in MEK solvent. The test was started by placing the index finger at 45 degree on the latex film and moving it forward and backwards. The test and the counting of the number of cycles was stopped (double rub), when MEK started scratching the film.

The samples for water absorption test were prepared from the casting of the latex or blends at room temperature and then annealed at 60 °C for one day. Polymer films with thickness of 0.5 mm were prepared and then immersed in deionized high-purity water. For the analysis, the samples were weighted after different time intervals.

Differential scanning calorimetry (DSC) analysis was performed to measure glass transition temperature (T_G) on a DSC, Q 2000, TA Instrument. The T_G was measured at a heating rate of 10 ºC/min with a temperature range of -50 ºC to 200 ºC.

Dynamic Mechanical Thermal Analysis (DMTA) were carried out using a dynamic mechanical thermal analyser DMA Q800, TA instruments with single cantilever tension geometry. We investigated the rheological properties by calculating the E', E" and tan delta at increasing temperature ramps of 4 °C /min.

For the kinetic analysis of the evolution of the crosslinking reaction, FTIR spectra were recorded using a Nicolet iS50 equipment. The spectra were registered with the resolution of 4 cm^{-1} with scan number 32. The samples were prepared by casting over CaF_2 support. The RT film formation was carried out at 23 °C with relative humidity of 55 % and for high temperature treatment, the film was placed in an oven with static air at 60 °C.

4.3. Results and Discussions

4.3.1. Preliminary experiments

4.3.1.1. Blends with different particle size and same T_G latexes

In this section, the preliminary results from the system having different particles size but the same hardness is presented. Therefore, component-1, having a solids content of 37 % with 87 nm particle size, and component-2 having a solids content of 47 % and 273 nm particle size

were blended with 30 / 70 polymer ratio of component-1 and component-2. There was no signs of coagulation during blend formation.

The mechanical properties of the polymer films obtained from the blends produced from different particle size latexes were studied using tensile test. Tensile strength and brittleness in the film was monitored. The effect of curing temperature was analysed by annealing the films at 60 °C. Figure 4.2 presents the mechanical properties of the films prepared from the blend films dried at RT and 60 °C. For comparison purposes, the data obtained for blends prepared with the same particle size in component-1 and component-2 (Chapter-3) have been also included in this graph.

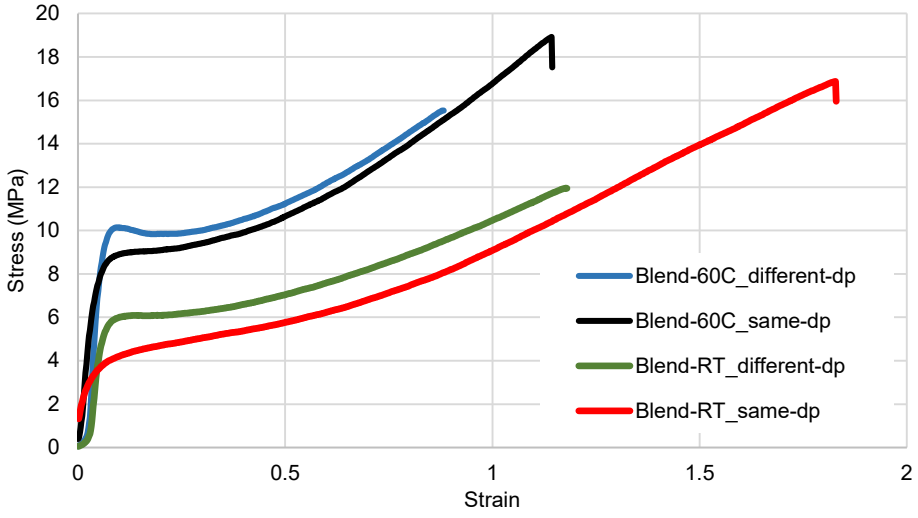

Figure 4.2. Comparison between the mechanical properties of crosslinked blends having similar particle size and different particle size.

It was found that in both systems, either with similar particle size or different particle size, the mechanical strength of the films (casted at same temperature) did not differ significantly as shown in Figure 4.2, even if slightly harder and more brittle films were obtained from the blend prepared from different particle size latexes.

Then, the morphology of the films having different particles size was analyzed to see if segregation had occurred during film formation. Figure 4.3 shows the TEM images of the Blend film dried at RT and stained with RuO_4 for 5 mins. The staining procedure employed, by which amine moieties of PEI are stained by RuO_4, allowed to easily monitor the distribution of smaller and bigger particles around the film. In any case, the small particles of component-1 did not bear PEI moieties, and the enamine group that is formed between the AAEMA moieties and the NH_4OH in this component, was supposed to disappear once the film was formed and the NH_4OH was evaporated. The presence of darker boundaries around the smaller particles might be because of the excess of PEI used in the system. In these images, we can see the distribution of smaller and larger particles in the final blend film. We did not find any difference in the images taken from the top and bottom of the final film. To check if there is any segregation in that film, the actual number of particles used in the system and the number of particles present in the TEM images of the film was calculated.

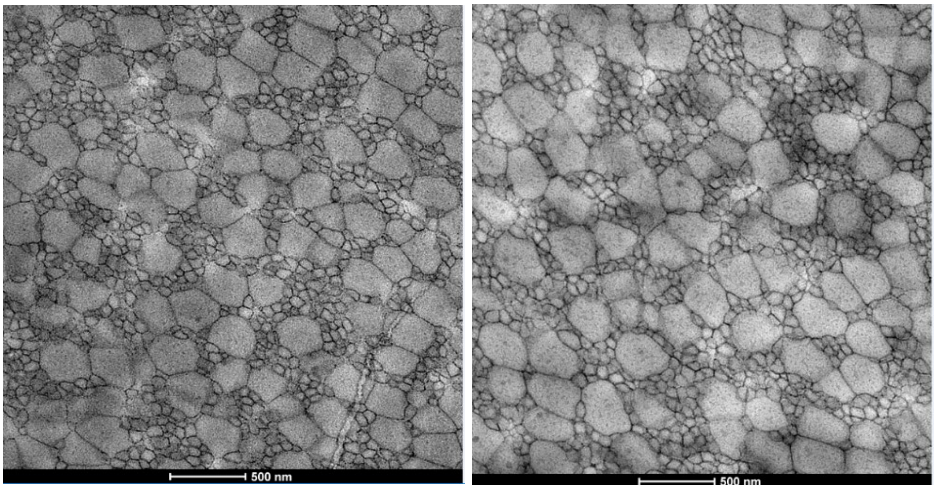

Figure 4.3. TEM images for Blend film prepared from large soft (70 %) and small soft (30 %) polymer latexes dried at RT and stained for 5 min with RuO_4. The image on left was taken from the top part of the film and the right image from the bottom part of the film.

We calculated that theoretically the ratio between the number of small and large particles was 13.2 for the Blend film. When the number of small and big particles were counted in both bottom and top film TEM images, it was found that the ratio of small to large particles was between 7 to 8. Therefore, we can say that some segregation had occurred between small and large particles in these films. The TEM images of C-0 used for the preparation was also analyzed and presented in Appendix II. The images obtained for C-0 were homogenous showing no such honeycomb pattern, which strengthens the hypothesis that the honeycomb pattern was formed because of the presence of PEI.

In order to see the distribution of components in a blend system having the same particles size in both latexes, styrene was introduced in one of the components to locate the position of this component (Appendix II). TEM images provided a clear positioning of each component by showing darker particles in the styrene containing component (see Appendix II). In that case, the average ratio between styrene containing and the non-styrene containing particles ranged from

0.8 and 1.2, showing a homogenous distribution of particles in the blend films when both components had the same particle size.

4.3.1.2. Blends with different particle size and T_G latexes

The preliminary results for the system having different particle size and T_G are presented in this section. Therefore, component-1, with a solids content of 44 %, 273 nm particle size, and a glass transition temperature of 22 °C, and component-2, with a solids content of 43.5 % and 130 nm particle size, and a T_G of 44.5°C, were blended with the same polymer % of each component.

The comparison of the mechanical properties between this system having different particle size and T_G with the system having same particle size and T_G is presented in Figure 4.4, together with their non-crosslinked counterparts. The tensile test of RT dried films of the bimodal system either crosslinked or non-crosslinked could not be performed as the films prepared were very brittle. Therefore, only the annealed films were evaluated. The non-crosslinked annealed film (Ref-blend-60C_diff-dp+T_G) was harder as well as more brittle as compared to (Ref-blend-60C_same-dp), due to the presence of high T_G particles. It can be seen that the fully crosslinked film prepared from the bimodal system containing different dp+T_G (Blend-60C_different-dp+T_G) becomes much harder and more brittle as compared to the system having same particle size (Blend-60C_same-dp). It can be concluded that the presence of crosslinking and high T_G particles showed a dramatic higher modulus as compared to crosslinked annealed film of similar particle size and T_G.

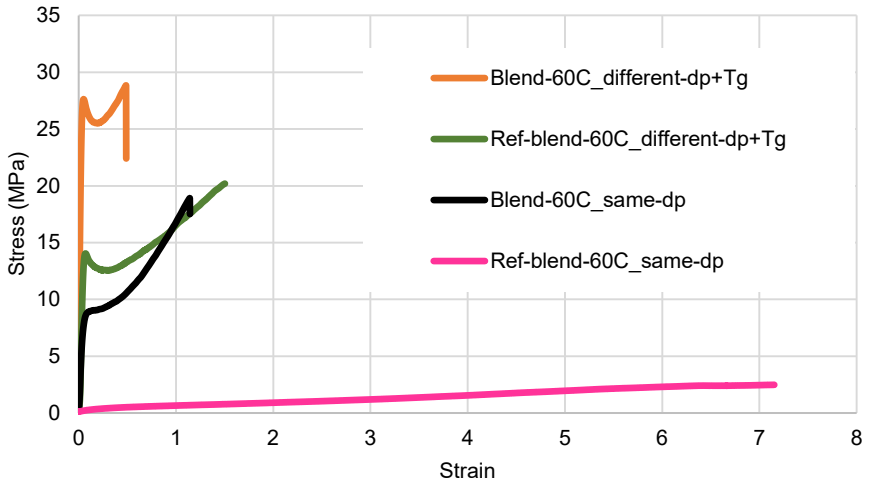

Figure 4.4. Comparison between the mechanical properties of the system with same particle size and T_G blend and the bimodal system having different particle size and T_G, Both crosslinked and non-crosslinked (Ref) films were annealed at 60 °C.

TEM analysis was also carried out to see the distribution of component-1 and 2 in the final blend film. Figure 4.5 shows the TEM images of the film with different dp + T_G dried at RT and annealed at 60 °C, stained with RuO_4 for 5 minutes. In these images, we can see the distribution of smaller and larger particles in the blend film. We did not find any significant difference between the RT and the annealed image of the film.

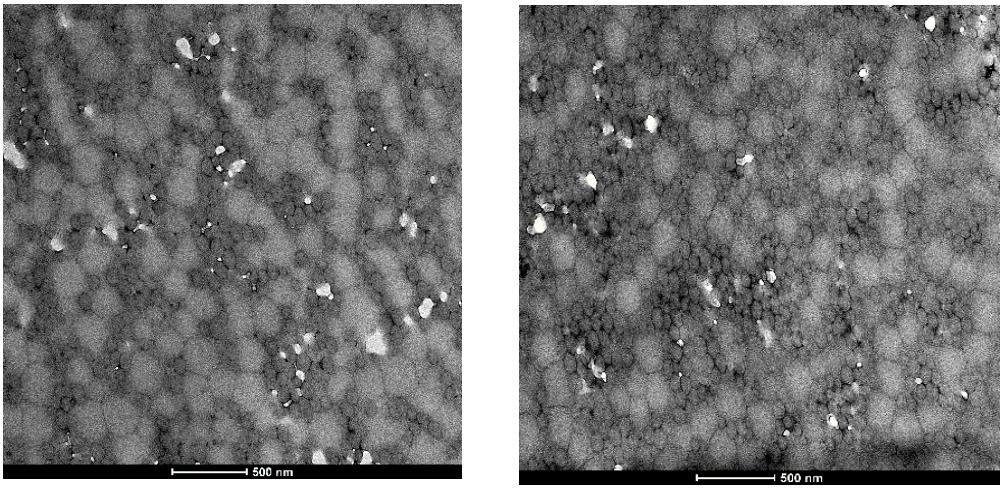

Figure 4.5. TEM images for blend film (different dp + T_G) stained for 5 min with RuO_4. The image on left was taken from the RT dried film and the right image from the 60 °C annealed film.

To check if there was any segregation in these film, we calculated the theoretical number of small and large particles used in the system and we counted the number of particles present in the TEM images of the films. We calculated that theoretically the ratio between the number of small particles to large particles was 9.3 for the blend films. When the number of small and big particles were counted in both bottom and top film TEM images, it was found that the ratio of small to large particles was between 6 and 6.5. Therefore, it seems that there had been segregation during film formation. However, in the cryosectioned TEM images of top and bottom surfaces of the film there was a similar distribution of both small and large particles, and apparently no difference could be noticed between both set of TEM images. In order to analyse this mismatch further, AFM images of film surfaces were analyzed to investigate where the missing small particles from the blend were located.

Figure 4.6 presents the AFM images of the blend film prepared by drop casting on mica substrate. The answer to the mismatch found by TEM images and the theoretical calculation between small and large particles was therefore found during AFM analysis of the blend film, as

we could see that there was an accumulation of small particles on the very top layer of the film as shown in Figure 4.6.

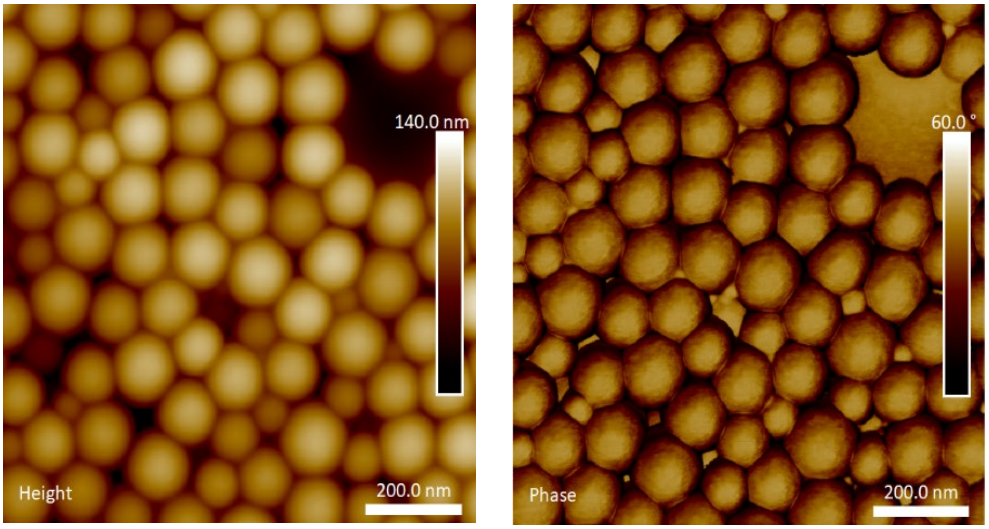

Figure 4.6. AFM images of the surface of the film prepared by drop casting of blend system with different dp and T_G.

The chemical resistance of the fully crosslinked films was also tested first by MEK double rub test and then by water absorption test. The resistance of the film against MEK solvent test is widely used in the paint industry because it provides a quick relative estimation of the degree of crosslinking without having to wait for long-term exposure results.

MEK resistance test results are presented in Table 4.7, showing how many cycles (double rubs) are required to scratch the film. In this study we had investigated the fully crosslinked films i.e., the films annealed at 60 °C. The blend film (annealed film) prepared from same particle size latexes, required only 12-15 cycles for scratch to appear in the film. The film prepared from different particles size latexes required nearly 250 cycles to show scratches on the film. Moreover, the resistance against MEK of the film prepared from different dp + T_G also increased with respect to the low T_G same dp system, as it required around 100 cycles for scratches to

appear in the film. It can be seen that a great improvement was achieved for both cases as compared to the system with same particles sizes. In case of the system having different dp + T_G, the presence of high T_G particles on the film surface (as shown by AFM) makes the film less resistant against MEK, as the film is very brittle on the surface creating small crack in the contact with MEK, which ended-up with a faster destruction of the film.

Table 4.7. Number of MEK double rubs required to scratch the blend films prepared at 60 °C.

Blend films	MEK cycles
Blend-60C_same-dp	12-15
Blend-60C_different-dp	~ 250
Blend-60C_different-dp+T_G	~100

If crosslinking is present in the polymeric film, the swelling and absorption of the film will definitely be affected. In our case, we studied the absorption of films using water as solvent. Figure 4.7 presents the results found for water absorption tests. The blend having same particle size i.e., Blend-60C_same-dp, showed more absorption of water in comparison to films produced from the systems having different particle size but same T_G i.e., Blend-60C_different-dp. Therefore, a better packing during film formation between small and large particles could have contributed to improve the water resistance properties. On the other hand, in case of "Blend-60C_different-dp+T_G", the chemical resistance was further improved by the presence of high T_G particles and the crosslinked network, as the % of water absorbed after 72 h was less than 1 %. It was also seen in the tensile strength of the films with this Blend-60C_different-dp+T_G, that there was a huge increase in the mechanical strength of the film.

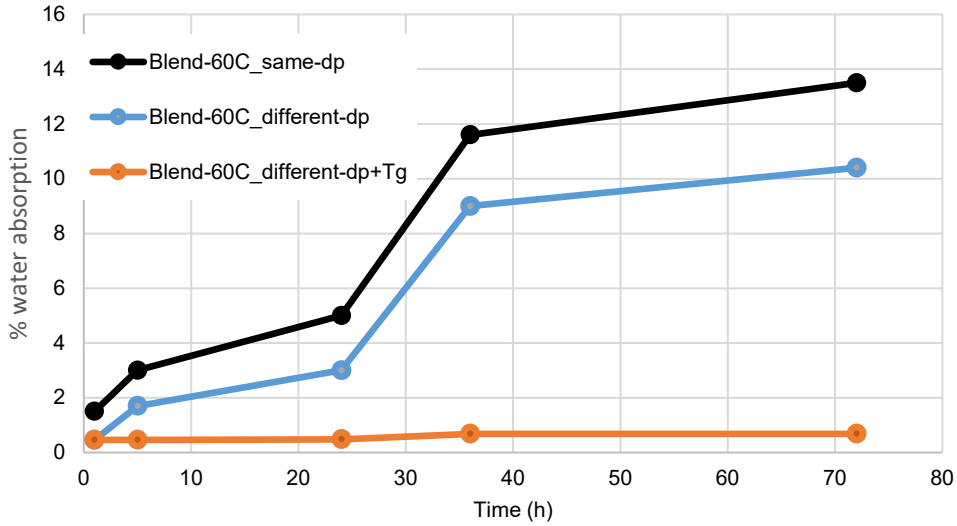

Figure 4.7. Water absorption tests result of blend films with same dp, different dp and different dp + T_G dried at 60°C.

It has been concluded that using different particles size and T_G, the tensile strength of the film increased and chemical resistance both in terms of water absorption and MEK resistance were also improved. A slight enrichment of small particles could be noticed on the surface of the films, but except for a small reduction of the MEK double rub test, no negative effect could be attributed to it. Therefore, in the next section higher scale synthesis for the crosslinking system has been carried out, in order to incorporate the crosslinking chemistry in actual coating formulations (Chapter 5).

4.3.2. Latexes synthesized at a higher scale

The solids content, final particle size, monomer conversion, MFFT and T_G of the latexes synthesized at a slightly higher scale are presented in Table 4.8. As it can be seen, large particles with particle sizes in the range 300-360 nm were obtained, while small particles were in the range

of 80-85 nm. On the other hand, soft particles had T_Gs around 20 °C and MFFT of around 9 °C, while hard ones had T_Gs around 53 °C and MFFT of around 42°C.

Table 4.8. Solids content, particle size, monomer conversions, T_G and MFFT of the latexes synthesised at larger scale with different particle size and T_G.

Latexes	Solids content (%)	Particle size (nm)	Monomer conversion (%)	T_G (DSC,°C)	MFFT (°C)
Latex 1_LS	44.5	357	95	20.5	9-10
Latex 2_LS	44.5	359	95	20.5	9-10
Latex 3_SS	33.5	84	97	21	8-9
Latex 4_SS	33.5	80	95	21	8-9
Latex 5_LH	44	300	96	54	42
Latex 6_SH	33.5	83	96	52	41-42

As it was mentioned in Table 4.5, four systems were studied blending these latexes: LS-S-H, LS-SH, LH-SS and SS-SH. Dynamic mechanical thermal analysis (DMTA) was used to measure the rheological properties of the crosslinked and non-crosslinked films prepared from these systems. In general, the presence of crosslinking increases the elastic modulus and decreases the viscous modulus or flow property (E'>E"). Therefore, the formation of crosslinking joint can be easily determined by the rheological properties of the film. The tan delta peak (calculated from the ratio of loss to storage modulus) also provides information related to the T_Gs of the film. The Modulus vs T curves for System LS_SS, System LS_SH, System LH_SS and System SH_SS using both drying conditions RT and RT + annealing at 60 °C are shown in Figures 4.9, 4.10, 4.11 and 4.12., respectively.

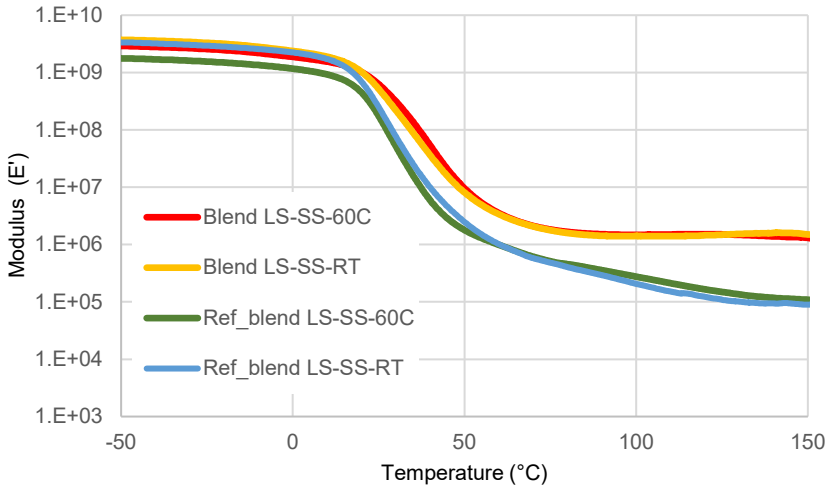

Figure 4.9. Modulus (E') vs T curves for the crosslinked and non-crosslinked films dried for 7 days at RT + annealed for one day at 60 °C for system LS_SS (blend having different particle sizes and same T_G latexes).

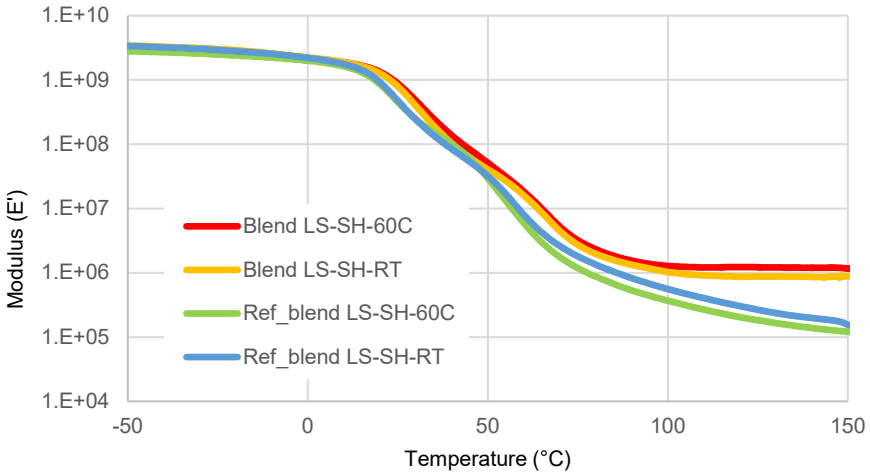

Figure 4.10. Modulus (E') vs T curves for the crosslinked and non-crosslinked films dried for 7 days at RT + annealed for one day at 60 °C for system LS_SH (blend having different particle sizes and different T_G latexes).

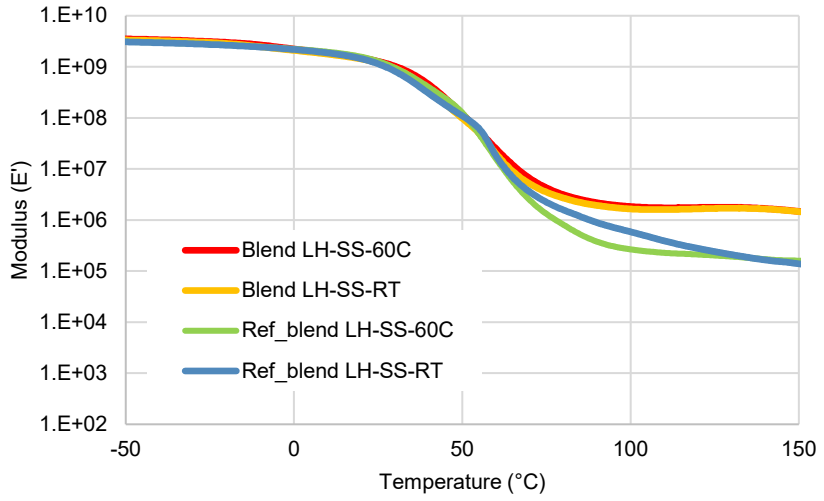

Figure 4.11. Modulus (E') vs T curves for the crosslinked and non-crosslinked films dried for 7 days at RT + annealed for one day at 60 °C for system LH_SS (blend having different particle sizes and different T_G latexes).

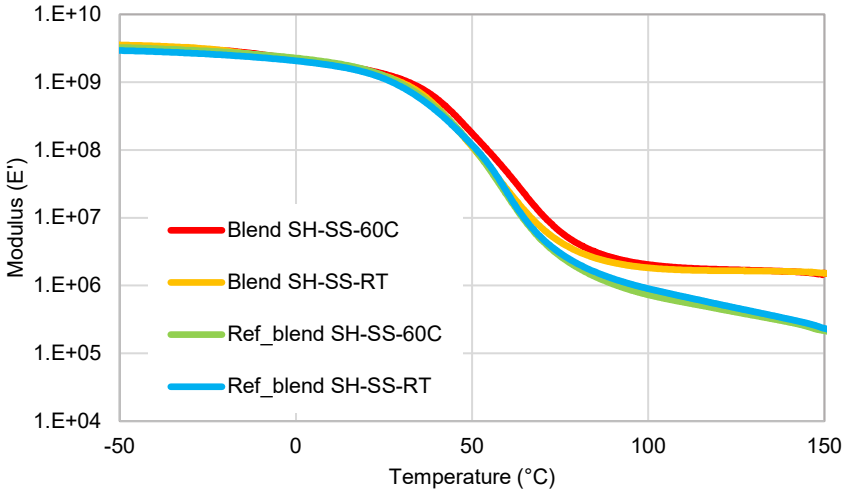

Figure 4.12. Modulus (E') vs T curves for the crosslinked and non-crosslinked films dried for 7 days at RT + annealed for one day at 60 °C for system SH_SS (blend having same particle sizes and different T_G latexes).

It can be seen in Figures 4.9, 4.10, 4.11 and 4.12, that the films with crosslinking and without crosslinking show the same pattern in the glassy state. However, when the curve enters the rubbery region, the presence of a plateau indicates the formation of a crosslinked network for Blend samples. This plateau has been seen in all the crosslinked films either dried at RT or at 60 °C, while non-crosslinked films showed no such plateau.

Tan delta curves from crosslinked and non-crosslinked films from System LS_SS, System LS_SH, System LH_SS and System SH_SS are shown in Figures 4.13, 4.14, 4.15 and 4.16 respectively.

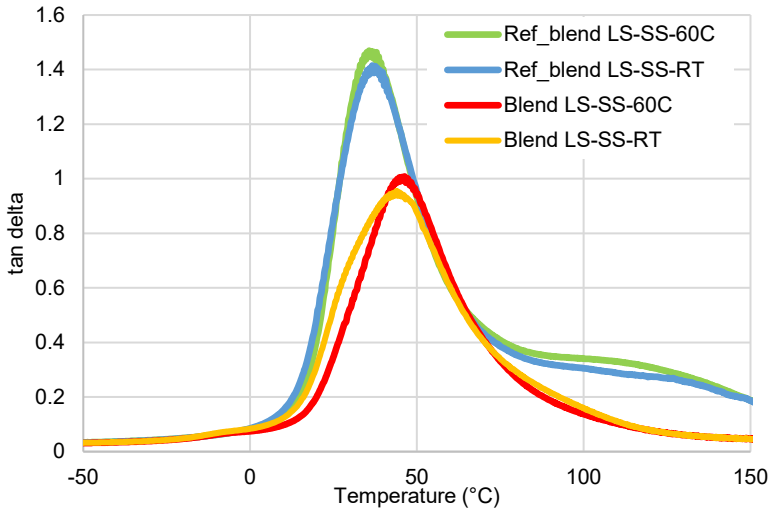

Figure 4.13. Modulus (E') tan delta curves for the crosslinked and non-crosslinked films dried for 7 days at RT + annealed for one day at 60 °C for system LS_SS (blend having same particle sizes and same T_G latexes).

System LS_SS comprises two latexes with different particle size but same T_G, therefore we found only one T_G (derived from tan delta peak) both in Ref-blend LS_SS and Blend LS_SS films, as shown in Figure 4.13. Furthermore, the decrease in the intensity of the peak from Ref -

blend LS_SS to Blend LS_SS films, and the shift to higher temperature indicate the movement of less amorphous phase in the annealed film, due to the formation of the crosslinked network. Moreover, there was a slight shift of tan delta peak from Blend LS_SS-RT to Blend LS_SS – 60 °C, showing the formation of more crosslinking joints, when the film was annealed at 60 °C, as already shown previously in Chapter 3.

Tan delta curves for System LS_SH and System LH_SS (having latexes with different dp and T_G) are presented in Figures 4.14 and 4.15. It has been seen that in both cases two T_G peaks can be observed, one indicating the presence of the softer phase and the other indicating the presence of the harder phase.

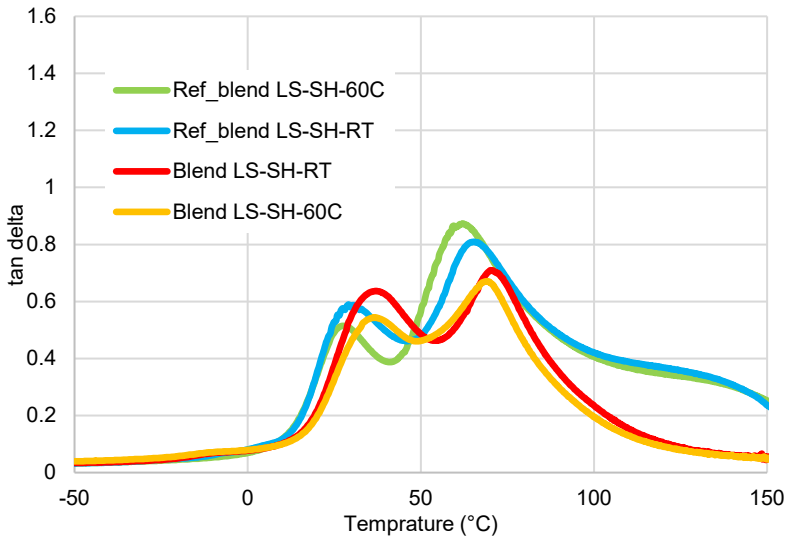

Figure 4.14. Modulus (E') tan delta curves for the crosslinked and non-crosslinked films dried for 7 days at RT + annealed for one day at 60 °C for system LS_SH (blend having same particle sizes and different T_G latexes).

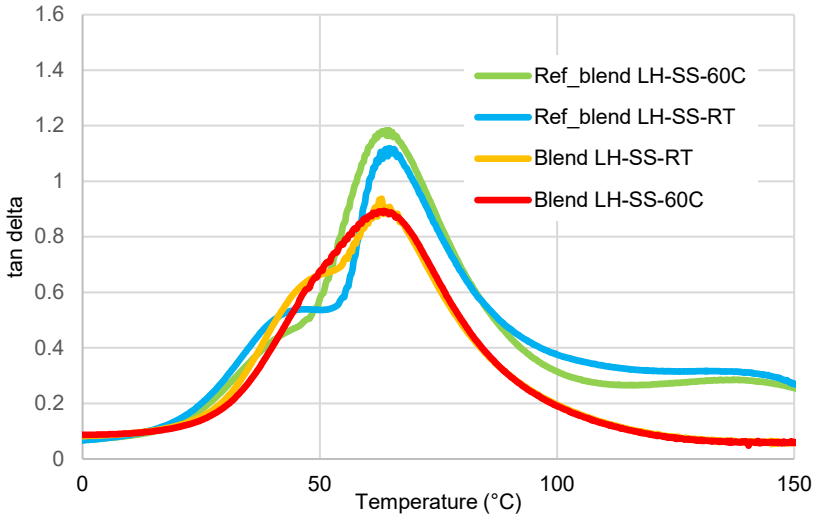

Figure 4.15. Modulus (E') tan delta curves for the crosslinked and non-crosslinked films dried for 7 days at RT + annealed for one day at 60 °C for system LS_SS (blend having same particle sizes and same T_G latexes).

Regarding the intensity of both peaks, the deconvolution of the curves has been done to separate the softer and harder phase (presented in Appendix III), and the results have been included in Table 4.9 and 4.10.

Table 4.9. Results of the deconvolution of tan delta curves obtained from DMTA for non-crosslinked systems dried at RT and annealed at 60 °C.

	Ref_blend-RT		Ref_blend-60 °C	
	First Peak % and T	Second Peak % and T	First Peak % and T	Second Peak % and T
LS-SH	52 % (29 °C)	48 % (66 °C)	25 % (28 °C)	75 % (62 °C)
LH-SS	30 % (44 °C)	70 % (66 °C)	8 % (38 °C)	92 % (64 °C)
SS-SH	15 % (37 °C)	85 % (64 °C)	9 % (34 °C)	91 % (65 °C)

Table 4.10. Results of the deconvolution of tan delta curves obtained from DMTA for crosslinked systems dried at RT and annealed at 60 °C.

	Blend-RT		Blend-60 °C	
	First Peak % and T	Second Peak % and T	First Peak % and T	Second Peak % and T
LS-SH	61 % (37 °C)	39 % (72 °C)	53 % (37 °C)	47 % (70 °C)
LH-SS	40 % (47 °C)	60 % (66 °C)	34 % (48 °C)	66 % (67 °C)
SS-SH	37 % (50 °C)	63 % (70 °C)	40 % (52 °C)	60 % (72 °C)

If LS-SH system is considered first, which had a 73/27 ratio of soft polymer/hard polymer, it can be seen that in the non-crosslinked film dried at RT, the amount of polymer in the softer phase peak is 52 %, lower than the 73 % of soft polymer coming from the large particles latex. This percentage is further decreased to 25 % in the non-crosslinked film annealed at 60 ºC. It can be concluded that the soft phase polymer diffuses and mixes with the harder phase polymer, producing a harder phase that presents lower T_G, as the amount of soft phase incorporated to it increases (66 ºC to 62 ºC). In the case of crosslinked LS-SH films, the T_G of both peaks increases with respect to the non-crosslinked films, and the ratio between soft and hard phases is more close to the 73/27 included in the blend. Therefore, there is less interdiffusion of polymer between particles in the crosslinked system, and the mobility of the chains in each phase is slightly restricted due to the crosslinking reactions.

Figure 4.16 and Figure 4.17 show the AFM images of non-crosslinked Ref_blend LS-SH-RT and crosslinked Blend LS-SH-RT cross-sectioned films, respectively. The micrographs of the non-crosslinked film show the presence of hard phase polymer surrounding softer polymer domains of around 300 nm (Figure 4.16). The hard phase polymer comes from the small hard polymer particles, which appear surrounding the large soft particles. However, in case of the crosslinked film where the hard phase polymer were also visible, these hard phase polymer seems to be still in the form of particles (Figure 4.17). Therefore, it can be concluded that in case of crosslinked film, the chain mobility in soft and hard phases is restricted by the formation of crosslinking that prevents the interdiffuion of the particles (similar conclusion has also been drawn in the deconvolution of tan delta results). However, in case of non-crosslinked films, some interdiffusion seems to have occurred between the hard phase and the soft one (Figure 4.16).

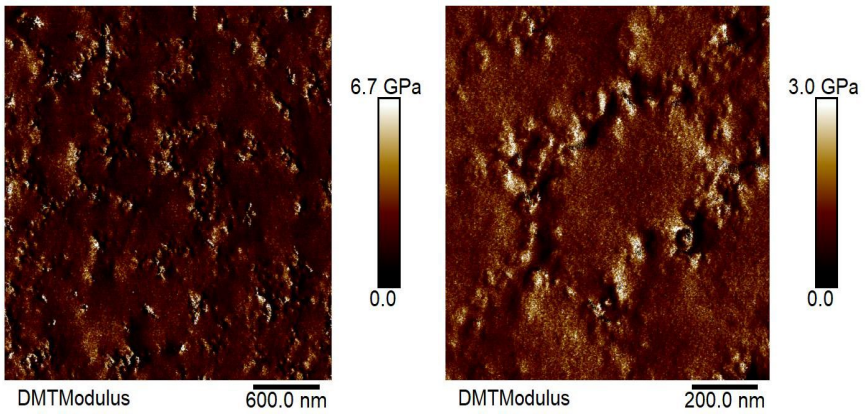

Figure 4.16. AFM images of the Ref_Blend LS-SH-RT non-crosslinked film dried at RT.

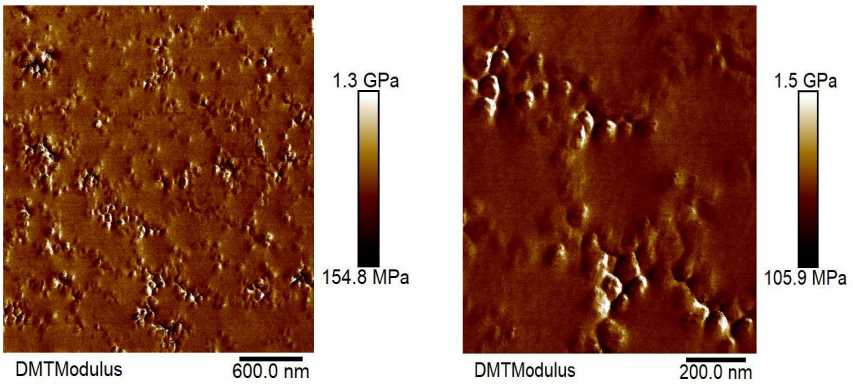

Figure 4.17. AFM images of the Blend LS-SH-RT crosslinked film dried at RT.

In the case of LH-SS system, which had initially a 50/50 polymer ratio, similar trends can be observed in the DMTA analysis compared to LS-SH system. There is a decrease in the soft phase percentage from 30 to 8 % in the non-crosslinked films when changing the drying temperature from RT to 60 ºC, while the percentage is maintained at 40 and 34 % in the crosslinked films dried at RT and 60 ºC respectively.

In case of the system having different T_G and similar particle size (Figure 4.18), tan delta presented a single band, with a shoulder at low temperatures. In order to calculate the amount of softer and harder phases present in the system, the deconvolution of the band has been performed as shown in Figure 4.19 and 4.20. The results of the area percentages and T of the two peaks have also been included in Table 4.9 and 4.10.

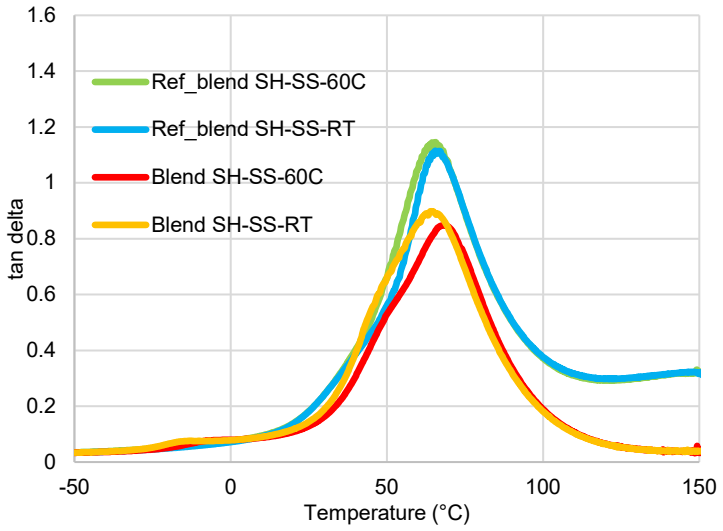

Figure 4.18. Modulus (E') tan delta curves for the crosslinked and non-crosslinked films dried for 7 days at RT + annealed for one day at 60 °C for system SH_SS (blend having same particle sizes and different T_G latexes).

It has to be remembered that the polymer ratio in SH-SS system is 50/50. However, as in the previous cases, in the non-crosslinked film, the amount of softer phase polymer was only 15 % in the film dried at RT, and it decreased to 9 % in the film annealed at 60 ºC. Compared to the LH-SS system, in which the initial polymer ratio was also 50/50, in this case, the initial amount of polymer in the softer region was much lower in the film dried at RT (15 % in comparison to 30 %). This can be attributed to the higher interfacial area between the hard and the soft domains in this SH-SS case, in which both polymer phases are contained in polymer particles of small

size, as compared to the LH-SS system. On the other hand, the percentage of soft and hard phase in the crosslinked system approaches more the initial amount included in the blends, 37/63 for the film dried at RT and 40/60 for the film annealed at 60 ºC. Furthermore, it can be pointed out that the T_G of both phases were the highest ones between the three cases with different T_G particles presented (50-52 ºC and 70-72 ºC). This can be due to the small particle sizes used in this case, in which the interfacial crosslinking affects more the mobility of the polymer phases.

a)

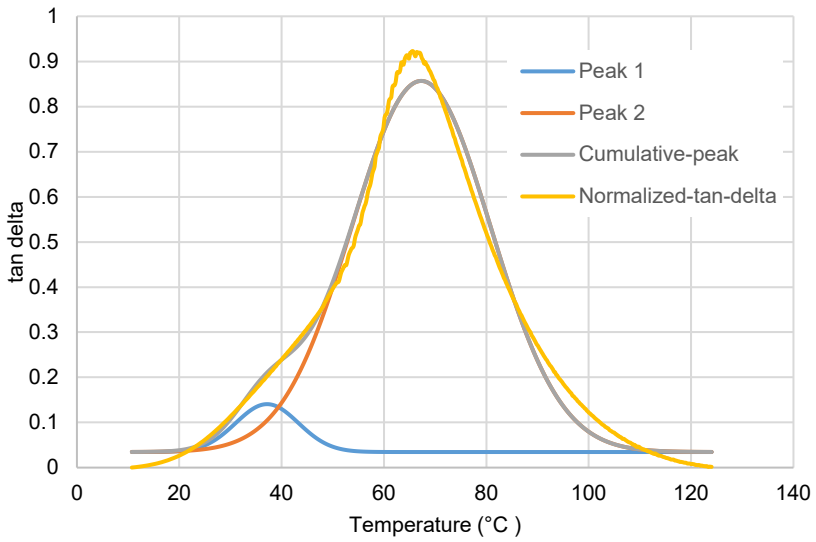

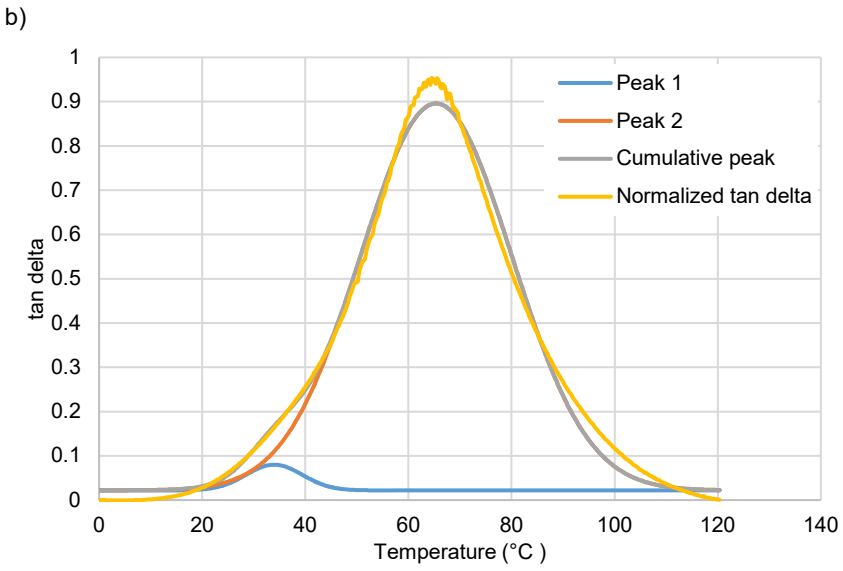

Figure 4.19. Deconvolution of Modulus (E') tan delta curves (a) Ref_blend SH-SS-RT(b) Ref_blend SH-SS-60C for system SH_SS (blend having same particle sizes and different T_G latexes).

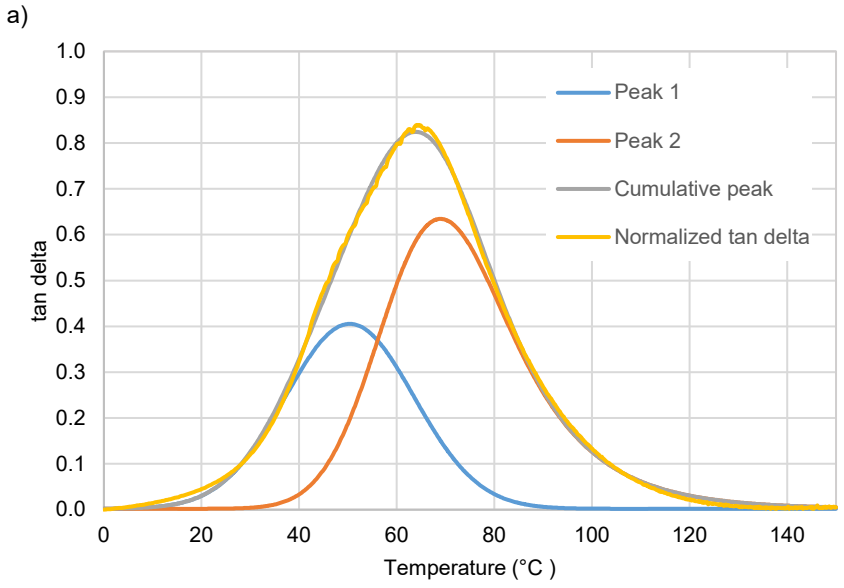

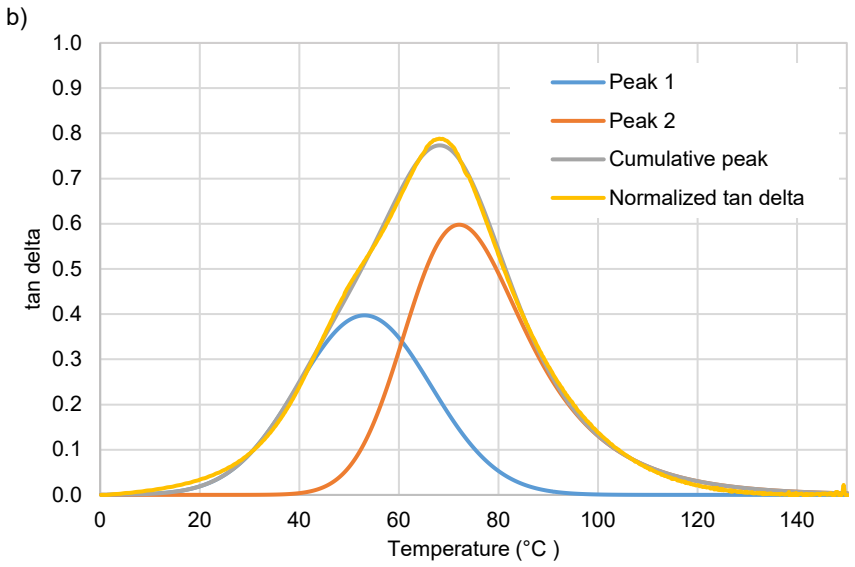

Figure 4.20. Deconvolution of Modulus (E') tan delta curves (a) Blend SH-SS-RT (b) Blend SH-SS-60C for system SH_SS (blend having same particle sizes and different T_G latexes).

In order to further analyze the morphology of SH-SS system, TEM and AFM images of the system were recorded. Figure 4.21 presents the TEM images of cryosections of Blend SH-SS-RT and Blend SH-SS-60 °C stained with RuO_4 for 10 and 5-mins, respectively. The formation of the honeycomb pattern indicated the presence of amines on the inter-particles spaces. As we had already seen for the system having same particle size and same T_G (see Chapter 3), the honeycomb pattern formed in the blend film indicated the occurrence of crosslinking in the shell of the polymer particles, which blocked the interdiffusion between the polymer particles. Therefore, these TEM images seem to validate the hypothesis stating that softer particles and harder polymer particles maintain their own identity and do not fuse into each other in the crosslinked film.

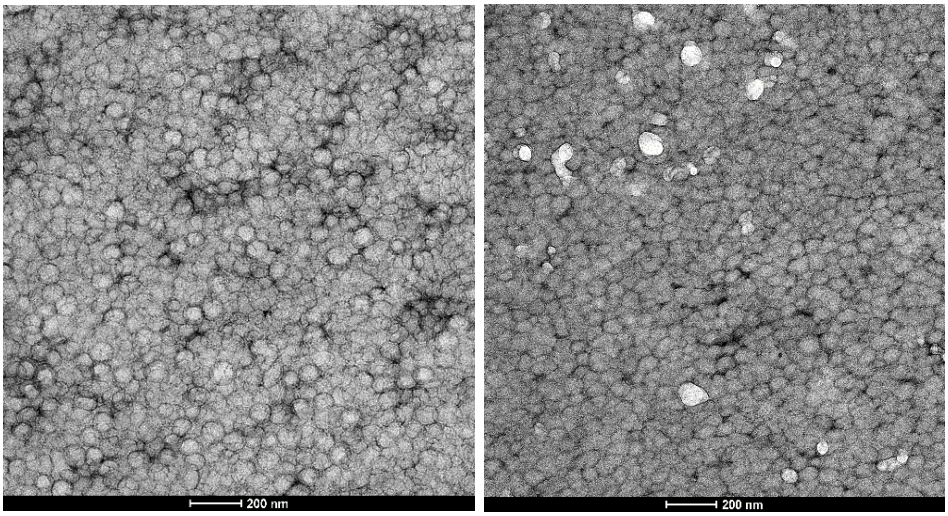

a) b)

Figure 4.21. TEM images of the crosslinked film of the system having same particle size but different T_G (a) Blend SH-SS-RT (b) Blend SH-SS-60C, stained with RuO_4 for 5 mins and 10 mins respectively.

In order to strengthen the stated hypothesis, AFM images of films cross-section were also analyzed. Figure 4.22 shows the AFM images of Ref_blend-SH_SS-RT and Ref_blend-SH_SS-60 °C. These films show quite homogenous modulus, with only some softer domains (or holes), supporting the hypothesis of a strong interdiffusion of polymer chains between the small particles, which would produce a film with an average T_G polymer between the two phases. Figure 4.23 presents the AFM images of Blend-SH-SS 60 cross-sectioned film. The darker spots represent the softer phase domains distributed in the matrix composed of a harder phase. This result indicates that softer particles were not fused into hard particles. Furthermore, it can be noticed that the modulus values in these images are higher than the ones obtained for the non-crosslinked system. As a results, the hardening of the films also observed in the crosslinked films by DMTA has also been proved by these AFM images.

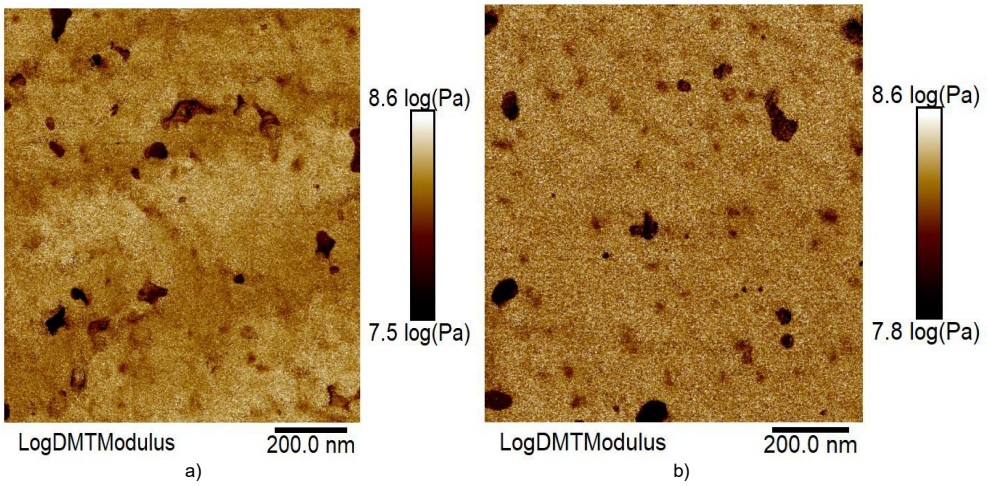

Figure 4.22. AFM images of the non-crosslinked film of the system having same particle size but different T_G (a) Ref_blend SH-SS-RT (b) Ref_blend SH-SS-60C.

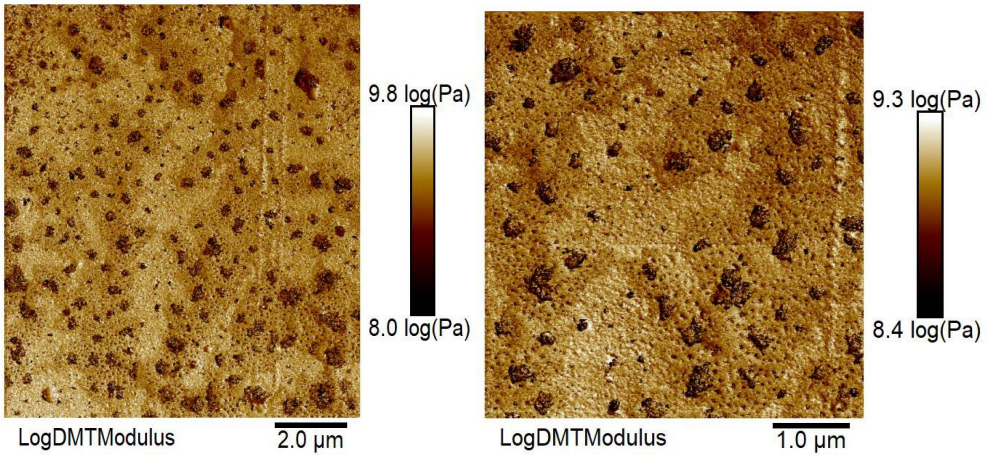

Figure 4.23. AFM images of the crosslinked annealed film at 60 °C of the system having same particle size but different T_G i.e., Blend SH-SS-60C.

The kinetics of the crosslinking reaction for the system having soft and same size particles, had already been presented in Chapter 3. In this section, the kinetics of the crosslinking reaction for the System SH_SS (composed of soft and high T_G particles) was followed via FTIR

spectroscopy. The detailed study for the formation of C-1 and C-2 has already been presented in Chapter 3. In the present study, the evolution of reaction has been followed analysing the carbonyl stretching region i.e., from 1800 cm^{-1} to 1500 cm^{-1}. Ideally, during the blend formation, the crosslinking reaction between the protected acetoacetoxy group of C-1 and the amine functionalized C-2 should happen, and all the primary amines coming from the protection of acetoacetoxy by NH_4OH in C-1 (1562 cm^{-1}) should disappear due to the reaction with PEI amines and the formation of secondary amines (1654 cm^{-1}). Therefore, it was decided to follow the evolution of reaction by recording the FTIR spectra for three days at RT and then annealing the film at 60 °C for 2, 3, 24, 48 and 62 hours (Figure 4.25).

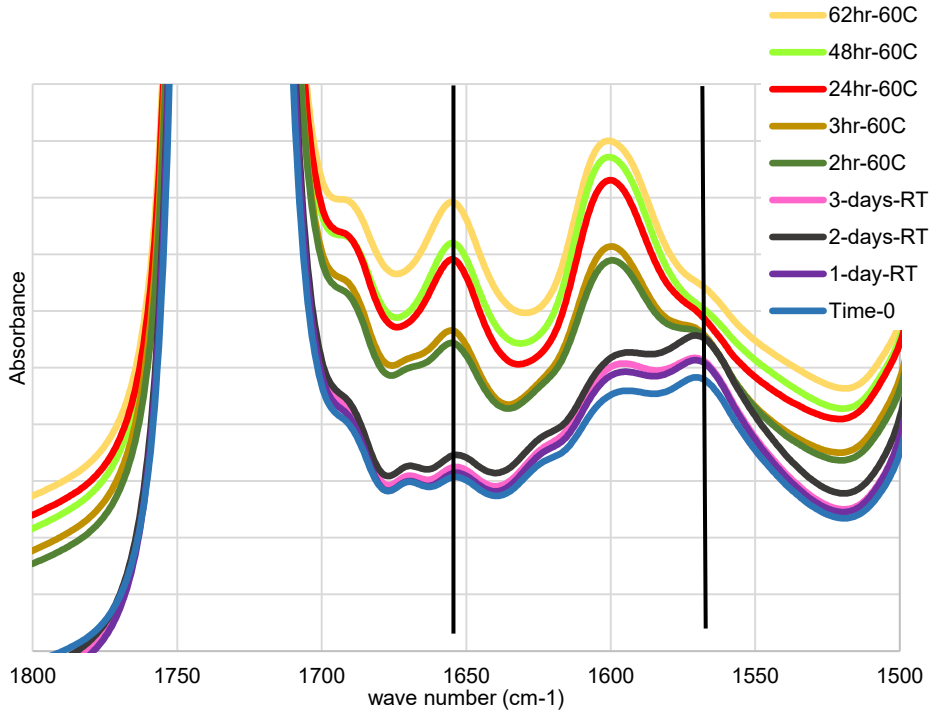

Figure 4.25. FTIR spectra in the carbonyl-stretching region after drying the Blend film at RT for 1, 2 and 3 days and then 2, 3, 24, 48 and 62 hours at 60 °C for the system having same particle size but different T_G (system SH_SS).

The conversion of the reaction was calculated based on the integration of the secondary amines peak at 1654 cm^{-1}, which was normalized with the carbonyl peak of acrylates at 1730 cm^{-1}. Equation 4.1 was applied to calculate the conversion of the reaction, considering that the conversion was negligible at time 0 and complete after 62 hours at 60 °C.

$$Percetage\ conversion = \frac{(Area)t-(Area)0}{(Area)\propto-(Area\ )0} \qquad \text{(Equation 4.1)}$$

Figure 4.26 presents the crosslinking percentage obtained during drying at room temperature for three days and annealing at 60 °C, for two repeated samples.

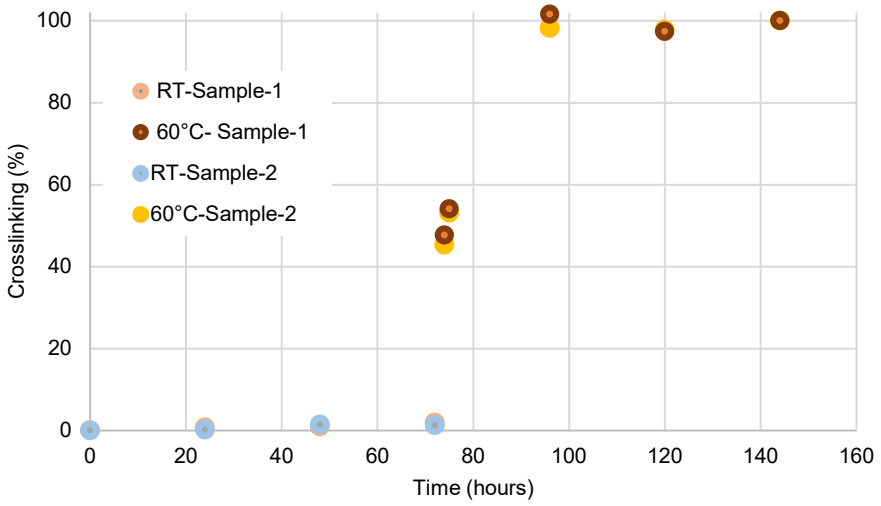

Figure 4.26. Crosslinking degree in Blend film calculated via FTIR analysis for the system having same particle size but different T_G latexes (system SH_SS).

It was noticed that the reaction did not proceed significantly at RT drying conditions but annealing for 2 hours after 3 days drying at RT, speeded up the process and a conversion of around 47 % was achieved. The conversion was further increased after 3, 24, 48 and 62 hours

at 60 °C, obtaining values of about 54 %, 97 %, 99 % and 100 % respectively. Similar results were obtained for both repeated samples. It was concluded that due to the presence of high T_G particles, the crosslinking reaction did not progress significantly at RT drying conditions, as it was seen in Chapter 3 when soft polymer phase particles were present in both components. Nevertheless, annealing at 60 °C, over the T_G of the hard particles (52 °C) again produced a fully crosslinked film, as in the case seen in Chapter 3.

4.4. Conclusions

AAEMA and amines based crosslinking chemistry has been further investigated by preparing systems with different particles size and T_G. In case of the system with different dp, it was seen that the annealed film (fully crosslinked film) showed better chemical resistance in terms of MEK resistance and water absorption as compared to the film with same particles size. Moreover, some improvement has also been seen in the tensile strength of the film. Moreover, in case of the system having different particle size and T_G, a dramatic improvement in tensile strength and water resistance performance was found as compared to the film produced with same particles size. Furthermore, some improvement was also noticed in terms of MEK double rub test as compared to the system with similar particle size. In general, we had concluded that by changing particle size and T_G in the blend film, mechanical and chemical properties of the film have been improved as compared to the film produced by same particle size latexes.

These preliminary results for systems having different sizes and hardness particles provide the platform to synthesize these systems in a bit higher scale and apply them for actual coating applications. Therefore, four different crosslinked systems were prepared based on

changing particle size and T_G parameter. First, the crosslinked and non-crosslinked films have been differentiated by analysing the DMTA and the formation of a plateau in the rubbery region has shown the formation of a crosslinked network. Tan delta curves have also been analysed to calculate the percentage of softer and harder phase in the final films. It has been seen that non-crosslinked films showed less amount of softer phase polymer compared to the one included in the blend and it further decreased while annealing at 60 °C. However, in case of crosslinked films, the ratio between softer and harder phases was almost the one included in the blend, meaning that crosslinking prevents the interdiffusion between soft and hard particles during film formation.

In case of the system having same particles size but different T_G, a detailed study of crosslinking has been done by analysing TEM and AFM images and FTIR spectroscopy. It has been noticed that a honeycomb pattern has been formed in the crosslinked film, suggesting again that crosslinking prevented the interdiffusion between the particles (as in Chapter 3). AFM images strengthen the result by showing a microstructure having a hard phase matrix with soft domains. By following the crosslinking kinetics via FTIR spectroscopy it has been found that crosslinking did not proceed significantly during drying at RT, due to the presence of hard T_G particles. However, annealing at 60 °C for 62 hours, above the T_G of the hard phase (52 °C) helped to complete the crosslinking reaction.

4.5. References

[1] E. Limousin, N. Ballard, J.M. Asua, Soft core–hard shell latex particles for mechanically strong VOC-free polymer films, J. Appl. Polym. Sci. 136 (2019) 47608. https://doi.org/10.1002/APP.47608.

[2] E.L. Brito, N. Ballard, Film formation of hard-core/soft-shell latex particles, J. Polym. Sci. 61 (2023) 410-421. https://doi.org/10.1002/POL.20220546.

[3] J. Feng, M.A. Winnik, R.R. Shivers, B. Clubb, Polymer Blend Latex Films: Morphology and Transparency, Macromolecules. 28 (1995) 7671–7682. https://doi.org/10.1021/MA00127A013/ASSET/MA00127A013.FP.PNG_V03.

[4] M. Winnik, J.Feng, Latex blends: an approach to zero VOC coatings, J. of C. Technology.68 (1996) 39-50.

[5] A.C.I.A. Peters, G.C. Overbeek, A.J.P. Buckmann, J.C. Padget, T. Annable, Bimodal dispersions in coating applications, Prog. Org. Coatings. 29 (1996) 183–194. https://doi.org/10.1016/S0300-9440(96)00629-7.

[6] S.T. Eckersley, B.J. Helmer, Mechanistic considerations of particle size effects on film properties of hard/soft latex blends, J. Coatings Technol. 69 (1997) 97–107. https://doi.org/10.1007/bf02696096.

[7] J.M. Geurts, M. Lammers, A.L. German, The effect of bimodality of the particle size distribution on film formation of latices, Colloids Surfaces A Physicochem. Eng. Asp. 108 (1996) 295–303. https://doi.org/10.1016/0927-7757(95)03404-8.

[8] S. Jiang, A. Van Dyk, A. Maurice, J. Bohling, D. Fasano, S. Brownell, Design colloidal particle morphology and self-assembly for coating applications, Chem. Soc. Rev. 46 (2017) 3792–3807. https://doi.org/10.1039/C6CS00807K.

[9] J. Feng, M.A. Winnik, Latex blends as an approach to zero VOC coatings, Polym. Mater. Sci. Eng. Proc. ACS Div. Polym. Mater. Sci. Eng. 76 (1997) 176.

[10] M.L. S. Lepizzera, C. Lhommeau, G. Dilger, T. Pith, Film-forming ability and mechanical properties of coalesced latex blends, J. Polym. Sci. Part B. 35 (1997) 2093-2101.

[11] A. Perez, E. Kynaston, C. Lindsay, N. Ballard, Semi-crystalline/amorphous latex blends for coatings with improved mechanical performance, J. Appl. Polym. Sci. 140 (2023) e53517. https://doi.org/10.1002/app.53517.

[12] D. Colombini, H. Hassander, O.J. Karlsson, F.H.J. Maurer, Influence of the Particle Size and Particle Size Ratio on the Morphology and Viscoelastic Properties of Bimodal Hard/Soft Latex Blends, Macromolecules. 37 (2004) 6865–6873. https://doi.org/10.1021/MA030455J.

[13] F.A.L. Dullien, Porous Media: Fluid Transport and Fluid Structures, Academic Press (1992).

[14] R.P. Kusy, Influence of particle size ratio on the continuity of aggregates, J. Appl. Phys. 48 (1977) 5301–5305. https://doi.org/10.1063/1.323560.

[15] A. Tzitzinou, J.L. Keddie, J.M. Geurts, A.C.I.A. Peters, R. Satguru, Film Formation of Latex Blends with Bimodal Particle Size Distributions: Consideration of Particle Deformability and Continuity of the Dispersed Phase, Macromolecules. 33 (2000) 2695–2708. https://doi.org/10.1021/MA991372Z.

[16] D. Colombini, H. Hassander, O.J. Karlsson, F.H.J. Maurer, Effects of thermal annealing on the viscoelastic properties and morphology of bimodal hard/soft latex blends, J. Polym. Sci. Part B Polym. Phys. 43 (2005) 2289–2306. https://doi.org/10.1002/POLB.20461.

[17] W. Herrera-Kao, M. Aguilar-Vega, Mechanical properties of latex blends films from polystyrene particles with different sizes in a butyl acrylate-co-styrene copolymer matrix, Polym. Eng. Sci. 49 (2009) 1736–1743. https://doi.org/10.1002/PEN.21405.

[18] E.P. Pedraza, M.D. Soucek, Bimodal particle distribution for emulsions: The effect of interstitial functional particles, Eur. Polym. J. 43 (2007) 1530–1540. https://doi.org/10.1016/J.EURPOLYMJ.2007.01.022.

[19] T. Tashima, M. Yamamura, Two-step migration of particles in evaporating bimodal suspension films at high Peclet numbers, J. Coatings Technol. Res. 14 (2017) 965–970. https://doi.org/10.1007/S11998-017-9946-1/FIGURES/5.

[20] M. Schulz, J.L. Keddie, A critical and quantitative review of the stratification of particles during the drying of colloidal films, Soft Matter. 14 (2018) 6181–6197. https://doi.org/10.1039/C8SM01025K.

El capítulo 5 está sujeto a confidencialidad por el autor

Chapter 6.

Conclusions

In this work, the interparticle crosslinking in waterborne coatings has been studied to achieve a dual objective; to prepare crosslinked coatings by avoiding water soluble / dispersable crosslinkers (under scrutiny by REACH regulation) and to study the behavior of crosslinking chemistry in two components systems for industrial implementation. The crosslinking chemistry has been studied between acetoacetoxyethyl methacrylate (AAEMA) functionalized polymer particles and amine functionalized polymer particles. The polymer particles have been synthesized by seeded semibatch emulsion polymerization using MMA/BA latexes containing 5% of AAEMA in the shell of the particles. For the preparation of amine functionalized polymer particles, three different amine compounds have been used; one smaller chain amine i.e., hexamethylenediamine (HMDA) and two longer chain amines i.e., polyethyleneimine (PEI) LUPASOL G-20 and PEI LUPASOL G-35. The amine functionalized polymer particles have been produced by reacting the amines solution with the AAEMA functionalized latex.

First, the crosslinking chemistry between AAEMA – amines in the system having shorter chain amines i.e., HMDA has been studied. In order to monitor the chemical structural changes, the crosslinking reaction has been followed by FTIR spectroscopy. It has been observed that reaction started at room temperature (RT) at a slow rate, reaching approximately 30 % of conversion after 3 days at room temperature. However, 2 hours of annealing at 60 °C were enough to achieve full conversion of the reaction. A similar kinetic study has been done by

measuring the rheological properties of the film, extracting the same conclusions. Moreover, the chemical resistance to water absorption and the mechanical strength also support the results, as the annealed film showed less water uptake and higher strength as compared to RT dried film.

Then, the investigation has been further proceeded by preparing AAEMA – amine based crosslinking chemistry with longer chain amines i.e., with PEI (LUPASOL G-20 and LUPASOL G-35). As the PEI has a branched chemical structure, it was expected to form a network of crosslinked joints as compared to HMDA based crosslinking system (which can only form linear crosslinking joints). In such crosslinked system, it is also important to analyze the film formation process together with the occurrence of the crosslinking reactions. Therefore, first the crosslinking reaction kinetics has been followed by FTIR spectroscopy and rheological measurements. Similar conclusions to the already seen for HMDA based crosslinking system have been observed. Namely, that the reaction proceeds at RT at a slow rate (one month required to complete the reaction at RT) but annealing at 60 °C speeds up the reaction, reaching complete conversion after 24 hours. In order to analyze film formation in this crosslinking chemistry, the interdiffusion between the polymer particles has been analyzed by fluorescence resonance energy transfer (FRET) and pyrene excimer fluorescence (PEF) experiment. It has been seen that FRET technique could not be used in this case, as PEI interferes with the donor fluorescence decay. By PEF, it has been seen that interdiffusion between the polymer particles is blocked because crosslinking is occurring in the shell of the polymer particles. Moreover, the TEM images also showed the formation of a honeycomb pattern, indicating the presence of amines in the interparticles spaces, strengthening the hypothesis that interparticle crosslinking is occurring before interdiffusion to produce a strong film. Moreover, the effect of the amount and the size of PEI used for the preparation of polymer particles functionalized with amines has also been studied. It has been seen that there is a threshold amount of PEI that needs to be used for

the preparation of hard films. If this amount is increased from the threshold value, the film becomes soft because of excess free PEI. When the larger size amine i.e., LUPASOL G-35 (Mw-2000 g/mol) instead of LUPASOL G-20 (Mw-1300 g/mol) is used, the tensile strength of the RT dried film is worse than for the system with LUPASOL G-20. Therefore, the time to achieve fully crosslinked films for the system with larger amines seems to be higher at RT, even if the mechanical properties were similar for both PEI when fully annealed films were measured.

The crosslinking chemistry between AAEMA – amine system has been then further studied by analyzing the effect of the particles size and T_G, therefore blend systems with different particles size and T_G have been prepared. In case of the system with different particles size in both components, the film showed a dramatic increase in the resistance against MEK solvent and some improvement in water resistance and tensile strength of the film as compared to the system with the same particles size in both components. In case of the system with different particles size and T_G, drastic improvements in water resistance and tensile strength have been seen as compared to the system with the same particles size. Therefore, it has been concluded that by changing the particles size and the T_G, the system is moving towards films with better chemical and mechanical properties. The distribution of large and small particles in the final film has been also investigated by TEM images. Although top and bottom images of the film have shown an homogenous distribution of small and large particles in both places, a small segregation of the small particles has also been seen on the very top surface of the films by AFM.

In order to move from studying the crosslinking chemistry in the dispersions, toward the real applications, coatings need to be prepared by incorporating the crosslinking dispersions in paint formulations. Therefore, four different crosslinking systems have been produced based on

the most promising blend systems studied i.e., Blend LS-SS (system with large soft and small soft particles), Blend LS-SH (system with large soft and small hard particles), Blend LH-SS (system with large hard and small soft particles) and Blend SH-SS (system with small hard and small soft particles). In order to identify the crosslinking in the final film, the rheological properties have been studied by DMTA. It has been seen that all films showed a plateau in the rubbery region, indicating the formation of crosslinked joints. Moreover, the crosslinking effect has also been seen in the tan delta curves, as the intensity of the peaks decreased in crosslinked films as compared to non-crosslinked films. The percentage of softer and harder phase in the final film has also been calculated by deconvolution of the peaks obtained from tan delta curve. It has been seen that non-crosslinked films showed less amount of softer phase than the one added in the blend and it further decreased while annealing at 60 °C. However, in case of crosslinked films, the ratio between soft and hard phases was almost the same as the one included in the blend, meaning that crosslinking prevents the diffusion of softer polymer into harder phase. TEM and AFM images of crosslinked and non-crosslinked films also support these hypothesis. The kinetics of the crosslinking reaction have also been analysed by FTIR spectroscopy in the system "Blend SH-SS" containing soft and hard particles of the same size. It has been noticed that, due to the presence of high T_G particles, the crosslinking reaction did not proceed significantly at RT. However, the reaction completed to almost full conversion by annealing at 60 °C for 144 hours.

Finally, paints have been formulated from the above mentioned four crosslinking systems for exterior wood coating applications. To have a reference for the crosslinked paints, non-crosslinked paints have also been formulated by just blending of the two components, without modifying component-2 with PEI moieities. It has been seen that crosslinking improved the performance in terms of better hardness development, less water absorption, improved wet adhesion, drastic improvement of the blocking resistance and reduced elasticity as compared to

non-crosslinked paints. In order to make a relative comparison between crosslinked paints, it has been noticed that in the bimodal systems having high T_G particles i.e., Blend LS-SH and Blend LH-SS, the hardness development, blocking resistance and water absorption were improved as compared to Blend LS-SS containing only soft particles. Moreover, further improvement in the performance of paints were seen on using small soft and hard particles i.e., Blend SH-SS. The effect of the amount PEI has been seen in Blend SH-SS in terms of better wet adhesion performance, as the system contained 50 % polymer containing PEI moieties that can also act as an adhesion promoter improving the wet adhesion performance. In any case, it has been seen that the presence of pigment particles and additives did not disturb the crosslinking reaction between AAEMA and amine containing particles.

In order to make a comparison with a commercial product, ACRONAL - EDGE 6283 (a self-crosslinking acrylic aqueous dispersion) has been chosen. Our crosslinked paints presented improved water resistance, blisters formation after 30 minutes and blocking resistance, both in terms of appearing of scratch and energy required to separate to stacked wood compared with the commercial Acronal paint. However, our crosslinked paints were worse in terms of hardness development with both time and temperature and wet adhesion performance. In our paints, PEI used in the binder acted as a wet adhesion promoter but in case of Acronal paint, it contained a double wet adhesion functionality, making the wet adhesion performance of Acronal better than the one of the paints. Although our system is based on a bimodal system with soft and hard particles, Acronal paint is described as a latex based on multiphase morphology with particles size of 60 nm. Therefore, the reason for better hardness might be hidden in the usage of multiphase morphology in small size particles, by developing more hardness with simultaneous control of the film formation.

Resumen y conclusiones

En este trabajo se ha estudiado la reticulación interpartícula en recubrimientos al agua para conseguir un doble objetivo; preparar recubrimientos reticulados evitando los reticulantes solubles/dispersables en agua (bajo el escrutinio de la regulación REACH) y construir base científica mediante el estudio del comportamiento de la química de reticulación para su posterior implementación industrial. Se ha estudiado la química de reticulación entre partículas de polímero funcionalizadas con metacrilato de acetoacetoxietilo (AAEMA) y partículas de polímero funcionalizadas con amina. Las partículas de polímero se han sintetizado mediante polimerización en emulsión semicontinua sembrada utilizando látex MMA/BA que contienen un 5 % de AAEMA en la cubierta de las partículas. Para la preparación de partículas poliméricas funcionalizadas con amina, se han utilizado tres compuestos de amina diferentes, una amina de cadena más pequeña, es decir, hexametilendiamina (HMDA) y dos aminas de cadena más larga, es decir, polietilenimina (PEI) LUPASOL G-20 y PEI LUPASOL G-35. Las partículas de polímero funcionalizado con amina se han producido haciendo reaccionar la solución de aminas con el látex funcionalizado con AAEMA.

En primer lugar, se ha estudiado la química de reticulación entre las aminas AAEMA en el sistema que tiene aminas de cadena más corta, es decir, HMDA. Para monitorear los cambios estructurales químicos, la reacción de entrecruzamiento ha sido seguida por espectroscopía FTIR. Se ha observado que la reacción comenzó a temperatura ambiente (TA) a un ritmo lento, alcanzando aproximadamente un 30% de conversión después de 3 días a temperatura ambiente. Sin embargo, 2 horas de curado a 60 °C fueron suficientes para lograr la conversión completa de la reacción. Se ha realizado un estudio cinético similar midiendo las propiedades

reológicas de la película, extrayéndose las mismas conclusiones. Además, la resistencia química a la absorción de agua y la resistencia mecánica también respaldan los resultados, ya que la película curada mostró menor absorción de agua y mayor resistencia en comparación con la película seca TA.

Luego se procedió al estudio de la reticulación basada en aminas con aminas de cadena más larga, es decir, con PEI (LUPASOL G-20 y LUPASOL G-35). Dado que PEI tiene una estructura química ramificada, se esperaba que formara una red de enlaces en comparación con el sistema de enlaces basado en HMDA (que solo puede formar enlaces lineales). En un sistema reticulado de este tipo, también es importante analizar el proceso de formación de la película junto con la aparición de reacciones de reticulación. Por lo tanto, la cinética de la reacción de entrecruzamiento se ha seguido primero mediante espectroscopía FTIR y mediciones reológicas. Se han observado conclusiones similares a las ya vistas para el sistema basado en HMDA. Es decir, la reacción procede a temperatura ambiente a un ritmo lento (se requiere un mes para completar la reacción a temperatura ambiente), pero el curado a 60 °C acelera la reacción, obteniendo conversión completa tras 24 horas. Para analizar la formación de película en esta química de reticulación, se analizó la interdifusión entre partículas de polímero mediante el experimento de transferencia de energía de resonancia de fluorescencia (FRET) y fluorescencia de excímero de pireno (PEF). Se ha visto que la técnica FRET no se podría utilizar en este caso, ya que la PEI interfiere en el decaimiento de la fluorescencia del donante. Usando PEF, se ha demostrado que la interdifusión entre partículas de polímero se bloquea porque la reticulación se produce en la cubierta de las partículas de polímero. Además, las imágenes TEM también mostraron la formación de un patrón de panal de abeja, lo que indica la presencia de aminas en los espacios entre partículas, lo que fortalece la hipótesis de que el entrecruzamiento entre partículas ocurre antes de la interdifusión para producir una película

fuerte. Además, también se ha estudiado el efecto de la cantidad y el tamaño de PEI utilizado para la preparación de partículas poliméricas funcionalizadas con amina. Se ha encontrado que existe una cantidad umbral de PEI que debe usarse para la preparación de películas duras. Si esta cantidad se incrementa sobre el valor umbral, la película se vuelve blanda debido al exceso de PEI libre. Cuando se utilizan aminas de mayor tamaño, es decir, LUPASOL G-35 (Mw-2000 g/mol) en lugar de LUPASOL G-20 (Mw-1300 g/mol), la resistencia a la tracción de la película seca a TA es peor que la del sistema con LUPASOL G-20. Por lo tanto, el tiempo para lograr películas completamente entrecruzadas para el sistema con aminas más grandes parece ser más largo a temperatura ambiente, incluso si las propiedades mecánicas fueron similares para ambos PEI cuando se midieron películas completamente curadas.

La química de entrecruzamiento entre AAEMA y el sistema de amina se ha estudiado más mediante el análisis del efecto del tamaño de partícula y la T_G, por lo que se han preparado sistemas de mezcla con diferentes tamaños de partícula y T_G en los dos componentes de la mezcla. En el caso del sistema con diferentes tamaños de partículas en ambos componentes, la película mostró un aumento dramático en la resistencia contra el disolvente MEK y cierta mejora en la resistencia al agua y la resistencia a la tracción de la película en comparación con el sistema con el mismo tamaño de partículas en ambos componentes. En el caso del sistema con diferentes tamaños de partículas y T_G, se han observado mejoras drásticas en la resistencia al agua y la resistencia a la tracción en comparación con el sistema con el mismo tamaño de partículas. Por tanto, se ha concluido que cambiando el tamaño de partícula y la T_G, el sistema avanza hacia películas con mejores propiedades químicas y mecánicas. Las imágenes TEM también han investigado la distribución de partículas grandes y pequeñas en la película final. Aunque las imágenes de zonas superior e inferior de la película han mostrado una distribución homogénea de partículas pequeñas y grandes en ambos lugares, también se ha visto una

pequeña segregación de las partículas pequeñas en la superficie superior de las películas por AFM.

Para pasar del estudio de la química de reticulación en las dispersiones a las aplicaciones reales, los recubrimientos deben prepararse incorporando las dispersiones con capacidad de reticulación en las formulaciones de pintura. Por lo tanto, se han producido cuatro sistemas de reticulación diferentes basados en los sistemas de mezcla más prometedores estudiados, es decir, Blend LS-SS (sistema con partículas blandas grandes y blandas pequeñas), Blend LS-SH (sistema con partículas blandas grandes y duras pequeñas), Blend LH-SS (sistema con partículas grandes duras y pequeñas blandas) y Blend SH-SS (sistema con partículas pequeñas duras y pequeñas blandas). Para identificar la reticulación en la película final, se han estudiado las propiedades reológicas mediante DMTA. Se ha visto que todas las películas mostraban una meseta en la región gomosa, lo que indicaba la formación de uniones entrecruzadas. Además, el efecto de entrecruzamiento también se ha visto en las curvas tan delta, ya que la intensidad de los picos disminuyó en las películas entrecruzadas en comparación con las películas no entrecruzadas. El porcentaje de fase más blanda y más dura en la película final también se ha calculado por deconvolución de los picos obtenidos a partir de la curva tan delta. Se ha visto que las películas no reticuladas mostraron menos cantidad de fase más blanda que la añadida en la mezcla y disminuyó aún más durante el curado a 60 °C. Sin embargo, en el caso de las películas entrecruzadas, la relación entre las fases dura y blanda era casi la misma que la incluida en la mezcla, lo que significa que el entrecruzamiento evita la difusión del polímero más blando hacia la fase más dura. Las imágenes TEM y AFM de películas entrecruzadas y no entrecruzadas también respaldan esta hipótesis. La cinética de la reacción de entrecruzamiento también ha sido analizada por espectroscopía FTIR en el sistema “Blend SH-SS”, que contiene partículas blandas y duras del mismo tamaño. Se ha observado que, debido a la presencia de

partículas con alta T_G, la reacción de entrecruzamiento no prosiguió significativamente a temperatura ambiente. Sin embargo, la reacción se completó hasta una conversión casi total por curado a 60 °C durante 144 horas.

Finalmente, se han formulado pinturas a partir de los cuatro sistemas de reticulación mencionados anteriormente para aplicaciones de revestimiento de madera exterior. Para tener una referencia para las pinturas reticuladas, también se han formulado pinturas no reticuladas simplemente mezclando los dos componentes, sin modificar el componente 2 con fracciones de PEI. Se ha visto que la reticulación mejoró el rendimiento en términos de mejor desarrollo de dureza, menor absorción de agua, mejor adherencia en húmedo, mejora drástica de la resistencia al bloqueo y menor elasticidad en comparación con las pinturas no reticuladas. Con el fin de hacer una comparación relativa entre pinturas reticuladas, se ha observado que en los sistemas bimodales que tienen partículas con T_G alta, es decir, Blend LS-SH y Blend LH-SS, el desarrollo de dureza, la resistencia al bloqueo y la absorción de agua mejoraron en comparación con Mezcla LS-SS, que contiene solo partículas blandas. Además, se observaron mejoras adicionales en el rendimiento de las pinturas al usar partículas pequeñas blandas y duras, es decir, Blend SH-SS. El efecto de la cantidad de PEI se ha visto en Blend SH-SS en términos de un mejor rendimiento de adhesión en húmedo, ya que el sistema contenía un 50 % de polímero con PEI, que también pueden actuar como un promotor de la adhesión mejorando el rendimiento de la adhesión en húmedo. En cualquier caso, se ha visto que la presencia de partículas de pigmento y aditivos no altera la reacción de reticulación entre AAEMA y partículas que contienen amina.

Para realizar una comparación con un producto comercial, se ha elegido ACRONAL - EDGE 6283 (una dispersión acuosa acrílica autorreticulante). Nuestras pinturas reticuladas

presentaron mejor resistencia al agua, formación de ampollas a los 30 minutos y resistencia al bloqueo, tanto en la aparición de rayaduras como en la energía requerida para separar la madera apilada en comparación con la pintura comercial Acronal. Sin embargo, nuestras pinturas reticuladas fueron peores en términos de desarrollo de dureza con el tiempo y la temperatura y el desempeño de la adherencia en húmedo. En nuestras pinturas, el PEI utilizado en el aglutinante actuó como promotor de la adhesión en húmedo, pero en el caso de la pintura Acronal, ésta contenía una funcionalidad de adhesión en húmedo doble, por lo que el rendimiento de la adhesión en húmedo de Acronal fue mejor que el de nuestras pinturas. Aunque nuestro sistema se basa en un sistema bimodal con partículas blandas y duras, la pintura Acronal se describe como un látex basado en una morfología multifásica con un tamaño de partículas de 60 nm. Por lo tanto, la razón de una mejor dureza podría estar oculta en el uso de morfología multifásica en partículas de pequeño tamaño, al desarrollar más dureza durante la formación de la película.

Appendix I.

A.I.1. Synthesis of latexes with different particle size and T_G

A.I.1. Synthesis of large and soft particles latex

For the preparation of large and soft particles, we followed the recipe shown in Tables A.I.1 and A.I.2. First, the seed was synthesized with batch emulsion polymerization (Table A.I.1).

Table A.I.1. Formulation used to produce the seed by batch emulsion polymerization for the preparation of large and soft particles latex

Ingredients	Seed Formation
Methyl methacrylate	11.42
Butyl acrylate	11.42
Water	76.47
Dowfax 2A1	0.46
$K_2S_2O_8$	0.23

Table A.I.2. Formulation used for the synthesis of MMA/BA/AAEMA latex with large and soft particles by semibatch emulsion polymerization.

Ingredients	Initial Charge (g)	Stream-1 Growth of the seed (g)	Stream-2 (g)
Seed amount	74.88		
Methyl methacrylate	3.809	373.89	
Butyl acrylate	3.809	373.83	
Water	590.4	165	130
Dowfax 2A1		6.29	
Methacrylic Acid		7.63	
$K_2S_2O_8$	1.404		2.6

Then, the growth of the seed was carried out by semi continuous emulsion polymerization. The initial charge of 74.88 g of seed latex, water and a small amount of monomers was added to the reactor. The initial charge was purged with nitrogen for 15 minutes, and after that a fraction of initiator was added. When a small increase of the temperature was observed, which means the reaction began, the rest of the ingredients were added in two different streams. The feeding rate for the first stream was 2.65 g /min and for the second one 0.22 g/min. When 50 % of feeding was completed, 49.60 g of AAEMA was added in the preemulsion of stream 1 (Table A.II.2). This synthesis was repeated twice to produce Latex 1_LS and Latex 2_LS, in order to check the repeatability of the synthesis.

A.I.2. Synthesis of small and soft particles latex

For the preparation of the small and soft particles latex, we have followed the recipe mentioned in Table A.I.3.

Table A.I.3: Formulation used to produce the seed by batch emulsion polymerization and the final latex by semibatch emulsion polymerization for the synthesis of MMA/BA/AAEMA latex with soft and small particle size.

Ingredients	**Seed (g)**	**Shell (g) Addition of the functional monomer**
Initial charge		1521
Methyl methacrylate	153.95	141.25
Butyl acrylate	154.20	140.335
Water	1231.613	50
SLS	6.17	5.65
$NaHCO_3$	1.604	
Disponil A3065		7.646
Methacrylic Acid		2.31
$K_2S_2O_8$	1.525	1.15
Acetoacetoxy ethyl methacrylate (AAEMA)		31

Batch emulsion polymerization was used for the preparation of the seed. Then 1521 g of this seed was used for the semibatch process. The formulation used for feeding in the semibatch

process is presented in the Table A.I.3 as well. The feeding rate for the shell preparation was 1.06 g/min. This synthesis was repeated twice to produce Latex 3_SS and Latex 4_SS, in order to check the repeatability of the synthesis.

A.I.3. Synthesis of large and hard particles latex

We prepared latex with big and hard particles by following the recipe mentioned in Tables A.I.4 and A.I.5. Initially the seed was produced by batch emulsion polymerization with the recipe presented in Table A.I.4.

TableA.I.4. Formation of seed for the preparation of seed for large and hard particles

Ingredients	Seed Formation
Methyl methacrylate	15.98
Butyl acrylate	6.852
Water	76.47
Dowfax 2A1	0.46
$K_2S_2O_8$	0.23

Then, an initial charge of 85.56 g of seed latex, water and a small amount of monomers were added to the reactor. The initial charge was purged with nitrogen for 15 minutes, and after that a fraction of initiator was added. When a small increase of the temperature was observed, which means the reaction began, the rest of the ingredients was added in two different streams. The feeding rate for first stream was 2.65 g /min and for the second stream 0.22 g/min of feeding rate was adopted. When 50 % of feeding was completed, 49.60 g of AAEMA was added in the preemulsion of stream 1. This way Latex 5_LH was produced.

Table A.I.5. Formulation used to produce the final MMA/BA/AAEMA latex with hard and large particle sizes by semibatch emulsion polymerization.

Ingredients	Initial Charge (g)	Stream-1 Growth of the seed (g)	Stream-2 (g)
Seed amount	85.56		
Methyl methacrylate	5.332	523.446	
Butyl acrylate	2.28	224.298	
Water	590.4	165	130
Dowfax 2A1		6.29	
Methacrylic Acid		7.63	
$K_2S_2O_8$	1.404		2.6

A.I.4. Synthesis of small and hard particles latex

We prepared a latex with small and hard particles by following the recipe mentioned in Table A.I.6. The prepared latex was named as Latex 6_SH.

Table A.I.6. Formulation used to produce the seed by batch emulsion polymerization and the final latex by semibatch emulsion polymerization for the synthesis of MMA/BA/AAEMA with small and hard particles.

Ingredients	Seed (g)	Shell (g) Addition of the functional monomer
Initial charge		1516
Methyl methacrylate	215.53	197.1095
Butyl acrylate	92.52	84.47
Water	1231.613	50
SLS	6.17	5.65
$NaHCO_3$	1.604	
Disponil A3065		7.646
Methacrylic Acid		2.31
$K_2S_2O_8$	1.525	1.15
Acetoacetoxy ethyl methacrylate (AAEMA)		31

Appendix II.

A.II. Particle location by incorporation of styrene in one of the blend components

A.II.1 Latex synthesis and experimental characterization

In the first stages of the PhD, and with the aim to locate the different latex components in a film produced by blending two of them, methyl methacrylate was changed for styrene (S) in the formulation of one of the latexes. Polystyrene has a T_G similar to the polymethyl methacrylate one, but if can be easily differentiated from an (meth)acrylate polymer by TEM in the final films. Therefore, component-2 containing the amine moiety was prepared containing S as follows. Table A.II.1 presents the formulation used to prepare the seed by batch emulsion polymerization.

Table A.II.1. Formulation of the seed produced by batch emulsion polymerization

Ingredients	Charge (g)
Methyl methacrylate	31.29
Butyl Acrylate	31.34
Water	250.31
SLS	1.255
$NaHCO_3$	0.326
$K_2S_2O_8$	0.31

This seed was used to produce the final latex by seeded emulsion polymerization with two feeding steps. We used 10 to 90 ratio of seed / monomer in the first feeding stage. The seed quantity used during the first stage of feeding was 42.78 g with no additional water, and the

formulation used in the feeding is presented in Table A.II.2; with a feeding rate of 0.442 g/min. In the second stage of feeding 31.5 g of extra water was added to maintain the solids content at 50 % and a feeding rate of 0.23 g/min was used (see formulation in Table A.II.2). The final latex contained particle sizes of 130 nm.

Table A.II.2. Formulation used in the two steps of growing of the seed by semibatch emulsion polymerization for the synthesis of MMA/BA/S/AAEMA latex

Ingredients	Feed (1) Growth of the seed	Feed (2) Addition of functional monomer
Methyl methacrylate	-	12.23
Butyl Acrylate	24.51	12.15
Styrene	24.76	-
Water	27.92	14.24
SLS	0.99	0.4915
Disponil A3065	1.34	0.662
Methacrylic Acid	0.467	0.20
$K_2S_2O_8$	0.2	0.1
Acetoacetoxy ethyl methacrylate (AAEMA)		4.4

Component-2 containing S was prepared by reacting this latex with polyethyleneinimine (PEI) by using the mole ratio of 7.7: 1 between N-H of PEI: AAEMA. On the other hand, component-1 was prepared with MMA/n-BA/ AAEMA latex with 5% AAEMA as mentioned in Chapter 3, with a particle size of 130 nm too (see section 3.2.2). The blend latex was prepared by mixing 50 % of each component.

The morphology of blend films was studied by means of Transmission Electron Microscopy (TEM). TEM analysis was carried out with a TecnaiTM G2 20 Twin device at 200 kV (FEI Electron Microscopes). The films were cryosectioned with a Leica EMUC6 cryoultramicrotome at 30 °C below the Tg of the sample, with a Diatome 45° diamond 30 knife, and the observations were made in the microscope (TEM), without any staining and after RuO_4 staining.

Tensile tests of the free standing films dried at room temperature (23 °C with relative humidity of 55 %) and annealed at 60 °C were performed on Universal testing machine TA.HD plus Texture Analyser at a crosshead speed of 0.42 mm/s. Samples with approximate length of 55 mm and 0.55 mm of thickness were used.

A.II.2. Results and discussions

The first difference that could be noticed from the blend films produced in Chapter 3, with MMA/BA/MAA/AAEMA in the formulation of both component-1 and component-2, is that the films were more opaque and even more yellowish when dried at 60 ºC when S was included in component-2, as shown in Figure A.II.1.b. Even if the film prepared from component-2 was transparent (Figure A.II.1.a), as it were all single component and blend films when no S was included in the formulations, the blends films became opaque. This opacity probably came from the presence of two different polymeric phases with different refractive indexes in its composition.

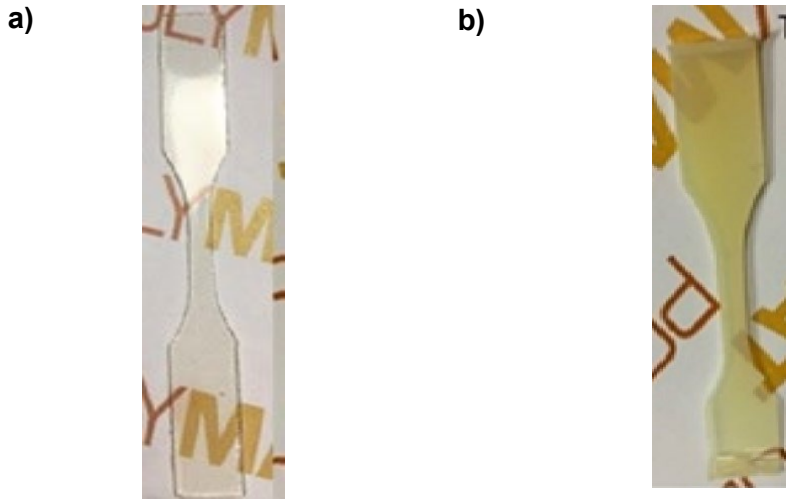

Figure A.II.1. a) Polymer film prepared from component-2 containing (MMA/BA/S/AAEMA) and b) Polymer film prepared from the blend at 60 ºC.

TEM analysis was therefore used to study the distribution of component-1 and 2 in the final blend films. Figure A.II.2 shows the TEM images of the blend film prepared in Chapter 3 and dried at RT, for comparison purposes. There on clear indication of any different phases as the film appearance is completely homogeneous.

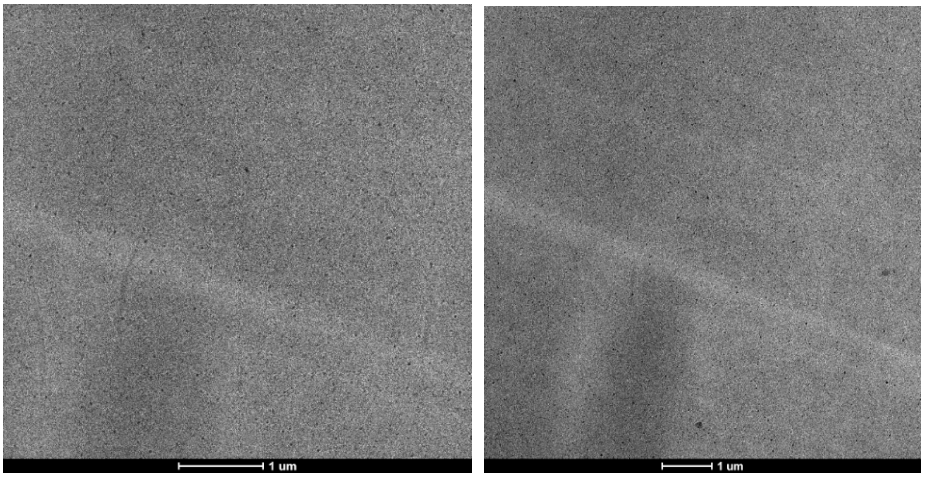

Figure A.II.2. TEM images for the blend film with same monomer composition in both components, dried at RT (system presented in Chapter 3 (MMA/BA/AAEMA)).

Figure A.II.3 shows the TEM images of the blend film having styrene in component-2. In the images, dark spots are homogenously distributed within all the film, clearly indicating the presence of styrene containing polymer phases spread all over the film. In order to quantify the distribution of S containing particles in the film, the cryosectioned films were stained with RuO_4, and analysed by TEM again (Figure A.II.4). This staining allows the differentiation of each polymeric particle in the final film, as RuO_4 stains preferentially the amine moieties that will be located in the interstitial spaces between the polymer particles. This way the counting of particles with and without S could be performed. In the different TEAM images analysed, the average of S containing particles ranged from 45 to 55 %. Therefore, it can be said that when the particle

size of the two latex components contained in a blend is the same, there is a homogeneous distribution of both components in the final blend film.

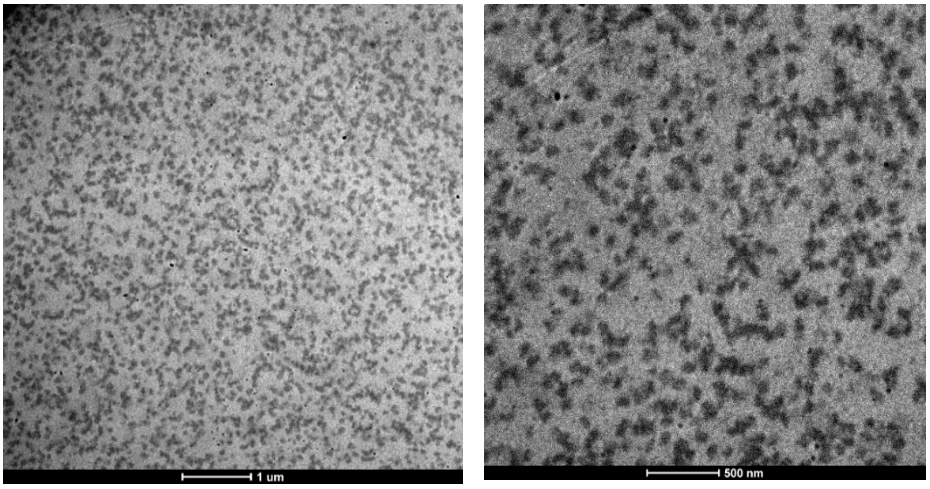

Figure A.II.3. TEM images for the unstained blend film having S in component-2 (MMA/BA/S/AAEMA) and MMA/BA/AAEMA in component-1, dried at RT.

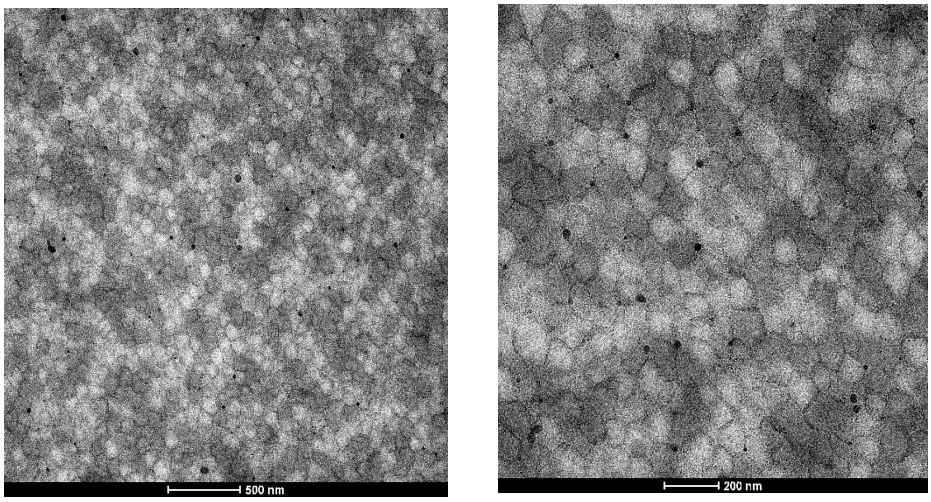

Figure A.II.4. TEM images for the RuO_4 stained blend film having S in component-2 (MMA/BA/S/AAEMA) and MMA/BA/AAEMA in component-1, dried at RT.

The mechanical properties of the sample produced from the blend containing S in Component-2 were also analized by tensile tests and compared to the blends produced with the same monomer composition (shown in Chapter 3). Figure A.II.5 presents the results, in which it can be seen that the general improvement of the mechanical properties observed when annealing at 60 ºC is reproduced in both systems, even if there was a slight increase in the Young's modulus for the samples containing styrene in their composition.

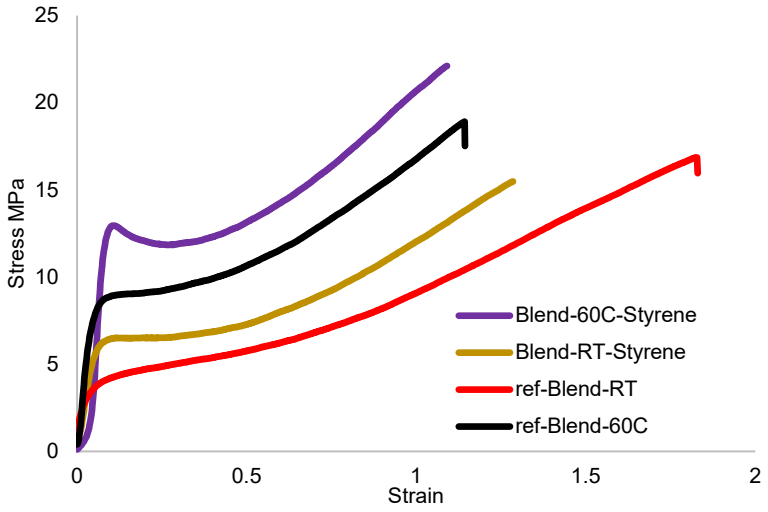

Figure A.II.5. Tensile test result comparison for blends dried at different temperature for the system with different monomer composition (BA/MMA/S/AAEMA) and the system with same monomer composition (BA/MMA/AAEMA).

Appendix III.

A.II. Deconvolution of DMTA tan delta curves in blend films

A.III.1 System LS-SH

In case of the system having different dp and Tg (System LS-SH), we had seen two clear peaks in tan delta, indicating the presence of softer and harder phases in the final film. In order to calculate the amount of softer and harder region in the final film, the deconvolution of the peak has been performed using a GaussMod fitting as shown in Figure A.III.1 and Figure A.III.2. It has been seen that the area calculated from softer region decreased from 51 % to 25 % in case of Ref_blend LS-SH-RT to Ref_blend LS-SH-60C (Figure A.III.1). However, in case of crosslinked blends i.e., Blend SH-SS-RT and Blend SH-SS-60C (Figure A.III.2) the deconvolution showed that the softer phase remained high at both drying temperatures, namely 43 % to 53 % for RT and 60 ºC dried samples. In case of non-crosslinked film, it has been seen that with the annealing conditions softer particles were diffused into harder phase. However, in crosslinked films due to the interparticle crosslinking, the diffusion between soft and hard phases was much more restricted, and the soft phase remained separated from the hard phase, even after drying at 60 ºC. .

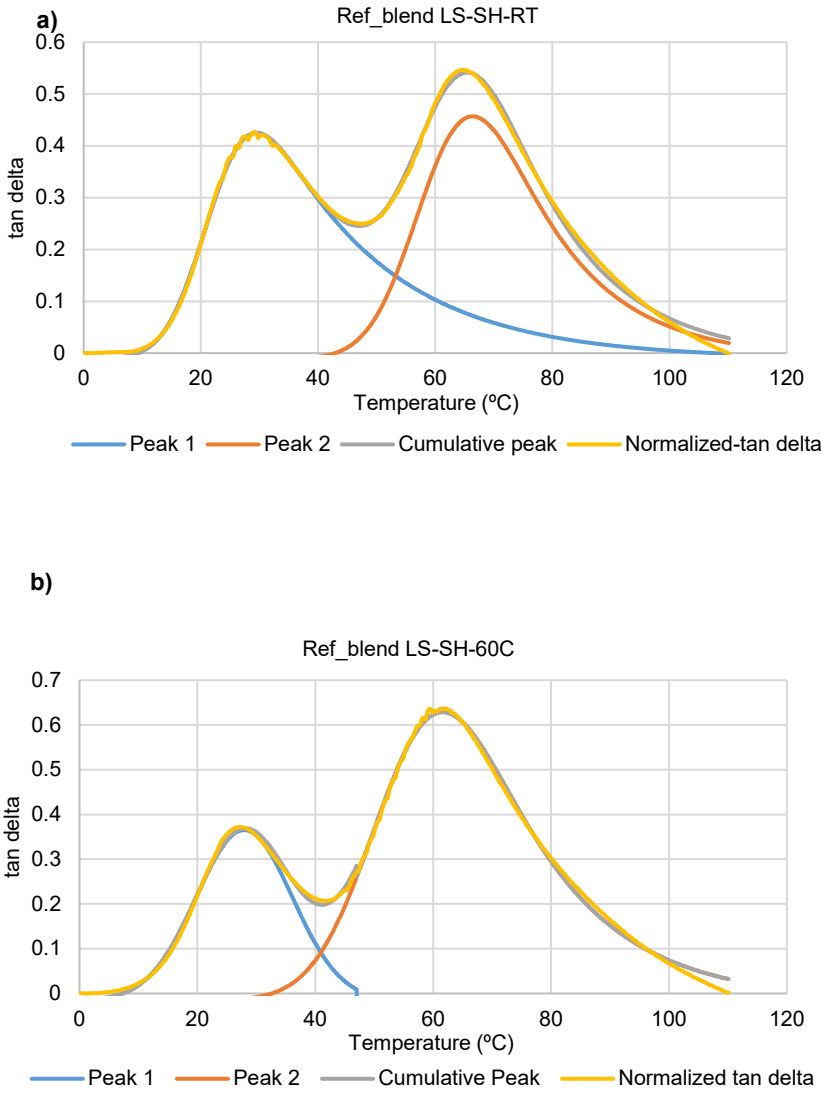

Figure A.III. 1. Deconvolution of Modulus (E') tan delta curves (a) Ref_blend LS-SH-RT (b) Ref_blend LS-SH-60C for system LS_SH (blend having different particle sizes and different T_G latexes).

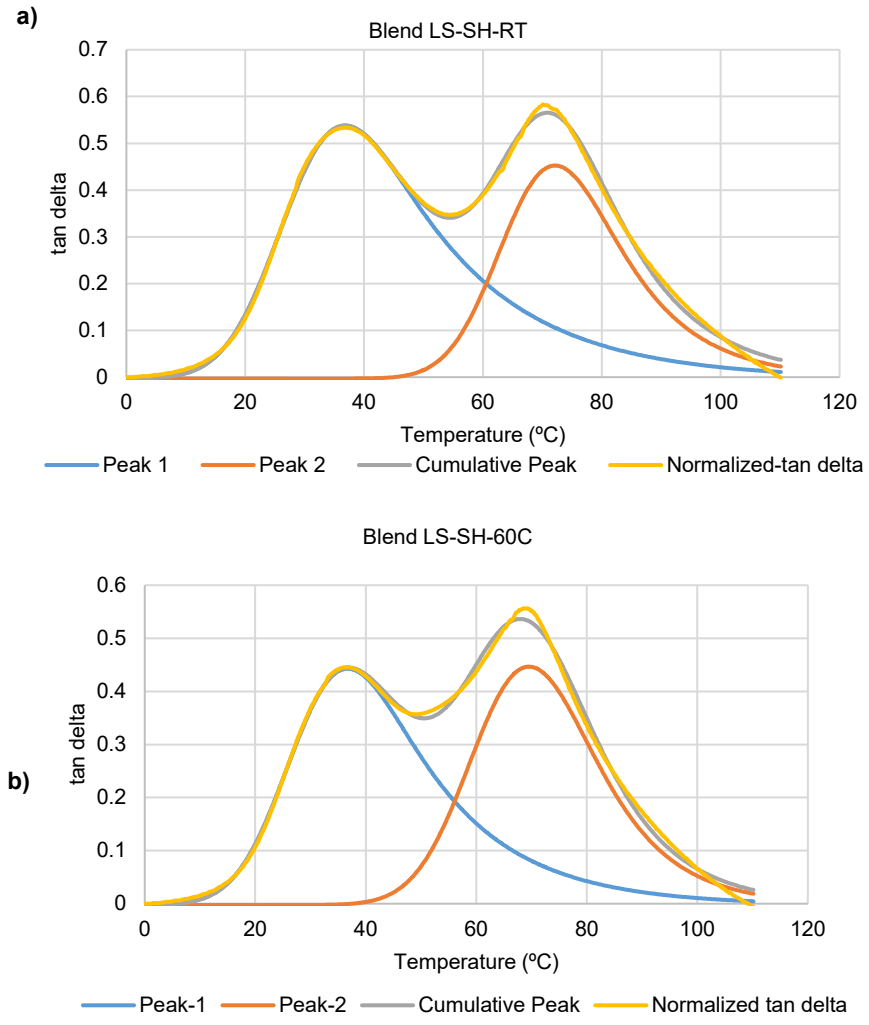

Figure A.III. 2. Deconvolution of Modulus (E') tan delta curves (a) Blend LS-SH-RT (b) Blend LS-SH-60C for system LS_SH (blend having different particle sizes and different T_G latexes).

A.III.2. System LH-SS

In this case, two clear peaks in tan delta could also be observed for the system LH-SS, indicating the presence of softer and harder phases in the film. The amount of soft and hard region polymer was calculated by the deconvolution shown in Figure A.III.3 and Figure A.III.4. In case of Ref_blend LH-SS-RT and Ref_blend LH-SS-60C, the calculated area of softer region decreased from 30 % to 8 % (Figure A.III.3) after drying at 60 ºC. However, in case of crosslinked blend i.e., Blend LH-SS-RT and Blend LH-SS-60C (Figure A.III.4) the amount of softer phase stayed at 40 % for RT and at 33.7 % for 60 ºC sample. Similar conclusions can be drawn in this case, as for crosslinked system the ratio of softer region remains high and after drying the sample at 60 ºC, showing that no or limited diffusion occurs between polymer particles of different T_G.

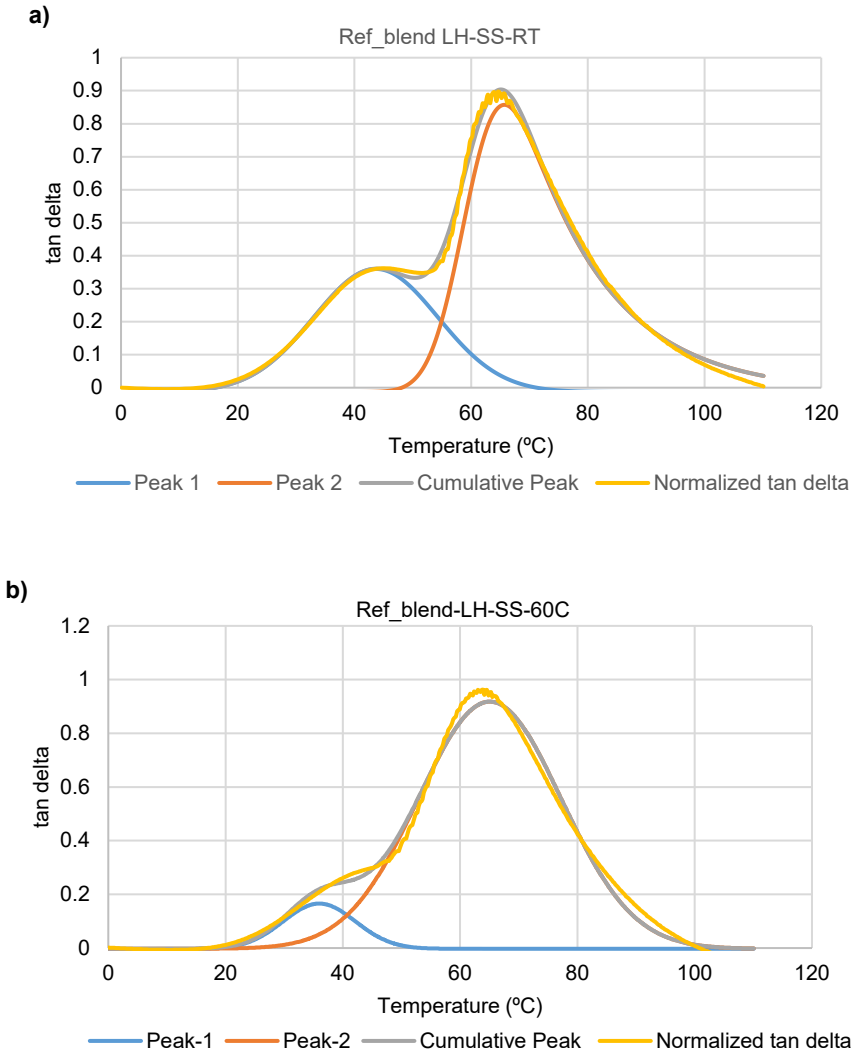

Figure A.III. 3. Deconvolution of Modulus (E') tan delta curves (a) Ref_blend LH-SS-RT (b) Ref_blend LH-SS-60C for system LH_SS (blend having different particle sizes and different T_G latexes).

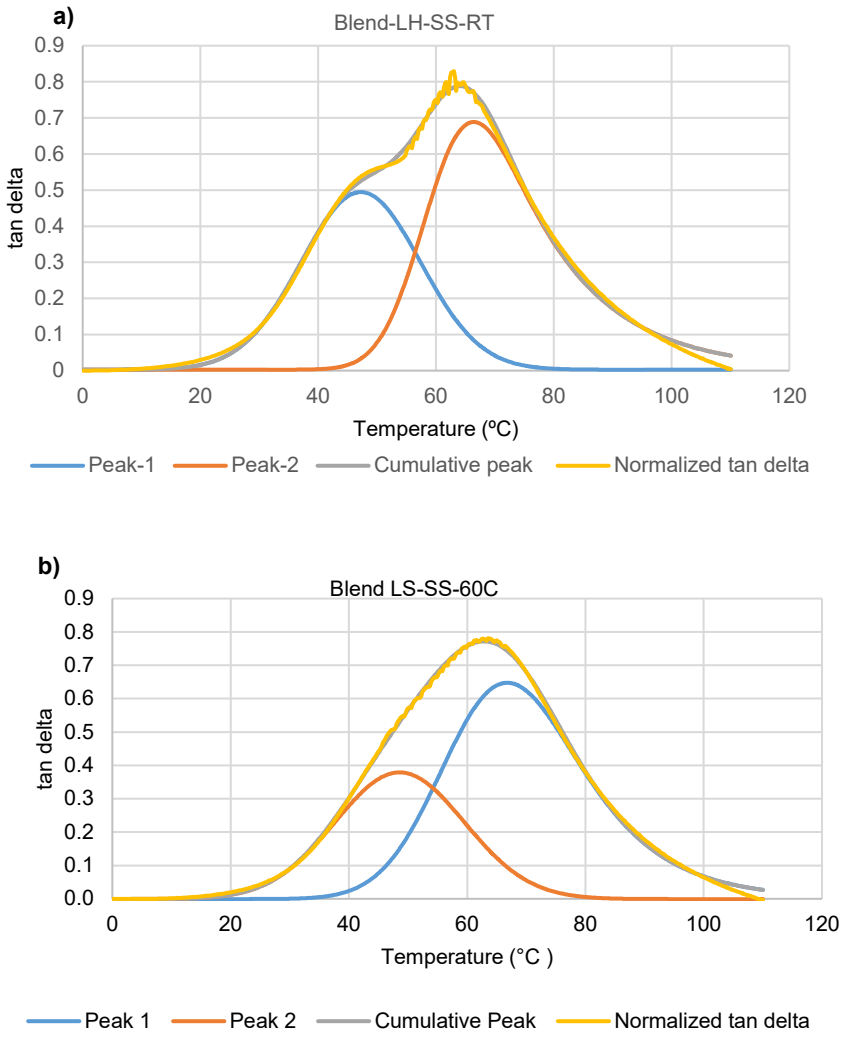

Figure A.III. 4. Deconvolution of Modulus (E') tan delta curves (a) Blend LH-SS-RT (b) Blend LH-SS-60C for system LS_SH (blend having different particle sizes and different T_G latexes).